NON-DESTRUCTIVE ASSESSMENT OF HOUSEHOLD REVERSE OSMOSIS WATER TREATMENT MEMBRANE BIOFOUILING

by

Stephen Donald Markwardt

A thesis submitted in partial fulfillment
of the requirements for the degree

of

Master of Science

in

Environmental Engineering

MONTANA STATE UNIVERSITY
Bozeman, Montana

May 2015

TABLE OF CONTENTS

TABLE OF CONTENTS – CONTINUED

TABLE OF CONTENTS – CONTINUED

TABLE OF CONTENTS – CONTINUED

TABLE OF CONTENTS – CONTINUED

LIST OF TABLES

LIST OF TABLES – CONTINUED

Table Page

LIST OF FIGURES

Figure Page

LIST OF FIGURES – CONTINUED

Figure Page

LIST OF FIGURES – CONTINUED

Figure Page

LIST OF FIGURES – CONTINUED

Figure Page

LIST OF FIGURES – CONTINUED

Figure Page

LIST OF FIGURES – CONTINUED

Figure Page

LIST OF FIGURES – CONTINUED

Figure Page

ABSTRACT

Reverse osmosis (RO) membrane treatment is well known for its ability to desalinate sea and brackish waters on a massive scale in large treatment plants. Conversely, RO membranes are also used to treat freshwater from questionable sources at the point of use. Both types of systems suffer from the negative effects of membrane fouling. There are four basic types of fouling: inorganic, colloidal, organic, and biofouling. Traditional methods for assessing fouling either cannot differentiate between the fouling types or destroy the membrane in the process. Currently, many new and innovative methods to non-destructively assess the degree and type of fouling inside a membrane unit are being researched. Most of these methods require the use of expensive electrodes and equipment which is not economical for point of use systems. This research was aimed at determining economical non-destructive methods to assess biofouling in point of use RO membrane treatment systems. Experimentation was performed on three parallel household RO membrane units operated under controlled feed water conditions to promote biofouling, inorganic fouling and a combination of both. Operational and biological parameters were monitored throughout the systems' lifespan. Membrane autopsies were also done to assess the degree and type of fouling. Statistical models were performed on the operational data to determine statistically relevant parameters between the fouling types that were subsequently validated by the membrane autopsies. Several non-destructive methods to assess the presence of biofouling were determined. Permeate flow rates decreased in a significantly different way when biofouling was present compared to when it was not. Large increases in permeate conductivity were also noted in membranes suffering from biofouling while they were not observed in membranes that had been inorganically fouled. The concentration of cell clumps in the retentate also increased in membranes experiencing biofouling while they did not increase in membranes that were inorganically fouled. These methods were found to not be sensitive enough to provide early warning for the presence of biofouling. However, these methods could be used to conveniently and economically assess the types of fouling problems being experienced household RO systems.

CHAPTER 1

INTRODUCTION

Reverse Osmosis (RO)

Osmosis and reverse osmosis are diffusion processes requiring a semipermeable membrane. Ideally, the membrane would only allow the passage of water. Imagine now that there are two types of water separated by the ideal semipermeable membrane; one with lower salt concentration than the other. In osmosis, water would diffuse through the membrane to the side with the highest salt concentration. This diffusion direction can be reversed if a pressure greater than the natural osmotic pressure of the system is applied to the fluid with the higher salt concentration, hence the name reverse osmosis. Reverse osmosis allows for the desalinization of sea water.

Reverse Osmosis Membrane Treatment Systems

There are a wide range of scales of application associated with reverse osmosis water treatment systems. To illustrate the possible range, the two opposite ends of the spectrum will be contrasted in this section.

Municipal RO Water Treatment Plants

Municipal RO water treatment plants used for the desalinization of brackish water or sea water for the production of potable water are large and costly installations. These plants operate continuously under very high operating pressures (greater than 600 psi) producing millions of gallons of potable water daily. They are also very complex,

utilizing hundreds of individual membrane units and retentate recycling streams. Membrane operations are closely monitored with sophisticated instrumentation by trained staff to ensure efficient plant operation.

Household RO Treatment Systems

Household membrane systems are small point-of-use systems and relatively inexpensive. They usually are used for the enhanced treatment of fresh water sources. These membrane systems operate under low pressures (40 – 100 psi) and produce water only on demand. Therefore, they operate intermittently and have low production volumes. Usually these systems consist of only one small membrane element. Upkeep and maintenance of the system is usually the responsibility of the owner.

Problems with RO Systems

While reverse osmosis water treatment membrane technology opens up new water sources for the production of potable water, there are several drawbacks to the technology. RO membrane treatment is very energy intensive, especially when it comes to sea water desalinization since large pressures (greater than 600 psi) are required and large quantities of water are being produced. Energy consumption is not that intensive household RO treatment systems since low operating pressures (40-100 psi) and low production volumes are normal.

One of the most severe problems associated with reverse osmosis membrane treatment and is ubiquitous between both municipal and household treatment systems is membrane fouling. Fouling is the attachment of foreign materials to the membrane

surface and other membrane elements which causes a decrease in production or an increase in energy to maintain production. There are four types of fouling: colloidal fouling, organic fouling, inorganic fouling and biofouling. All these fouling types are driven by different mechanisms and generally require different procedures for their mitigation and/or removal.

Assessing Membrane Fouling

It is important for treatment system operators to be able to distinguish the degree and type of fouling occurring within the RO membrane. Currently, this is done through membrane autopsies. During a membrane autopsy, the targeted membrane is taken offline and cut open to assess the state of fouling. Unfortunately, this destroys the membrane in the process so it must be discarded.

New methods are now being researched and developed that would allow for the determination of the degree and type of fouling without the need for membrane autopsies. These so called non-destructive methods would allow membrane system operators to assess the proper fouling mitigation efforts while the system is still operational. Most if not all the literature on non-destructive fouling assessment is devoted to large municipal RO membrane treatment plants and tends to require advanced and expensive instrumentation.

Experimental Goal

Experimentation was conducted with the goal of finding non-destructive methods to assess the presence of biofouling in household RO water treatment membranes. This

was done by inducing accelerated biofouling, inorganic fouling and a combination of both in membrane elements. Membrane autopsies were performed to determine the degree and type of fouling in each membrane element. A wide variety of parameters were monitored during membrane operation. These parameters were compared on the basis of fouling type that had occurred in each membrane element with the goal of finding different data trends based whether biofouling was present or not.

Thesis Outline

This thesis is divided into several chapters. Chapter 2 provides background data about reverse osmosis membrane treatment systems. It also details some of the current work being done with the development of non-destructive methods to assess membrane biofouling. Chapter 3 provides information about the experimental system and methods used during experimentation. Chapter 4 describes the experimental results and the statistical analyses used to validate the proposed non-destructive methods. Chapter 5 is a detailed discussion of the results and it compares and contrasts the results of this experiment with the results from other research. Chapter 6 is an in depth discussion of the non-destructive methods that were found through this research and outlines the required methodology and the potential pitfalls of each. Finally, the appendices detail the experimental methodologies that were not successful.

CHAPTER 2

LITERATURE REVIEW

Water Issues

Almost 97% of the Earth's water occurs as salt water in the oceans, while only about 1% exists as liquid fresh water (Bouwer, 2000). Bouwer (2000) also states that great imbalances between the distribution of these limited freshwater sources and human populations exist, resulting in regions with water scarcity and shortages. Furthermore, Bouwer (2000) states that growing populations and higher standards of living will further stress these limited freshwater supplies. If that isn't enough, changing climate patterns create great uncertainties in the continued availability and distribution of freshwater sources throughout the planet. All of these circumstances will pose heavy burdens on freshwater resources in the future (Bouwer, 2000). Therefore, it is essential to find alternative sources for procuring freshwater for potable use.

With such large a percentage of the Earth's water being salt water, desalinization is a logical option for creating freshwater. Reverse osmosis (RO) is becoming a widespread desalination method used to produce fresh water from brackish or sea water sources (Sim et al., 2013). In fact, about 72% of all desalination in Europe is performed through the use of RO membranes (Fritzmann et al., 2007). Desalinization is usually performed in large treatment plants with multi-million dollar price tags operating under high pressures and producing millions gallons of fresh water daily. Alternatively, small RO membrane systems are now being used to treat water of questionable quality from

wells or produced by non-optimized municipal treatment plants. These small, low cost, point-of-use systems treat small quantities of water on demand at low operating pressures.

Unfortunately, both types of systems are not without their potential problems and drawbacks. Outside of increased cost of treatment (purchase of membranes, energy costs, maintenance costs, etc.) both systems suffer from fouling with biofouling being the most troublesome type of fouling to control. It is desirable for RO system operators to be able to determine the type of fouling occurring inside the membrane elements so proper mitigation measures can be employed.

Basics of Reverse Osmosis Systems

Both municipal RO membrane treatment plants and household RO treatment systems can be broken into the same fundamental components. A schematic of the components can be found in Figure 1 and are discussed in greater detail below.

RO membranes allow for the treatment of a wide range of source waters including sea water, brackish groundwater and fresh water. Before this water is fed into the RO membrane it undergoes pretreatment. Pretreatment conditions the source water for optimal RO membrane performance. In household RO membrane systems, it is essential that pretreatment remove any chlorine that may be present in the source water since it is damaging to the membrane.

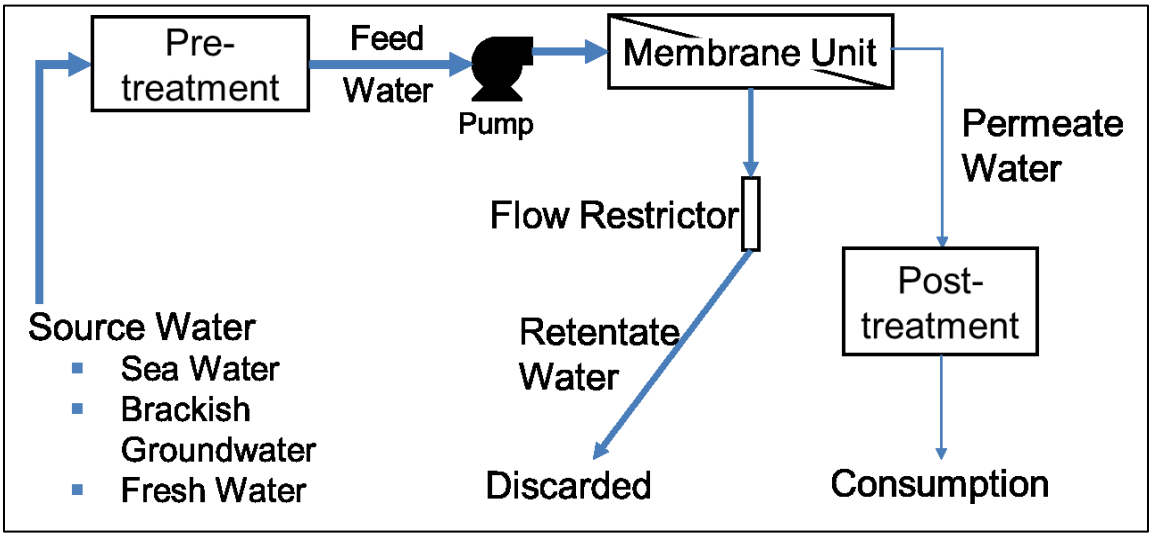

Figure 1: Basic process schematic for a RO membrane water treatment system.

Pressure is needed to drive reverse osmosis. This pressure is often supplied to the system through pumps. The retentate flow restrictor works in conjunction with the pump by restricting the flow out of the membrane element. It allows the system to operate at a pressure high enough to induce fluid flux through the membrane and without it no permeate production would be possible.

There are three process streams associated with RO membrane filtration. The feed stream consists of the source water that has undergone pretreatment. Feed water is the water that enters the membrane element. Permeate water is the clean production water that has fluxed through the membrane and is considered potable. Retentate water is the water that did not flux through the membrane. It is a concentrated waste stream that must be discarded. In a typical household RO membrane system, for every one part feed water, 2/3 exits as retentate while 1/3 exits as permeate.

Produced permeate water undergoes some kind of post treatment in both the household and municipal RO membrane treatment systems. In municipal treatment systems, salts are added back into the permeate to prevent corrosion of the distribution network.

Reverse Osmosis Membranes

Most reverse osmosis membranes on the market today are spiral would membranes. Spiral wound membranes have several key components that are essential for their operation. These components can be seen in Figure 2.

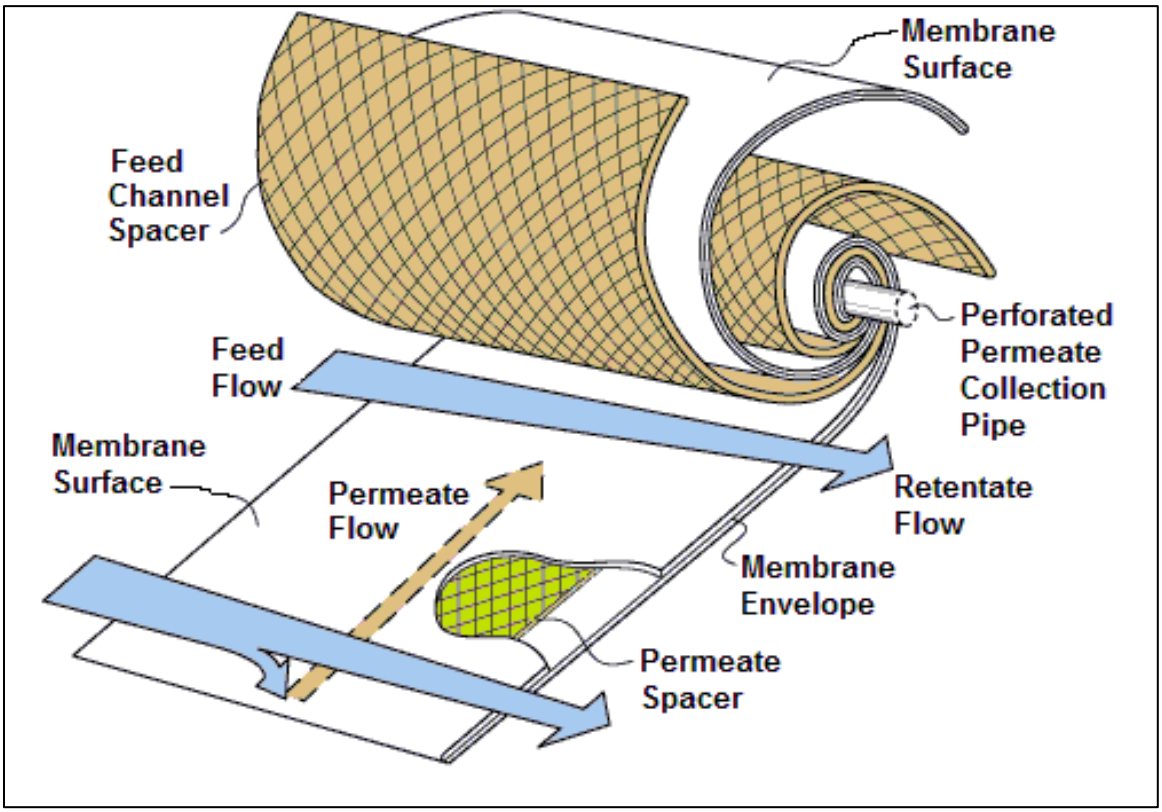

Figure 2: Spiral wound RO membrane. Image modified from www.mtrinc.com.

Perforated Permeate Collection Pipe

The perforated permeate collection pipe is the back bone of the membrane element. It is a tube that is closed on one end with small holes drilled along its length. The mouth of the membrane envelope is sealed to the perforated permeate collection pipe around the outside of these holes. This allows for fluxed water to flow down the inside of the membrane envelope through the perforations and out the open end to the collection pipe.

The Membrane Envelope

The membrane envelope is two membrane sheets that have been laid on top of each other and fused together along three edges. This creates a membrane envelope pocket in which fluxed water (permeate water) flows through to the perforated permeate collection pipe. The membrane envelope design allows for a large active membrane area since water flux can occur on both sides of the envelope

Permeate Spacer

The permeate spacer is a fine mesh that is inserted into the membrane envelope pocket. Its main purpose is to keep the membrane envelope pocket open and allow permeate water to flow to the perforated permeate collection pipe. If the permeate spacer was not employed, the membrane envelope pocket would be flattened due to the large pressure differential between the feed/retentate stream and the permeate stream thus preventing any permeate water from getting to the perforated permeate collection pipe.

Feed Channel Spacer

The feed channel spacer is a coarser screen than the permeate spacer that lies on top of the membrane envelope. The primary purpose of the feed channel spacer is to create a space where feed water can flow over the membrane element allowing for fluid flux. The feed channel spacer also creates turbulence which helps scour away any inorganics that have precipitated onto the membrane surface. Unfortunately, research has found that the feed channel spacer is also ideal habitat for biofilm growth (Vrouwenvelder et al., 2011a).

Outer Wrap

The membrane envelope and feed channel spacer are wrapped tightly around the perforated permeate collection pipe forming a cylinder. The outer wrap (not shown in Figure 2) is adhered to the very end of the membrane envelope and feed channel spacer at the opposite end that was attached to the perforated permeate collection pipe. The outer wrap is then wrapped around the element and sealed to itself to prevent the membrane element from unrolling.

Fouling of Reverse Osmosis Membranes

One of the most significant problems with RO water treatment, besides the increased cost of treatment, is membrane fouling. Fouling is the accumulation of foreign materials from the feed water on the active membrane surface and/or on the feed channel spacer to the point of causing operational problems (Pandey et al., 2012). Fouling of membranes results in increased power consumption and a reduction of membrane

lifespan which are major operational and economic issues for the feasibility of membrane treatment (Kavanagh et al., 2009). Most literature has separated fouling into four different types: inorganic fouling, colloidal fouling, organic fouling and biofouling (Pandey et al., 2012; Vrouwenvelder et al., 1998).

Inorganic Fouling

Inorganic fouling is the precipitation of dissolved solids on the membrane surface. This happens because the concentrations of dissolved solids increases in the direction of flow along the membrane due to the reduction of flow volume because of permeate production. Depending on water properties within the membrane, the concentration of one or more solutes may exceed its solubility product and form a precipitate on the membrane surface (Pandey et al., 2012). This precipitate formation is also referred to as scaling. Inorganic fouling can be controlled through the use of anti-scalants and pretreatment (Vrouwenvelder et al., 2011a).

Colloidal Fouling

Colloidal fouling is the attachment of biologically inert particles and colloids to the surface of the membrane. This causes fouling by cake formation on the membrane's surface which decreases flux and membrane performance (Pandey et al., 2012). Excessive colloidal fouling can be prevented by extensive pretreatment (Vrouwenvelder et al., 2011a).

Organic Fouling

Organic fouling is the deposition of non-viable organic matter on the membrane surface (Al-Juboori and Yusaf, 2012). Some of the possible organic compounds linked to fouling include humic substances, amino acids, sugars and aromatic acids (Pandey et al., 2012). Currently, there are no known methods to control organic fouling (Vrouwenvelder et al., 2011a).

Biofouling

Biofouling is the attachment and growth of microorganisms to form a biofilm on the membrane surface and/or feed channel spacer in a membrane unit to the point where economical operation is impacted (Flemming, 1997; Pandey et al., 2012; Vrouwenvelder and van der Kooij, 2001). Microorganisms are ubiquitous to technical water systems and even if 99.99% of all aqueous bacteria could be removed in RO feedwater, enough still exist to gradually colonize the membrane unit (Flemming et al., 1997)

Of all the fouling types, biofouling is the most detrimental to long term operation (Pandey et al., 2012). Today, biofouling is recognized as at least a contributing factor to more than 45% of all membrane fouling (Komlenic, 2010). Biofouling also poses severe risks to membrane operations because it is currently uncontrollable (Vrouwenvelder et al., 2011a). Biofouling increases system energy demand, increases cleaning requirements and decreases membrane life (Flemming and Tamachkiarow, 2003).

Traditional Methods for Assessing Fouling

Membrane system operators need tools to assess the degree and type of fouling occurring in the membrane units in order to run the system efficiently and apply effective membrane cleaning techniques. Traditionally, methods such as monitoring pressure drops, measuring fluid flux across the membrane and performing membrane autopsies have been used to monitor or determine membrane fouling. Traditional methods suffer from severe drawbacks. Monitoring pressure drops and flux decline can gauge severity of fouling but cannot determine the type. Autopsies can determine the degree and type of fouling but require the membrane to be taken offline. Autopsied membranes must also be discarded after autopsy analyses are completed. Furthermore, new high flux membranes have complicated the use of traditional methods in monitoring fouling (Tay and Song, 2005).

Monitoring Pressure Drops

Two different changes in pressure can be monitored in a membrane system. They are trans-membrane pressure (TMP) drop and feed channel pressure (FCP) drop. The TMP drop is the drop in pressure from the feed stream to the permeate stream and is created by the resistance of the membrane and any fouling layers to fluid flux through the membrane. TMP will increase under constant flux operating conditions as the membrane is fouled due to the increased resistance caused by the fouling layer. The FCP drop is the pressure drop from the feed stream to the retentate stream and is created in the feed water channel of the membrane by frictional resistance to the fluid flow by obstructions, such as feed spacers and biofilm accumulation (Vrouwenvelder et al., 2011a).

One traditional practice for monitoring membrane fouling is based on the increase of TMP at a constant flux. However, this method is not sensitive enough to detect membrane fouling early since fouling is probably well established before a change in TMP can be detected (Sim et al., 2013). Furthermore, studies have also shown that only the FCP was affected by the formation of biofilm, making TMP useless for detecting this type of fouling (Vrouwenvelder et al., 2011a).

Biofouling has been linked to an increase in FCP drop. The research performed by Vrouwenvelder et al. (2011a) indicated that an increase in the FCP drop across the lead membrane in large municipal water treatment membrane units is most likely caused by biofouling. Furthermore, they found that the use of very accurate (and expensive) differential pressure transmitters over the lead membrane detected an early increase in FCP drop resulting from biofouling. However, high concentrations of inorganics may also contribute to increased FCP drop so it is not totally indicative of biofouling (Vrouwenvelder et al., 2011a).

Monitoring Flux Across the Membrane

Since the 1960's membrane fouling was indicated or measured by a flux decline in the RO process (Kavanagh et al., 2009; Tay and Song, 2005). The premise behind using flux as a fouling indicator is that at constant salt concentration and applied pressure, any increase in overall membrane resistance due to the accumulation of a foulant on the membrane surface will result in a flux decline (Tay and Song, 2005). Flux decline was a preferred tool to assess fouling since it was non-destructive and the

membrane could remain online. Unfortunately, this method, while non-destructive, cannot be used to elicit the type of fouling present.

Measuring flux decline to indicate fouling worked well for older membranes that generally had higher resistance. This method is less effective with the newer, more permeable membranes since these new membranes can operate in two different regimes: thermodynamic equilibrium and mass transfer limited (Tay and Song, 2005). Tay and Song (2005) found that when membranes were operating in the thermodynamic equilibrium regime, resistances doubled but no significant decline in flux was detected. However, a significant decrease in flux occurred when the system began operating in the mass transfer limited regime. This method is no longer sensitive enough to detect membrane fouling early since fouling is probably well established before a decline in flux can be detected (Sim et al., 2013).

Membrane Autopsies

Membrane autopsies are a precise and accurate way to determine the type of fouling present on a membrane surface. In Flemming et al. (1997), a standard procedure to perform an autopsy was described. Essentially, to perform an autopsy, the membrane in question is removed from the process stream and opened. Representative swatches are cut from the opened membrane and a large assortment of analyses can then be performed on the swatches. Al-Juboori and Yusaf (2012) detailed and extensively listed many of the analyses that are possible on membrane samples obtained from autopsies.

While autopsies determine the extent and type of fouling, they destroy the membrane. An autopsied membrane cannot be repaired and returned to use and

therefore, must be discarded. Routine autopsies are not economical in plant operations and should only be performed in extenuating circumstances. Autopsies, however, are extremely useful laboratory tools to validate potential non-destructive methods to assess fouling (Al-Juboori and Yusaf, 2012). Vrouwenvelder et al. (2011a) extensively used autopsies to correlate sessile ATP with various operational parameters and to assess the degree of biofouling.

Non-destructive Methods to Assess Membrane Fouling

At a minimum, non-destructive methods need to determine the type of fouling present in a membrane. Ideally, these methods would be able to be performed in situ without the need to shut down membrane operations therefore increasing operation time and water production. Furthermore, an ideal non-destructive method would be able to detect and determine fouling type early to enable easy cleaning and prevent irreversible damage.

Non-destructive methods would make membrane water treatment more economical. First, membrane autopsies would only need to be performed under extenuating circumstances, thus reducing the amount of membranes needing to be replaced. Second, these non-destructive methods would enable the determination of fouling type thus giving insight to the cleaning treatment required and saving money on cleaning costs.

Currently, reliable non-destructive in situ detection of fouling remains an important research topic (Dixon et al., 2012). The next sections of this paper are devoted to some of the non-destructive methods to assess membrane biofouling that are currently

being developed and/or validated in the scientific community. All these methods have been developed with large municipal RO membrane treatment systems in mind. This means they often employ expensive instrumentation which is justifiable by the multi-million dollar price tag of these types of systems. Many of these methods are not economical for the point-of-use membrane systems though the fundamentals behind each method could possibly be applied to point-of-use systems in a more economical way. The methods for non-destructive analysis of biofouling can be broken into three general categories. These are based on feedwater properties, devices that mimic conditions inside the membrane and monitoring/detecting parameters unique to biofouling.

Methods Based on Feedwater Properties

Methods based on feedwater properties tend to be predictive in nature. It is difficult to correlate the state of membrane fouling solely from the properties of the feedwater (Hwang et al., 2012). However, they do provide important information regarding the likelihood of biofouling. This information could be useful for validating results obtained from other methods.

Assimilable Organic Carbon (AOC). AOC refers to the fraction of total organic carbon that can be utilized by defined mixtures of bacteria (Escobar and Randall, 2001). A detailed description of equipment and methodology concerning the determination of AOC as modified for use in RO feed waters are published (Eaton et al., 1998). Basically, known amounts and strains (usually 2) of bacteria native to RO feedwater are inoculated into pasteurized samples of that RO feedwater. After a week, the inoculated samples are plated each day for the next 3 days. Plates are then incubated and each bacterial strain is

counted. Knowing the bacterial concentration of each strain and its yield with respect to acetate, an AOC value can then be calculated in µg acetate as carbon per liter (Ac-C/L).

Severe biofouling was observed on membranes with feedwater that had an AOC concentration exceeding 80 µg Ac-C/L (Vrouwenvelder and van der Kooij, 2001). However, AOC was not sensitive enough to be used for an early warning of membrane biofouling (Vrouwenvelder et al., 2011b). Furthermore, AOC analysis does not produce results in a timely fashion. From the start of the analysis, at least 13 days are required before final results can be calculated. This time lag is not desirable in monitoring situations since feedwater conditions could have easily changed by the time results are ready.

Biofilm Formation Rate (BFR). The development and methodology behind assessing the BFR has been published (van der Kooij et al., 1995). Essentially, RO feedwater flows down through a vertical glass column. Inside this column are removable glass or Teflon cylinders. Over time, biofilm grows on the cylinders. At desired time points, the cylinders can be removed and the attached bacteria quantified. Final results yield an amount of biomass (normally as ATP) per unit area and time.This method is predictive for analyzing the risk of biofouling and cannot actually assess the current state of biofouling on the membrane (Kappelhof et al., 2003). It was found that severe biofouling occurred with feed water that had a BFR value exceeding 120 pgATP/cm^2·d (Vrouwenvelder and van der Kooij, 2001). However, other tests with RO feedwater showed that BFR values from the monitor were 5-100 times lower than those on the membrane (Vrouwenvelder et al., 2011a). Furthermore, it was shown that BFR was not

sensitive enough to be used for an early warning of membrane biofouling (Vrouwenvelder et al., 2011b)

Membrane Fouling Simulator (MFS)

Devices that mimic conditions inside the membrane are simplified and scaled down versions of the membranes used for production. They are constructed with the same membrane and feed channel spacer as the membrane units they are to monitor. A portion of the RO feedwater is then passed through the device and fouling progression is monitored. One such device, designed specifically to monitor biofouling is described below.

The membrane fouling simulator (MFS) is essentially a small monitoring device placed directly ahead of the main membrane units in the process stream. Several different versions of the MFS exist with each being geared for use in different circumstances. For instance, high pressure MFSs monitor flux. Lower pressure versions have a transparent window so biofouling on the feed channel spacer can easily be observed. Finally, a PVC MFS exists solely for use with nuclear magnetic resonance microscopy. Extensive development information and background research for this device can be found in Vrouwenvelder et al. (2011a).

The MFS monitors operational parameters through visual observation with the use of a sight window and through destructive sampling of the membrane coupon within the MFS (Vrouwenvelder et al., 2011b). Care must be taken to ensure conditions within the MFS are scaled to accurately mimic the conditions within the membrane the MSF is to represent. Results detailed in Vrouwenvelder et al. (2011a) showed that the MFS

mimicked biofouling conditions within the membrane well. They also showed that the MFS is a versatile device for use in research and development.

Monitoring / Detecting
Parameters Unique to Biofouling

Methods in this category involve determining and detecting parameters that are unique to biofouling. Unlike all the other types of fouling, biofouling is caused by living organisms which eat, grow, proliferate and excrete substances. If any parameters associated with these factors can be detected and/or monitored, they could be indicative of biofouling.

Specific Oxygen Consumption Rate (SOCR). Kappelhof et al. (2003) conducted research to determine if SOCR is a viable means of assessing the degree of biofouling within a membrane unit. Many microbiological activities require oxygen. By measuring the rate at which oxygen is consumed, the amount of biomass can be inferred. Generally, the greater the observed SOCR, the more biomass that exists within the system. In these experiments, SOCR was measured in the retentate stream when the membrane unit was offline. Results showed that the SOCR increased 14 days prior to an increase in normalized pressure drop (Kappelhof et al., 2003). Unfortunately, SOCR measurements can only be performed when membrane units are at a standstill (Kappelhof et al., 2003). This is detrimental for large scale reverse osmosis membrane water treatment plants because overall plant production is reduced. However, this method could be a valid method for point-of-use RO membrane units that operate intermittently.

Flow Cytometry (FCM). FCM is a technique used to rapidly and accurately count bacterial cells (Dixon et al., 2012). Bacterial cells from sampled water are dyed with a fluorescent stain and passed through the flow cytometer. The cytometer can detect and quantify the fluorescent emissions and thus a bacterial concentration can be calculated.FCM was used by Dixon et al. (2012) at a full scale reverse osmosis plant to see if it was a valid means of assessing biofouling. Their results from the FCM analysis showed large variations attributed to several operational parameters such as changing raw sea water bacterial concentrations, shock chlorination in the system and shock acidification. Furthermore, the use of FCM is limited if cells are agglomerated by extracellular polymeric substances (Dixon et al., 2012). This poses problems with the use of FCM in biofouling assessment since research found that at most, only 33% of the total effluent cells in biofouled tube reactors existed as single cells (Behnke et al., 2011). This would result in large FCM errors.

Fluorescence Spectrum-based Assessment. Research has shown that proteins and humic-like substances in extracellular polymeric substances (EPS) of biofilm can be successfully characterized through the use of fluorescence excitation emission matrices (EEMs) (Sheng and Yu, 2006). With this technique, certain molecules of the EPS re-emit absorbed light at different wavelengths and can be measured via fluorescence spectroscopy (Hwang et al., 2012). As membranes biofoul, EPS and cells slough off the membrane and may be detectable in the retentate stream with this method.

Experimentation was conducted by Hwang et al. (2012) to determine the relevance of using fluorescence spectrum-based methods to detect RO membrane

biofouling. In their experiments, a fluorescence EEM of foulants sampled from a biofouled membrane was used as a reference. EEMs of retentate samples were then compared to the reference using advanced mathematical techniques to determine the Euclidean distance between the two matrices. They proposed that the smaller the Euclidean distance between the retentate EEMs and the reference, the greater the degree of biofouling in the membrane unit.

Results detailed in Hwang et al. (2012) indicated that fluorescence spectrum-based assessment for biofouling is a promising technique. The Euclidean distance between the retentate EEMs and the reference EEM grew smaller as the membrane fouled. Retentate EEMs also showed their greatest distance from the reference after cleaning procedures were applied.

Electrical Impedance Spectroscopy (EIS). Another tool being researched for non-destructive biofouling analysis is EIS. EIS works by injecting a number of known sinusoidal alternating currents at known frequencies across the membrane surface and measuring the potential difference (voltage) across that surface including the phase difference between the voltage and current (Kavanagh et al., 2009). From this data, capacitance and conductance can be determined, and the variation of these properties with frequency can be used to determine the number of "layers" which compose the system of interest (Kavanagh et al., 2009). The data can also be displayed in Nyquist plots of imaginary impedance vs. real impedance that help to more clearly reveal the presence of various elements and processes occurring on and near the membrane surface (Sim et al., 2013).Sim et al. (2013) conducted experiments using EIS to detect fouling

caused by dosed silica and bovine serum albumin (BSA) in a membrane fouling simulator with flux. They found that the shift of the Nyquist plots for fouling with silica was very different than the shift observed with fouling by BSA. This may allow for the differentiation between organic/biofouling (simulated by the BSA) and inorganic/colloidal fouling (simulated by the silica). Under mixed fouling conditions (simultaneous dosing of silica and BSA), Sim et al. (2013) found that EIS data seemed to reflect the predominant fouling layer which is also beneficial in selecting a proper cleaning method. Furthermore, they found that EIS responded almost immediately to any changes that occurred on the membrane surface. This could enable early detection of fouling type on the membrane surface and preemptive corrective cleaning to prevent the development of severe fouling. Further development and research is needed on this promising technique.

Nuclear Magnetic Resonance (NMR) Microscopy. Significant NMR microscopy research has been performed on RO membranes (Graf von der Schulenburg et al., 2008; Pintelon et al., 2010; van Loosdrecht et al., 2012; Vrouwenvelder et al., 2011a). For these studies, the ^{1}H of water molecules was used as a passive tracer. They were able to successfully image a RO membrane in a laboratory setting and found that as biofouling progressed, a larger distribution in velocities was observed. Their finding also indicated that minimal biofouling had a substantial impact on flow field homogeneity.NMR is not without its potential problems. It can only be performed in the absence of magnetic metals which may be an issue in large scale RO membrane water treatment plants. Experimentation in Vrouwenvelder et al. (2011a) was conducted only under biofouling

conditions. Therefore, it is not clear if the other fouling types will produce similar results to those observed with biofouling. More research in this area is needed.

Methods Currently being Researched

Unilever of Hindustan, India is currently funding research at the Montana State University Center for Biofilm Engineering concerning the non-destructive assessment of biofouling in household point-of-use RO membranes. The operational environment of these membranes differs greatly from those utilized in large municipal treatment plants. Point-of-use RO membranes see intermittent use throughout the day; therefore, there are long stagnation periods where no water is flowing through the membrane. They also generate far less permeate water than the membranes used in large municipal plants. Point-of-use membranes are also scattered throughout the countryside and are relatively inexpensive, unlike the membranes used in large municipal plants which are conveniently co-located and come with a hefty price tag. That being said, sophisticated technical options for non-destructive fouling assessment are not economically relevant. Given these factors, low cost methods with the ability to determine whether biofouling or inorganic fouling was affecting the membrane were researched. These methods should also be able to be performed onsite or from samples that could be easily transported to a nearby laboratory. Some of the methods being researched are described in the following subsections.

Degree of Cell Clumping in the Retentate

Biofilm development occurs in three phases: induction, logarithmical growth and plateau (Flemming, 1997). As the biofilm grows, parts of it slough off and end up in the retentate stream. According to Flemming (1997), biofilm detachment should become more prevalent as the biofilm nears the plateau phase. Cell clumping analysis was performed using a procedure similar to that outlined in other prior research (Behnke et al., 2011; Wilson et al., 2004). Clumping analyses were performed on the retentate stream and were correlated to the actual state of membrane biofouling determined through the use of autopsies.

Cell clumping analysis has been used successfully in the past. A model predicting the rate of detachment events of a certain size was created through clumping analysis in Wilson et al. (2004). Furthermore, in Behnke et al. (2011), clump sizes and frequency of occurrence were successfully measured in biofouled tube reactors. Findings from Dixon et al. (2012) further support the use of clumping analysis since they attributed cell clumping to some of the error in their FCM analysis.

Increase of Protein and / or Carbohydrate
Concentration in the Retentate

This method employs the same biofilm fundamentals that were exploited in Hwang et al. (2012) with their fluorescence spectrum-based assessment research. Essentially, as biofilms slough, a large portion of that sloughed material is EPS, which contains proteins and carbohydrates. It was the purpose of this research to see if simpler, colorimetric methods can be used to detect an increase in retentate protein and/or

carbohydrate concentration. Collected data was correlated to the actual state of membrane fouling through the use of autopsies.

Change in Total Organic Carbon (TOC) from Retentate to Feed

This method is based on the detection of bacterial metabolic activity. It follows similar fundamental ideas to those employed by the AOC and BFR analyses. The thought is that bacteria in the biofilm will consume TOC as it passes through the feed channel of the membrane. As the amount of biofilm increases, so to should the TOC consumption. Therefore, TOC was measured in the feed and retentate streams in the hope that a net loss could be detected. It was also hoped that this loss in carbon would increase as biofouling increased. The collected data was correlated to the actual state of membrane fouling through autopsies.

Feed Channel Pressure (FCP) Drop

Biofouling has been linked to an increase in FCP drop. The research performed by Vrouwenvelder et al. (2011a) indicated that an increase in the FCP drop across the lead membrane in large municipal water treatment membrane units is most likely caused by biofouling. However, they also found that high concentrations of inorganics may also contribute to increased FCP drop so it is not totally indicative of biofouling. Perhaps, significantly greater FCP drops would be observed in membrane units suffering from biofouling. Given the previous research, this method may not be sensitive enough predict biofouling early since FCP drops have also been observed with inorganic fouling.

Difference between Retentate and Feed Biological Parameters

As stated earlier, biofilm development occurs in three phases: induction, logarithmical growth and plateau and biofilm detachment should become more prevalent as the biofilm nears the plateau phase (Flemming, 1997). As cells grow and detach from the biofilm, an increased amount of cells should be seen in the retentate compared to the feed. System operation naturally concentrates contaminates in the retentate stream due to permeate production. This concentration factor can easily be accounted for by multiplying retentate concentrations by the ratio of retentate flow to feed flow, thus allowing the difference between concentrations between streams to be analyzed. The biological parameters monitored were adenosine triphosphate (ATP), heterotrophic plate counts (HPCs) and direct cell counts.

Literature Review Summary

RO membrane treatment is a promising technology to handle future water demands and water quality requirements. However, this technology is not without its problems. One of the greatest problems encountered in RO membrane water treatment is fouling with biofouling being the predominant concern. Traditional methods to assess RO membrane fouling either cannot determine the prevalent fouling mechanism or they require destructive sampling of the membrane. Also, new high flux membranes have made early non-destructive detection of fouling by traditional methods difficult.

New and exciting techniques for the non-destructive methods targeting biofouling were reviewed. AOC and BFR are methods based on feedwater properties and are

predictive in nature. However, they tend to underestimate the actual degree of fouling within the membrane and are not sensitive enough to be used as early indicators of biofouling. The MFS is designed to mimic the fouling conditions inside a membrane. Research has shown they do this well, but the flow through the device must be scaled correctly. SOCR detected biomass growth inside the membrane two weeks before a pressure drop was detected, but it can only be performed when the system is offline. FCM was used to try to assess biofouling but suffered severely from plant operation conditions and cell clumping. Fluorescence spectrum-based assessment, EIS, and NMR microscopy all showed very promising results when it came to non-destructively assessing biofouling in the membrane. However, technical issues must be overcome before they can be implemented in full scale RO membrane treatment plants.

Research was conducted to determine non-destructive method(s) to assess biofouling in household point-of-use RO membranes. To keep the assessments economical, (these are small, inexpensive systems) technically simple and inexpensive methods were researched. Methods involved monitoring the size and frequency of cell clumps from sloughing biofilm in the retentate, monitoring for an increase of protein and/or carbohydrates in the retentate from sloughing biofilm, monitoring for consumption of TOC by organisms between the feed and retentate streams, monitoring the feed channel pressure drop and comparing the difference of biological parameters between the retentate and feed streams. Data were then compared to membrane autopsy results for confirmation of the type and extent of fouling

These methods were tested in an experimental system employing three parallel household reverse osmosis membranes. Membrane units were operated under similar conditions to those experienced in the feed. Different feed water types were employed to influence the type of fouling in each membrane unit. Parameters in the process streams were monitored as the membranes fouled under various fouling types in order to determine suitable non-destructive methods for distinguishing biofouling from inorganic fouling.

CHAPTER 3

MATERIALS AND METHODS

Experimental Design

Reactor Setup

The experimental system consisted of three parallel household reverse osmosis lines which employed the use of three major components to replicate field conditions in a laboratory setting. These components are the reverse osmosis units, the feed tanks and the dose tanks. Each reverse osmosis line had its own reverse osmosis unit and feed tank, but all three lines shared the same dosing tanks. Figure 3 displays the setup for one reverse osmosis line. To ensure consistent system operation, all system pumps were controlled by the Control Company's Traceable® Outlet Controllers (Control Company, Cat # 5090, Friendswood, Texas, USA). The controllers were calibrated bimonthly so they remained synchronized. These control units enabled system operation without the need for a technician to be present.

Reverse Osmosis Unit. A reverse osmosis unit consisted of a 75 GPD reverse osmosis (RO) membrane (DOW Filmtec, Cat # TW30-1812-75, Minneapolis, MN, USA), membrane housing, tubing and a 450 mL/min flow restrictor. Liquid-filled pressure gauges (McMaster-Carr, Cat # 3708K21, Santa Fe Springs, CA, USA) were used in conjunction with 0.008 inch orifice diameter pulsation-dampening snubbers (McMaster-Carr, Cat # 3820K27, Santa Fe Springs, CA, USA) to measure feed and

retentate stream pressures. A RO booster pump (SHURflo, Cat # 8075-142-313, Costa Mesa, CA, USA) was employed so the system operated at desired pressures.

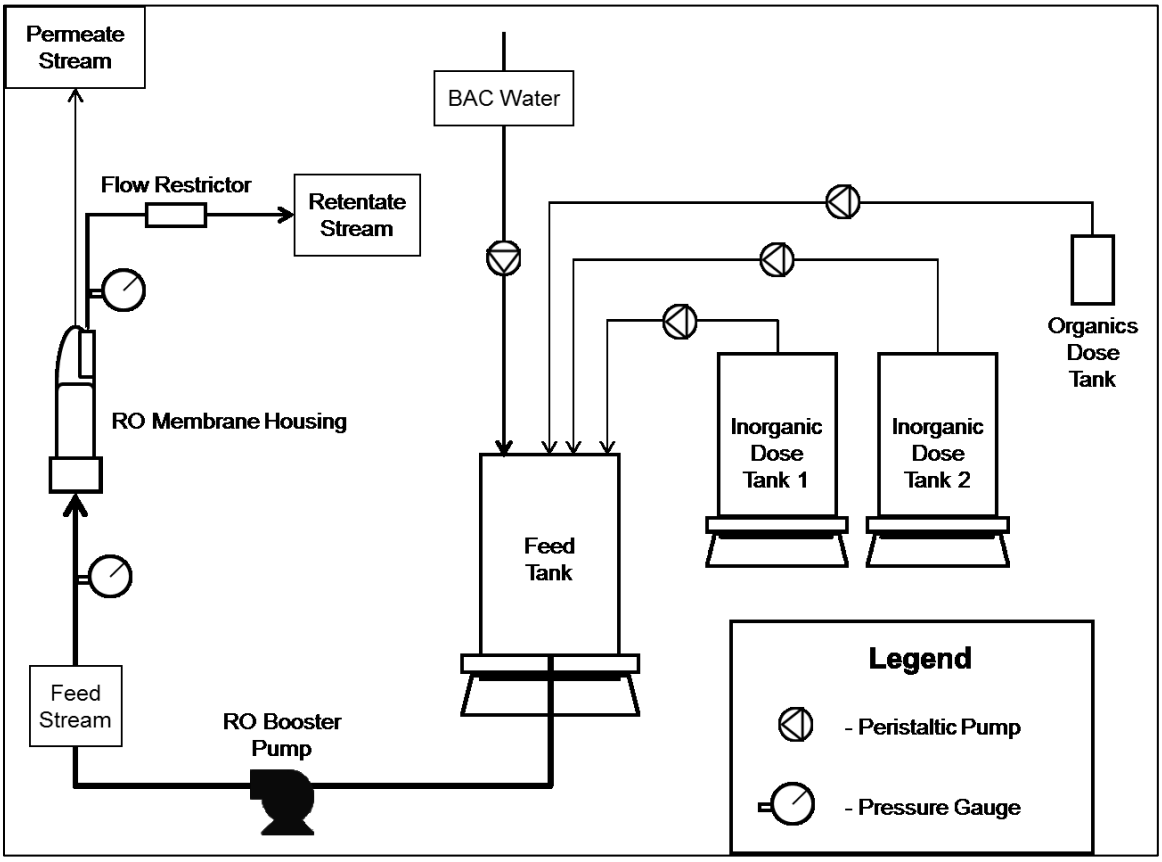

Figure 3: Process schematic for one of the three parallel RO membrane lines. The same dose tanks were used by all three RO membrane lines.

Feed Tank. Each reverse osmosis membrane line had its own feed tank. The feed tanks were 15 L Nalgene wide mouthed carboys plumbed to contain 13.8 L of feed solution. Peristaltic pumps were used to fill each feed tank by pulling water from a reservoir. This reservoir was continuously fed by Bozeman (Montana, USA) tap water which had flown through a granular activated carbon (GAC) column and a biologically activated carbon (BAC) column. These columns removed background chlorine and

carbon from the tap water and were a source of indigenous bacteria for the colonization of the membrane systems. Henceforth, this water will be referred to BAC water after the BAC column it flowed through. The feed tanks and all transparent tubing were protected from light to prevent the growth of photosynthetic organisms. The feed tanks were also continually mixed using magnetic stir plates (Barnstead/Thermolyne, Cat # 846725, Dubuque, IA, USA) to ensure uniform dispersal of dosed solutions.During Phase I, BAC water constantly flowed through each feed tank at a rate of 35 mL/min. This constant flow provided good conditions for biofilm growth and made cleaning difficult. By the end of Phase I, a visible biofilm had grown on the bottom of the tank. To combat this issue in the remaining phases, feed tanks were filled with BAC water 1.5 hours prior to each membrane run. A drain line for each feed tank was also implemented so any remaining feedwater could be removed from the feed tank via peristaltic pumps. The tanks were then rinsed with approximately 2 L of BAC water and drained three times after each run to remove any residual feed solution. Tanks were also cleaned monthly with a mild bleach solution and sponge. After cleaning, the feed tanks were thoroughly rinsed, drained and air-dried to ensure no bleach residual remained.

Dose Tanks. Desired feed solution concentrations were achieved by dosing each feed tank with solutions from three dose tanks; Organic Dose Tank, Inorganic Dose Tank 1 and Inorganic Dose Tank 2. Constituents and concentrations for each dose tank are displayed in Appendix A.The organic dose solution was replaced biweekly. During each replacement, the organic dose tank and lines were rinsed and autoclaved to ensure sterility. New organic dose solution was made from a filter sterilized 20x concentrated

organic dose solution stored at 4°C and autoclaved nano-pure water. Proper dilution was obtained with sterile measuring vessels in a laminar flow hood.

Inorganic dose solutions were changed every 2 weeks by mixing the proper constituents with nano-pure water. These constituents were separated into two different tanks to prevent precipitation of solids at the dose concentrations. The inorganic dose tanks were protected from light to prevent the growth of photosynthetic organisms.

Dosing solution was added to each feed tank from the dose tanks via peristaltic pumps. Dosing stopped 4 minutes prior to each membrane run to ensure uniform dispersion of the dosed solutions. Dosing pumps were calibrated each time the dose solution was replaced. Additionally, the inorganic dose pump performance was monitored through checking feed water conductivity.

Operational Considerations

The experimental system was designed and built so that field conditions could be modeled as closely as possible. For replicate analysis, the experimental system had three parallel reverse osmosis lines. The operational goal of the system was to generate around 10 L of permeate water per day per reverse osmosis line. Initial tests on the membrane units revealed that an operation time of 14 minutes would create 3.3 L of permeate. Running the system three times a day on eight hour intervals resulted in the targeted permeate water production.

Feed solution concentrations were chosen to provide accelerated fouling. Organic constituents were chosen to promote biofilm growth and allowed for a 100:10:1 molar carbon: nitrogen: phosphorus ratio, respectively. Inorganic constituents were chosen to

match field conditions stipulated by the project sponsor. Targeted feed concentrations were 10 ppm total organics and 500 ppm total inorganics to encourage both inorganic fouling and biofouling, 10 ppm total organics and 150 ppm inorganics (background inorganics concentration from BAC water) to promote biofouling and 0 ppm total organics and 500 ppm total inorganics to favor inorganic fouling. Table 1 and Table 2 display feed concentrations for each phase and feed constituent information, respectively. Initially, in Phase I, a feed solution of 2 ppm organic carbon and 500 ppm inorganic carbon was used. After 49 days of operation, no significant reduction in performance was detected therefore the organics concentration was raised to 10 ppm.

Table 1: An overview of experimental feed water properties and concentrations by experimental Phase.

Constituent	Phase I Before Day 49 [ppm]	Phase I Post Day 49 and Phase IV Combined [ppm]	Phase II and Phase IV Organics [g/L]	Phase III and Phase IV Inorganics [g/L]
L-Glutamic Acid	0.123	0.613	0.613	-
L-Aspartic Acid	0.139	0.693	0.693	-
L-Serine	0.146	0.729	0.729	-
L-Alanine	0.124	0.618	0.618	-
D(+)Glucose	0.125	0.625	0.625	-
D(-)Galacturonic Acid Monohydrate	0.147	0.736	0.736	-
D(+)Galactose	0.125	0.625	0.625	-
D(-)Arabinose	0.125	0.625	0.625	-
Monobasic Potassium Phosphate	0.045	0.227	0.227	-
$CaCl_2$	74.703	74.703	-	74.703
$MgCl_2*6H_2O$	43.672	43.672	-	43.672
$Al_2(SO_4)_3*16H_2O$	1.464	1.464	-	1.464
Na_2SO_4	20.195	20.195	-	20.195
$MgSO_4*7H_2O$	30.040	30.040	-	30.040
$NaHCO_3$	218.611	218.611	-	218.611
$MnSO_4*H_2O$	0.157	0.157	-	0.157
Background TDS	150	150	150	150
pH	7.80 – 7.88	7.80 – 7.88	7.41 – 8.14	8.20 – 8.32

Table 2: Reference information for feed water dosing chemicals used during analyses.

Constituent	Manufacturer	Catalog Number	Reference Information
L-Glutamic Acid	Fisher Scientific	A125-100	www.fishersci.com
L-Aspartic Acid	Sigma	A9256-100G	www.sigmaaldrich.com
L-Serine	Alfa Aesar	A11179	www.alfa.com
L-Alanine	Amresco	0106-500G	www.amresco-inc.com
D(+)Glucose	Fisher Scientific	D16-500	www.fishersci.com
D(-)Galacturonic Acid Monohydrate	Fluka	48280-25G-F	www.sigmaaldrich.com
D(+)Galactose	Alfa Aesar	A12813	www.alfa.com
D(-)Arabinose	Alfa Aesar	A10357	www.alfa.com
Monobasic Potassium Phosphate	FisherBiotech	BP362-500	www.fishersci.com
$CaCl_2$	Alfa Aesar	L13191	www.alfa.com
$MgCl_2*6H_2O$	Alfa Aesar	12288	www.alfa.com
$Al_2(SO_4)_3*16H_2O$	Sigma	A7920	www.sigmaaldrich.com
Na_2SO_4	BDH	0836-VBD-2.5KG	www.bdhme.com
$MgSO_4*7H_2O$	Alfa Aesar	A14491	www.alfa.com
$NaHCO_3$	BDH	0865-VBD-12KG	www.bdhme.com
$MnSO_4*H_2O$	Fisher Scientific	M113-500	www.fishersci.com

Analytical Methods

Operational Analytical Methods

The following sections detail the analytical procedures used to collect data during the operational portion of the experiments. This portion consisted of the time points when the reverse osmosis membranes are producing permeate water. A detailed list of analyses performed based on phase and process stream can be found in Table 3

Table 3: Operational analyses performed based on phase and sample location.

Phase	Feed Loading	Process Stream	Operational Analyses
Phase I	10 ppm Organics 500 ppm Inorganics	Feed	Pressure, ATP, HPC, Direct Counts, TOC, Conductivity,
		Retentate	Pressure, Flow, ATP, HPC, Direct Counts, Cell Clumping, TOC, Conductivity
		Permeate	Flow, ATP, HPC, Conductivity
Phase II	10 ppm Organics 150 ppm Inorganics	Feed	Pressure, ATP, HPC, Direct Counts, TOC, Conductivity, pH, Temperature
		Retentate	Pressure, Flow, ATP, HPC, Direct Counts, Cell Clumping, TOC, Conductivity, Concentrated Protein
		Permeate	Flow, ATP, HPC, TOC, Conductivity
Phase III	0 ppm Organics 500 ppm Inorganics	Feed	Pressure, ATP, HPC, Direct Counts, TOC, Conductivity, pH, Temperature
		Retentate	Pressure, Flow, ATP, HPC, Direct Counts, Cell Clumping, TOC, Conductivity
		Permeate	Flow, ATP, HPC, TOC, Conductivity
Phase IV	1 replicate of each feed loading type	Feed	Pressure, ATP, HPC, Direct Counts, Conductivity, pH, Temperature
		Retentate	Pressure, Flow, ATP, HPC, Direct Counts, Cell Clumping, Conductivity, Hydrogen Sulfide
		Permeate	Flow, ATP, HPC, Conductivity

Sampling and Nomenclature. The following procedure was used for all operational samples unless noted otherwise. Sampling was performed during the morning run. Samples from the retentate and permeate were collected in sterile test tubes directly from the outlets of their respective lines after 2 minutes of system operation to ensure that the system was operating at a pseudo steady state. Retentate stream analysis suggested a flushing effect that occurred over the first 1 minute of system operation. During this time, planktonic cells that had reproduced while the system sat stagnant were flushed from the system. Sampling at a pseudo steady state was preferred since it could be easily reproduced in the field. Samples from the feed tanks were collected via pipette and placed in sterile test tubes. Retentate and permeate samples were collected by directly filling sterile test tubes with the effluent of each line. Samples were then stored at 4°C until relevant analyses could be performed. To keep samples organized, an alphabetical and numerical nomenclature was used, for example GP071413-2. The first letter in the nomenclature determines which of the three parallel RO lines the sample came from. Each RO line was color-coded (blue, yellow, and green) during setup to ensure no false connections. The second letter in the nomenclature determines the sample location on the determined RO line. These letters were followed by the date the sample was taken and the final number denoted the sample replicate number. Table 4 cyphers the nomenclature. Thus, the aforementioned example would be the second replicate sample taken from the green line's permeate stream on July 14, 2013.

Table 4: Cypher for nomenclature used in operational analyses.

RO Line		Sample Location	
G =	Green Line	F =	Feed Water
B =	Blue Line	R =	Retentate Water
Y =	Yellow Line	P =	Permeate Water

Pressure and Flow. Pressure and flow were measured daily during each phase. Pressure was read to the nearest 0.5 psi from liquid-filled pressure gauges in conjunction with 0.008 in. orifice diameter pulsation-dampening snubbers on the feed and retentate lines. Increases in pressure indicate increased flow resistance which can be caused by the growth of fouling layers. Pressure data was normalized to the initial observed pressure drops. For trans-membrane pressure, this would be the drop of pressure from the feed to the permeate line. For feed channel pressure drop this would be the pressure drop between the feed and retentate lines. This was done by subtracting the initial calculated pressure drops from all subsequent calculated pressure drops.

Permeate and retentate flows were measured using a stopwatch and a graduated cylinder by filling the graduate cylinder with effluent from both lines for a measured period of time. Decrease in permeate flows indicate a reduction in flux across the membrane surface often caused by the increased thickness of a fouling layer. Addition of the retentate and permeate flows results in the rate at which feed water was processed. Permeate flow data was normalized by taking the ratio of the current measurement to the initial measurement (F_t/F_0).

Adenosine Triphosphate (ATP) Luminescence. ATP was monitored in the feed, retentate and permeate process streams and was used to provide measurement of the active biomass in each stream. Increased biomass in process streams could indicate biofouling. ATP analysis was done using BacTiter-Glo™ Microbial Cell Viability Assay Kit (Promega, Cat G8230, www.promega.com) and a Lumitester C-110 luminometer (Kikkoman, SN 015811, Japan). Undiluted samples were run in triplicate following a single tube method where 100 µL of suspended reagent was added to 100 µL of sample. Each tube was then shaken for 2 seconds and then incubated for 10 minutes before luminescence was recorded with the luminometer.A standard curve was run each time the ATP analysis was performed to correlate the luminometer readings to molar ATP concentrations. The standard curve was generated using 10 mM rATP (Promega, Cat # P1132, www.promega.com) using serial dilutions between 10^{-7} M and 10^{-11} M ATP. A blank solution consisting of autoclaved nano-pure water was also analyzed. All standard curve measurements were performed in triplicate.

During Phase I, ATP luminescence measurements were performed daily with one standard curve measured each week. This method was deemed inferior since it did not account for variation of the luminescence enzyme performance as it aged. For the remaining phases, ATP luminescence was performed either tri-weekly or bi-weekly with a standard curve run for each analysis.

Heterotrophic Plate Counts (HPCs). Heterotrophic organisms were monitored in the feed, retentate, and permeate streams by spread plating triplicate samples. HPCs were another method to quantify organisms in process streams. An increase of organisms

between process streams may be indicatory of biofouling. Spread plates were performed on a bi-weekly or tri-weekly basis in all phases. Samples were serially diluted in autoclaved nano-pure water so that 30-300 colonies would be produced on a single plate from 100 µL of sample. The dilution water was also plated to check for contamination issues. For initial permeate spread plates, a sample volume of 1 mL was used to attain statistically relevant counts. All spread plates were made with Difco™ R2A agar (Becton, Dickison, and Company, Cat # 218261). All samples were incubated at 28°C for 7 days before being counted on a Leica Colony Counter (Leica Inc., Buffalo, NY, USA).

Direct Counts. Direct cell counts were performed weekly on the feed and biweekly on the retentate waters. In most cases, permeate counts remained too low to be counted. Direct counts were used to quantify organisms in process streams. An increase of organisms between process streams may be indicatory of biofouling. For feed waters, 5 mL of undiluted sample was stained with LIVE/DEAD® BacLight™ Bacterial Viability Kit (Life Technologies, Cat # L7012, www.lifetechnologies.com) stains using 500 µL of a 1:150 stain solution. For the retentate, 2.5 mL of undiluted sample was stained with the same stains but 500 µL of a 1:300 stain solution was used. Later, 5 mL of retentate sample was analyzed using the same stain solution as in the feed analyses. After staining, samples were incubated for 45 minutes in the dark. All samples were filtered onto a black polycarbonate membrane (Maine Manufacturing LLC, Cat # 1215609, Sanford, ME, USA) with a 0.2 µm pore size and a 25 mm diameter. The membrane was analyzed with fluorescence microscopy using a Nikon Eclipse E800 and 100x Nikon oil emersion lens. Initially, twenty frames of reference per membrane were

analyzed. After Phase II, the imaging equipment was upgraded and thirty-five frames of reference were captured to ensure the same area was being analyzed. For each frame of reference, two images for live or dead cells were captured by using different filters. Live cells were imaged with a FITC filter at an excitation wavelength of 495 nm. Dead cells or cells with damaged membranes were imaged using a TRITC filter at an excitation wavelength of 552 nm. Images were captured using the software MetaVue® for fluorescence image capturing. The two images from the same frame of reference were combined using the color combine function found in MetaMorph® image analysis software. The color threshold function in MetaMorph® was then used to define cell areas in the image that were brighter than 55 on a scale from 0 - 255. Once thresholded, the cells with areas between 5 and 350 pixels were counted by the software. The pixel values were later adjusted to compensate for upgraded imaging equipment and to ensure consistency throughout all phases.

Cell Clumping. The color combined microscope images from the direct counts were also used to determine the extent of cell clumping in the retentate. An increase in cell clumping in the retentate could indicate sloughing of biofilm from system elements. Using MetaMorph® image analysis software's color threshold function, areas brighter than 55 on a scale from 0 - 255 were defined as cells or clumps. The software then determined the pixel area of all thresholded cell and clump areas greater than 5 pixels. All the area data for that given sample and day was exported to MS Excel® 2010 and an average cell area was determined by finding the arithmetic average of cells with pixel areas between 5 and 350 pixels. The measured cell and clump areas were divided by the

calculated average to determine the approximate number of cells per clump. The pixel values were later adjusted to compensate for upgraded imaging equipment and to ensure consistency throughout all phases.

Clump data was analyzed in three ways. The first way was to see if the percent of clump occurrences based on total occurrences increased as the system biofouled. Occurrences are individual events of single cells and clumps of a certain size range observed in the sample. For example, if a sample had 210 single cells, 20 clumps of >10 cells and 100 clumps between 2 and 10 cells, that sample would have 210 single cell occurrences, 20 occurrences of clumps of >10 cells, 100 occurrences of clumps between 2 and 10 cells, and 330 total occurrences. The second way was to compare the number of cells that existed in certain clump size ranges and single cells to the total number of cells observed in the sample. This was performed by summing all the single cells, summing all the cells that existed in the clumps between 2 and 10 cells, and summing all the cells that existed in clumps >10 cells. The sum of all the cells in those three categories resulted in the total number of cells. A percent of cells that existed in those categories was calculated as fouling progressed in the membrane. An increase in percent of cells in clumps could indicate biofilm sloughing. The third and final way was to monitor the concentration of clumps > 5 cells in the retentate stream and see if it increased as the system biofouled.

Conductivity. Conductivity was measured in the feed, retentate and permeate process streams weekly. It was used to ensure proper inorganic dosing in the feed tanks and to assess the passage of inorganics across the membrane. Conductivity was also used

to calculate total dissolved solids (TDS) in each process stream which was used to determine membrane failure through percent TDS removal. Permeate conductivity data was normalized by taking the ratio of the current measurement to the initial measurement (C_t/C_0).In Phases I and II, conductance was measured with a Traceable® automatic temperature compensating digital conductivity meter (Fisher Scientific, Cat # 967053, www.fishersci.com). Even though the meter had automatic temperature compensation, sample temperatures were still adjusted to 25°C by placing sample vials in a warm water bath before conductance was measured. Conductivity of the samples was calculating by measuring the conductance of a 0.01 M KCl standard and determining a cell constant for the conductivity meter.During Phases III and IV, conductivity was directly calculated with an Accumet AP65 portable conductivity meter (Fisher Scientific, Cat # 13-636-AP65A, www.fishersci.com) with an Accumet two cell conductivity probe 1.0 (Fisher Scientific, Cat # 13-620-168, www.fishersci.com). Sample temperatures were again adjusted to 25°C before measurements were taken. To check the accuracy of the conductivity meter, conductivity of a 0.01 M KCl solution was measured.

Additional Operational Analyses. Retentate protein quantification and total organic carbon (TOC) mass balances were also performed. These analyses proved to be not sensitive enough to provide valid data. Further information concerning the retentate protein and TOC analyses can be found in Appendix C and Appendix F, respectfully.

Membrane Autopsy Analytical Methods

Membrane autopsies were performed to determine the type and extent of fouling in every phase. The time points of the autopsies vary by phase. In Phase I and Phase IV,

all membranes were autopsied upon membrane failure. Membrane failure was defined as the time point when TDS removal dropped below ~75% and/or a ~50% reduction in permeate flow was seen. Since performance in these household systems is not extensively monitored and system maintenance is solely up to each household, it is realistic that membrane units are run to this degree of failure. In Phase II and Phase III membrane autopsies were performed when a membrane replicate achieved a set parameter milestone. In this case the milestones were 1/3 of the predicted maximum increase in trans-membrane pressure, 2/3 the predicted maximum increase in trans-membrane pressure and membrane failure. Maximum increase of trans-membrane pressure was predicted by subtracting the initial trans-membrane pressure from the maximum pressure of the RO booster pump.

A variety of analyses were performed during autopsy. Sessile ATP, HPCs, direct counts, protein and carbohydrates were used to quantify the amount of biomass on the membrane surface. Sessile spacer ATP was used to compare the amount of active biomass that had accumulated on the feed channel spacer between Phases III and IV. Sessile calcium was used in Phase IV to determine the presence of calcium carbonate scale on the membrane surface. Focus emission scanning electron microscopy (FESEM) and cryo sectioning were used to visualize membrane foulants. FESEM enabled visualization of the surface of the foulant while cryo section enabled analysis of the profile of the foulant.

The experimental membranes had an active surface area (area where flux was possible) of 4,800 cm^2. The assays measuring sessile quantities of ATP, HPCs, direct

counts, protein, carbohydrates, and calcium carbonate used membrane swatch sizes of 36 cm^2 at 3 sample locations for a total of 108 cm^2. These assays analyzed 2.2% of the active membrane surface.

Sampling and Sample Preparation. The following procedures were used during membrane autopsies unless noted otherwise. During an autopsy, each membrane was carefully cut open and unrolled. A sterile scalpel was then used to cut out membrane swatches of a desired size from selected areas of the membrane surface. Permeate and retentate flow spacers were not included in the membrane sample. Table 5 shows a list of analyses performed and the required sample preparations.

Membrane swatches were then transferred to sterile petri plates with sterile forceps. Autopsy utensils were sterilized by soaking in a 75% ethanol solution for at least 1 minute. Utensils were then flamed to remove any residual ethanol prior to use. Ten milliliters of autoclaved nano-pure water was added to the petri plate and the fouled membrane surface was scraped with a sterile policeman to dislodge any attached biofilm. Scraped swatches were rinsed with a portion of the water in the petri plate via pipette. Following rinsing, the sample water was transferred from the petri plate to a labeled sterile sample vial via pipette. Sample vials were vortexed with a Vortex-Genie 2 (Scientific Industries, Model # G-560, Bohemia, NY, USA) intermittently for 30 seconds at speed setting 9. Sample vials where stored on ice or at 4°C until analyses could be performed.

Table 5: Sample size and preparation for autopsy analyses.

Analysis	Swatch Area [cm^2]	Sample Preparation
Sessile ATP	36	Scraped in 10 mL autoclaved nano-pure water
Sessile HPC	36	Scraped in 10 mL autoclaved nano-pure water
Sessile Direct Counts	36	Scraped in 10 mL autoclaved nano-pure water
Sessile Protein	36	Scraped in 10 mL autoclaved nano-pure water
Sessile Carbohydrates	36	Scraped in 10 mL autoclaved nano-pure water
Sessile Spacer ATP	16	Scraped in 10 mL autoclaved nano-pure water and vortexed thoroughly with mesh
Calcium Carbonate	36	None
FESEM	1	Air dried and iridium coated
Cryo Sectioning	1	Stained and incased in OTC

During autopsies in Phase III and Phase IV, a portion of the scraped sample was aliquotted to be homogenized for a comparison study between homogenized and non-homogenized samples. Samples were prepared using a homogenizer (IKA, Model # T25S1, Staufen im Breisgau, Germany) for 30s at 20,500 rpm. Between samples, the homogenization probe was cleaned by homogenization of a 70% ethanol solution and sterile water. See Appendix B for more detailed methods and results of the comparison study.

Phase III and Phase IV also saw the analysis of the membrane feed channel spacer. A 4 cm x 4 cm square was cut from the spacer mesh over the same areas where membrane swatches were cut with a sterile scalpel. The spacer sample was then transferred to sterile petri plate with sterile forceps. Autopsy utensils were sterilized by soaking in a 75% ethanol solution for at least 1 minute. Utensils were then flamed to remove any residual ethanol prior to use. Ten milliliters of autoclaved nano-pure water

was added to the petri plate and the spacer mesh was thoroughly scraped with a sterile policeman to dislodge any attached biofilm. The sample water and spacer swatch were transferred from the petri plate to a labeled sterile sample vial via pipette and forceps, respectively. The sample vial was vortexed with a Vortex-Genie 2 (Scientific Industries, Model # G-560, Bohemia, NY, USA) intermittently for 30 seconds at speed setting 9. Sample vials where stored on ice or at 4°C until analyses could be performed.

Control Preparation. During each autopsy, swatches of new membrane were used for background concentration controls in the following autopsy analyses: sessile carbon, sessile carbohydrates and sessile protein. These swatches required their own special preparation since they are covered with chemicals to help preserve the membrane surface during storage. To remove these chemicals, membrane swatches were submerged in boiling nano-pure water for 10 minutes. Upon removal from the boiling water, the swatches where rinsed with nano-pure water and then stored in a sterile container at 4°C until use. Prior to use, they were rinsed again with nano-pure water.

Sample Nomenclature. To keep samples organized, they were labeled based on a letter and number nomenclature, for example G2-101113. The letter stands for which one of the three parallel membranes the sample was taken. This lettering is identical to that displayed in Table 4. The letter was followed by a number which indicates the distance along the feed channel in the direction of flow where the samples were taken. The number 1 indicated a sample location at the front of the membrane, 2 indicted a sample location at the center of the membrane and 3 indicated a sample location at the end of the membrane. The sample location is still considered random since samples with the same

number tag were not taken at the exact location across all the autopsied membranes. The sample location indicator was followed by a dash and then the date the sample was taken. Therefore the example sample would have been taken from the green line membrane, at the center of the membrane on October 11, 2013.

Sessile Carbohydrates. The phenol-sulfuric acid method was used to determine the concentration of sessile carbohydrates which is indicative of biomass on the membrane surface. 200 µL of 5% w/v phenol solution (Ricca Chemical Company, Cat # 5738-16, riccachemical.com) was added to 200 µL of sample in a clean glass test tube. One milliliter of concentrated sulfuric acid (Fisher Scientific, Cat # A300-S212, www.fishersci.com) was rapidly and directly added to the mixed sample solution. Samples stood for 10 min prior to being shaken rigorously. The samples stood for another 30 min and were transferred to disposable cuvettes (VWR, Cat # 97000-586, us.vwr.com) before absorbance was measured at 490 nm using a Genesys 10uv Scanning spectrophotometer (Thermo Scientific, SN 2LGN161001, Madison, WI, USA). A standard curve was created by using D-glucose (Fisher Scientific, Cat # D16-500, www.fishersci.com). All samples and standards were run in triplicate.

Sessile Protein. Sessile protein concentrations were determined using a Coomassie Plus (Bradford) Assay Kit (Pierce Biotechnology, Cat # 23236, www.thermoscientific.com/pierce). Sessile protein is indicatory of biomass on the membrane surface. The kit's Micro Test Tube Protocol was exactly followed. Standards were made following kit procedure and using bovine serum albumin (Pierce Biotechnology, Cat # 23209, www.thermoscientific.com/pierce). Mixed

samples/standards and reagents were transferred to disposable cuvettes (VWR, Cat # 97000-586, us.vwr.com) and absorbance was read at 595 nm with a Genesys 10uv scanning spectrophotometer (Thermo Scientific, SN 2LGN161001, Madison, WI, USA). All samples and standards were run in triplicate.

Focus Emission Scanning Electron Microscopy (FESEM). FESEM was used to visualize the degree and type of foulant on the membrane surface. A 1 cm x 1 cm swatch was carefully cut from the membrane and placed in a sterile petri plate with a forceps. Care was taking to minimize any possible damage to the membrane surface. Samples were air dried and stored at 4°C. Just prior to analysis, samples were prepped using a sputter coater (Emitech, Model # K575X, www.quorumtech.com) with an iridium target. Images were captured with a Zeiss Surpa 55VP using secondary electron imaging (SEI). Images were acquired at 500X and 4000X magnification for every sample.

Cryo Sectioning. Cryo sectioning was used to analyze the thickness of the fouling layer on the membrane surface. A 1 cm x 1 cm swatch was carefully cut from the membrane and placed in a sterile petri plate on a piece of filter paper dampened by sterile nano-pure water. A 1.5μL/mL LIVE/DEAD® BacLight™ Bacterial Viability Kit (Life Technologies, Cat # L7012, www.lifetechnologies.com) stain solution was created using filter sterilized reverse osmosis water and 200 μL of this stock stain solution was gently pipetted onto the fouled surface of the membrane swatch. Swatches were incubated for one hour in the dark. Residual stain solution was removed by gently rinsing the sample with filter sterilized reverse osmosis water. Rinsed samples were placed on dry filter paper in sterile petri plates to remove any excess water prior to freezing. Tissue Tek

O.C.T. compound (Sakura Finetek, Cat # 4583, Torrance, CA, USA) and dry ice were used to encapsulate the swatch. The O.C.T. compound was first placed on the fouled side of the swatch and allowed to freeze. Next, a sharp scalpel was used to peel off the support layer of the membrane thereby significantly reducing the thickness of the membrane. Finally, the back of the swatch was covered with the O.C.T. compound and allowed to freeze. Samples were labeled and stored at -60°C until cryo sectioning and microscopy could be performed.

Cryo sectioning was performed with a Leica CM1850 cryostat (Lieca Inc, Buffalo Grove, IL USA). A 5µm slice thickness was used. Sliced sections were mounted on Superfrost™ Plus slides (VWR, Cat # 48311-703, us.vwr.com). Sections were imaged using a Nikon Eclipse E800 and a 20x Nikon or 40x Nikon lenses. Images were captured using the software MetaVue® for fluorescence image capturing. Image analysis was performed using MetaMorph® image analysis software. Image pixels were calibrated to actual distance in µm using the calibrate distances function under the measure menu. Distance calibrations were performed earlier by imaging a micrometer under the relevant objective magnifications and measuring the amount of pixels in 1 µm. Distances were measured by drawing lines using the single lines tool provided in the regions tools located under the regions menu.

Sessile Calcium. Sessile calcium was used to detect the presence of deposited calcium carbonate on the membrane surface which is indicatory of inorganic fouling. Calcium analysis began by cutting 6 cm x 6 cm swatches from the membrane and placing them in sterile petri plates. A 10% hydrochloric acid (HCl) solution with a pH of 0.7 was

dripped onto each swatch with a pipette. Swatches were carefully observed for the presence of bubbling within the HCl solution. If bubbles were observed, scaled calcium carbonate was present.

Other Autopsy Analyses. Sessile ATP, HPCs and direct counts were performed during autopsy in order to quantify active organisms on the membrane surface which was used to assess the degree of biofouling. These analyses followed the same procedures detailed in the operational analytical methods section of this chapter.Statistical Analysis

Statistical models were run to determine if the differences in measured operational parameters were significantly different between feed types. The operational data for each line was truncated at the point where membrane failure occurred. This was done so any trailing data would not impact the models. On certain data sets, Log_{10} transforms were performed to linearize the data i.e. retentate cell clumping and HPCs. The models specifically compared the significance of interactions between the feed types and the monitored parameter that was analyzed.

Using the statistical software package Minitab^{TM} v. 17, general linear models (GLMs) were created to assess the relationships between trans-membrane pressure drop and the potential non-destructive analysis parameter of interest which was differentiated by feed type. General linear models are a type of regression analysis where certain factors are either considered fixed or random. In this study, feed type was considered a fix factor. Each individual membrane analyzed was given its own unique reactor code. This reactor code was used as a random effect that was nested within feed type. Residual

plots and histograms were also created for each model to ensure that the datasets met the assumptions associated with the GLM and ANOVA analysis

Trans-membrane pressure drop was chosen to be the response for the GLM because it is a good assessment of the degree of membrane fouling. As fouling layers develop, the resistance to fluid flux across the membrane increase. To overcome this increased resistance, the TMP drop must also increase. Feed type was used as a fixed effect factor in the GLMs. Feed type is the only factor in the experiment that was controlled. Comparing autopsy data with the feed types, it was determined that biofouling was present in the combined and organic feed types but not observed in the inorganics feed type which made feed type a good indicator for type of fouling present. The hypothesized indicatory parameters were treated as covariates in the GLM.

ANOVAs were performed on the GLMs using the combined and inorganic feed types as baselines for comparisons. The significance of interaction between the feed type and covariate were of the most interest. The interaction represents the slope of the regression line and was the best way to differentiate between the observed trends in operation data based on feed type which is a good descriptor of the type of fouling occurring within the membrane. If the interactions in organics and combined line were significantly different, a p value ≤ 0.05, from the inorganics the tested parameter was determined to be a promising non-destructive indicator of biofouling.

CHAPTER 4

EXPERIMENTAL RESULTS

Phase I Results

The goal of Phase I was to fail the RO membranes through combined inorganic fouling and biofouling. Furthermore, it was also used to pilot the experimental system and determine estimated experimental lengths. Initially, a feed solution of 2 ppm organics and 500 ppm inorganics was fed through the three parallel RO membrane lines (line 1, line 2 and line 3). After 49 days (roughly 1500 L feed passed), the organics concentration was increased to 10 ppm to decrease the time to system failure. All three membrane lines were run to failure. Membrane failure was defined as the time point when TDS removal dropped below ~75% and/or a ~50% reduction in permeate flow was seen. On average, the membranes operated for 94 days passing around 2,800 L of feed water before failure as seen in Figure 4. After every line was determined to have reached failure, membranes were removed from their housings and autopsied.

Phase I Operational Data

All results are normalized by an accumulated volume of feed water passed through the membrane. This volume was found by taking the run time and multiplying it by the measured flow rate. On days when flow rates were not measured (weekends and holidays), the measured flow rates from the day prior and the day after the break were averaged. That averaged value was then used to calculate a volume of feed water.

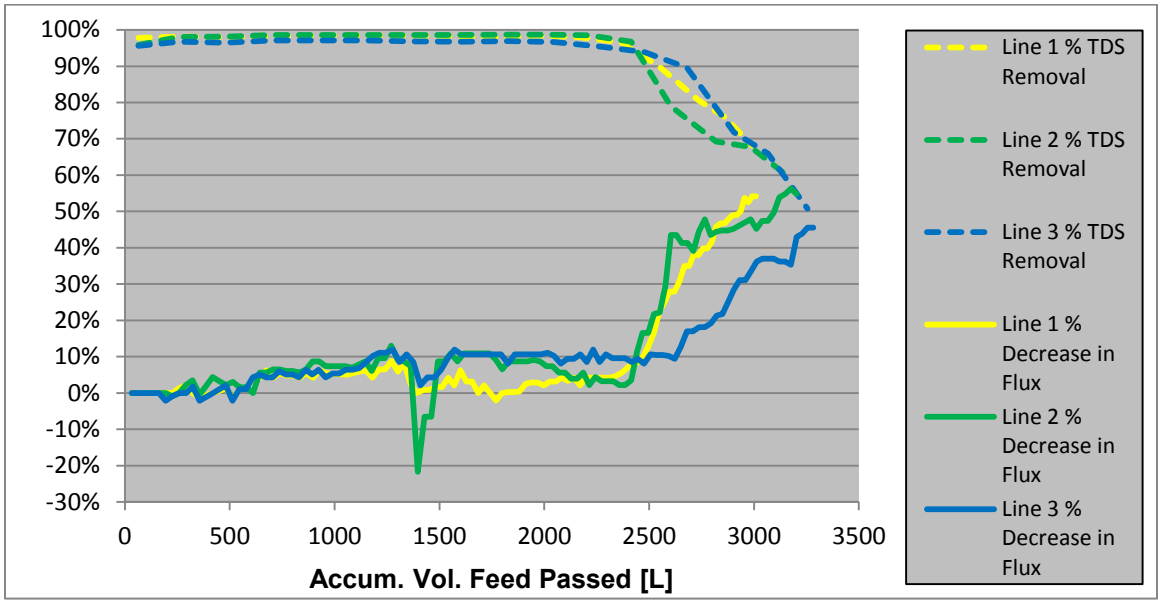

Figure 4: Progression of Phase I fouling indicators.

System Operation. During Phase I, feed tanks were constantly filled with BAC water at the rate of 35 mL/min. The wet environment and residual organics concentration within the tank provided an ideal environment for biofilm growth. By the end of Phase I, a visible biofilm had grown on the bottom of the tanks. To combat this issue in the remaining phases, feed tanks were filled with BAC water 1.5 hours prior to each membrane run and rinsed and drained after each membrane run.

Pressure and Flow. Trans-membrane pressure drop, the change of pressure from the feed line to the permeate line, increased at a constant rate for all three lines during the first 1,000 L of feed water passed. After this point, the rate of trans-membrane pressure drop increased dramatically for line 1. Trans-membrane pressure drop rates in lines 2 and 3 increased to a similar rate observed in line 1 after the increase of the feed water

organics concentrations. Trans-membrane pressure plateaued when the maximum pump head of the RO booster pumps was achieved.

No noticeable increase in feed channel pressure drop was observed during the initial 49 days of the experiment. Upon the increase of the organics concentration in the feed water, an increase in feed channel pressure drop was observed as displayed in Figure 5. Feed channel pressure drop increased to a maximum of 6 psi in line 1, 7 psi in line 2 and 4 psi in line 3.

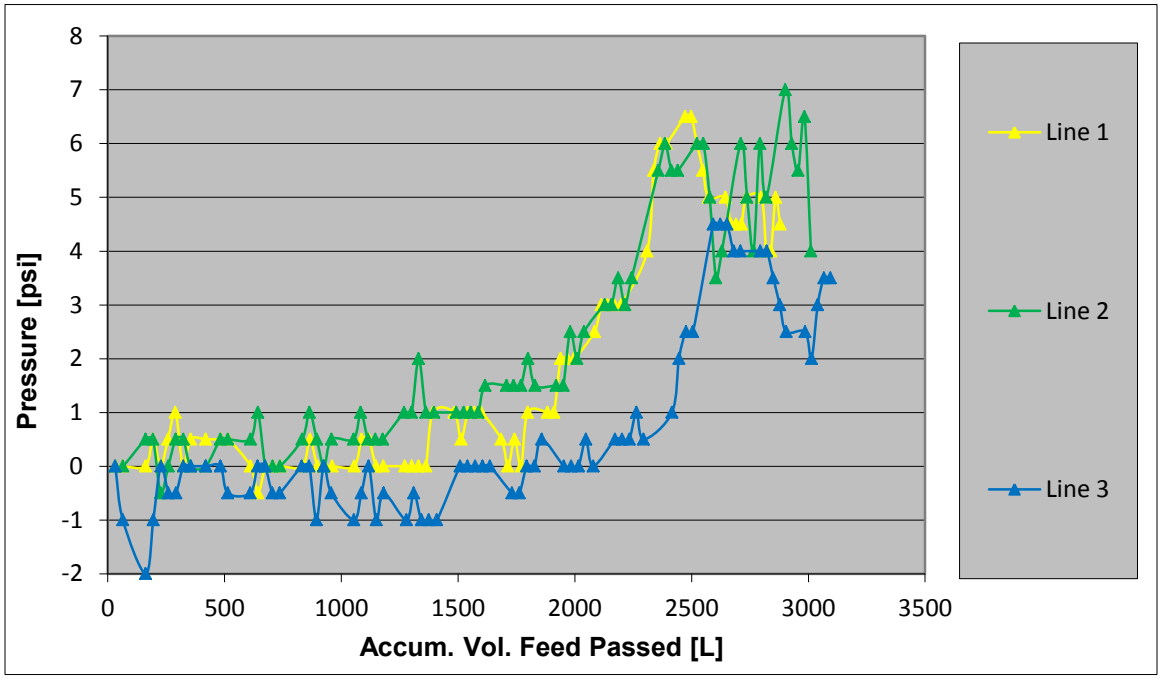

Figure 5: The increase in the feed channel pressure drop over the duration of Phase I.

Permeate flow rates remained constant for all three lines until about 2,500 L of feed water passed. At this point, permeate flows began to decline at different rates for all three lines. Retentate flow rate data showed more variability than that of the permeate. Retentate flow rates were consistent for all three lines until 1,100 L of feed water passed.

At this point, the retentate flow rates diverged for all three lines with no consistent trends. Flow data is displayed in Figure 6.

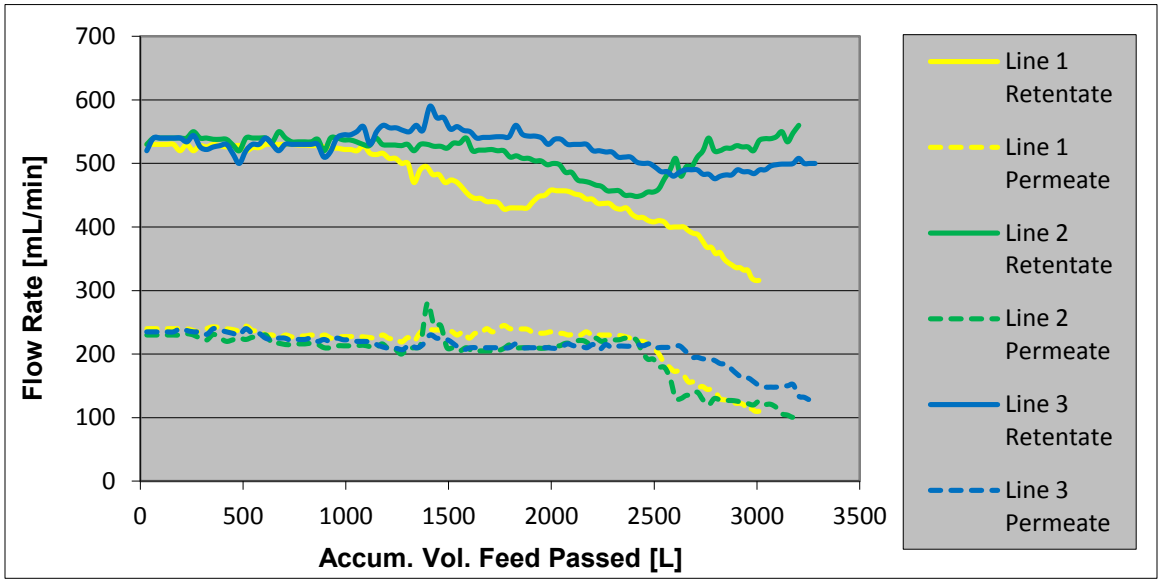

Figure 6: Retentate and permeate flow rates during Phase I.

ATP Luminescence. Feed and retentate ATP values were compared to each other by subtracting feed ATP from adjusted retentate ATP. Results from this analysis are displayed in Figure 7. During the first 1,500 L of feed water passed (first 49 days of operation), feed and retentate values were similar. A large spike in feed water ATP can be seen around 2,000 L of feed water passed in lines 2 and 3. Just prior to 2,500 L of feed water passed, more ATP is detected in the retentate than in the feed for all three experimental lines.

Permeate ATP remained around the limits of detection until near the end of the experiment and then increased rapidly in lines 2 and 3. Line 1 permeate ATP did not show a significant increase during the experiment.

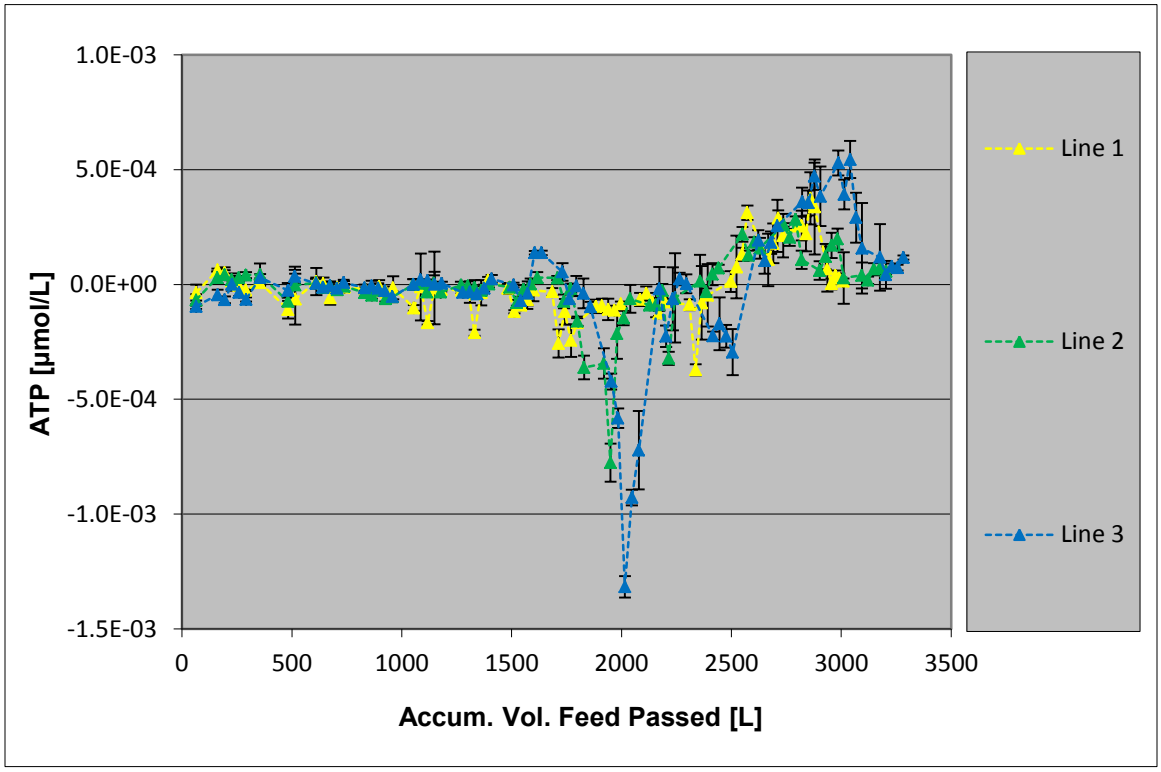

Figure 7: Difference between retentate and feed ATP (adjusted retentate ATP – feed ATP) during Phase I.

HPCs. The difference between the retentate and feed HPCs (adjusted retentate HPCs – feed HPCs) is displayed in Figure 8. The difference oscillated around negative 0.25 Log_{10}(CFU/mL) for the first 1,500 L of feed water passed. A large spike in HPC counts in the retentate was observed after 1,500 L feed water passed. Another spike in retentate HPCs was observed around 2,500 L of feed water passed.

HPCs in the permeate began to increase shortly after raising the organics in the feed water. An exponential increase in the permeate counts was observed for all three lines, followed by a decrease in the counts in all lines near the end of the experiment.

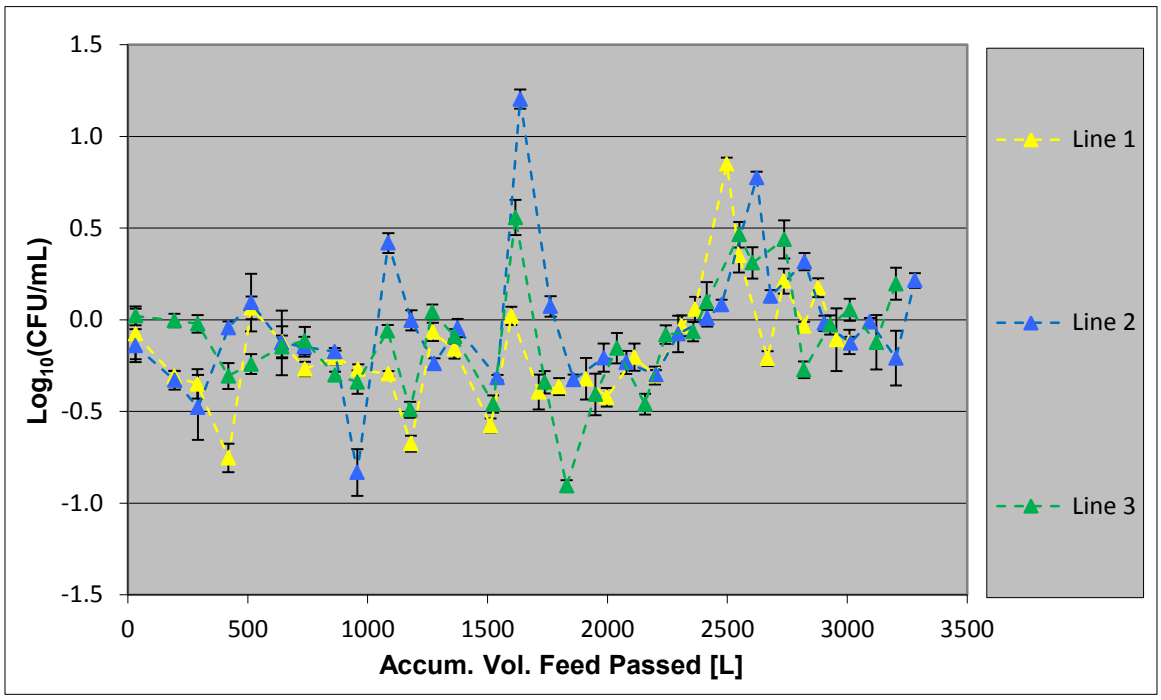

Figure 8: Difference between retentate and feed HPCs (adjusted retentate HPCs – feed HPCs) during Phase I.

The proportions of different colony types also changed as the system aged. Most notable was the appearance of black fuzzy colonies (most likely mold) near the end of Phase I that became more numerous at the time of shut-down.

Direct Counts. Direct microscopy counts of the feed remained fairly constant throughout Phase I near 1.00E+05 cells/mL. Direct counts in the retentate were of the same order of magnitude as those observed in the feed water during the first 2,300 L of feed water passed. After that point, direct counts in the retentate increased by an order of magnitude to 1.00E+06 cells/mL for all lines. Direct counts were not performed in the permeate since they were too low to count.

Cell Clumping. Cell clumping analysis was performed in the retentate streams of each RO line. Three types of clumping analyses were performed: clumping based on percent total occurrences, clumping based on percent of total cells and concentration of clumps greater than 5 cells. No increases were observed based on percent occurrences. Single cells were around 78% of total occurrences while clumps between 2 to 10 cells and clumps >10 cells remained around 21% and 1%, respectively. Distributions based on percent total cells exhibited a great deal of variation. In general no increasing trend was noticed. Single cells made up about 43% of total cells on average. However, the concentration of clumps > 5 cells began to dramatically increase after 2,500 L feed water passed. Lines 2 and 3 had a maximum of 50,000 clumps/mL while line 1 had a maximum of 25,000 clumps/mL. Clump concentration data is displayed in Figure 9.

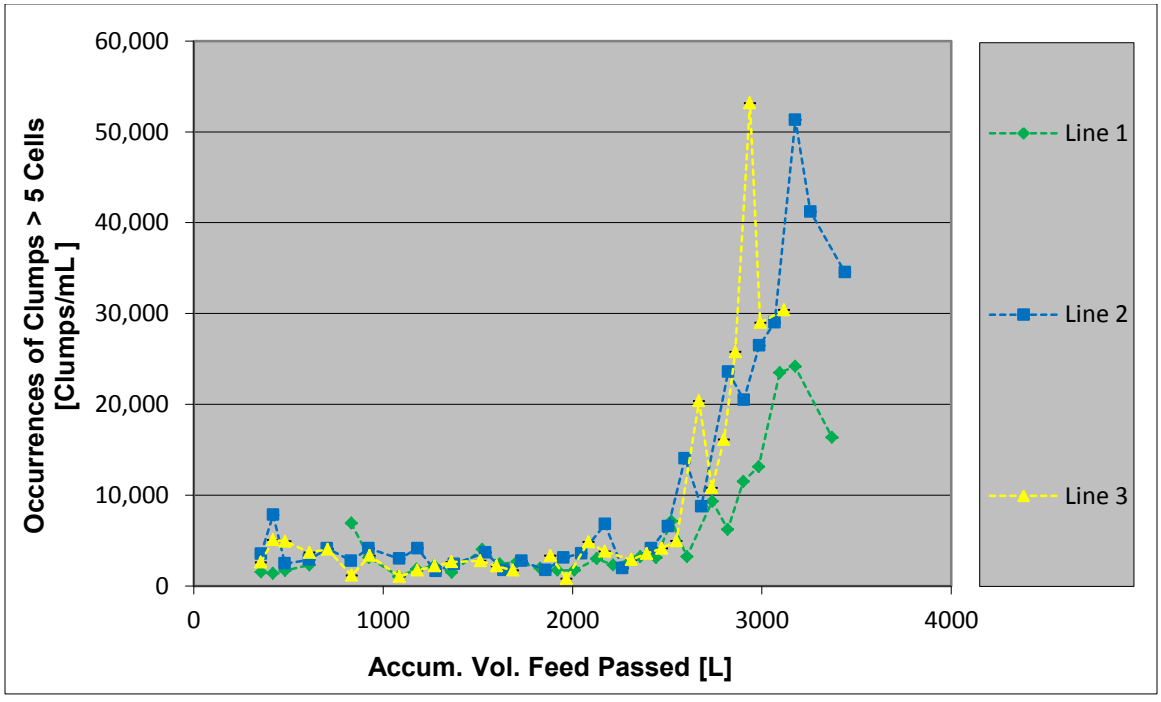

Figure 9: Retentate cell clumping throughout the duration of Phase I. All lines were combined loaded.

Conductivity. The measured conductivity in the feed water was consistent throughout the experiment excluding the one point when one of the inorganic dose pumps failed in the line 2. Retentate conductivity remained constant until the membranes began to fail. Conductivity in the permeate remained constant until around 2,500 L of feed water passed and then increased rapidly. Results from the conductivity analysis are displayed in Figure 10

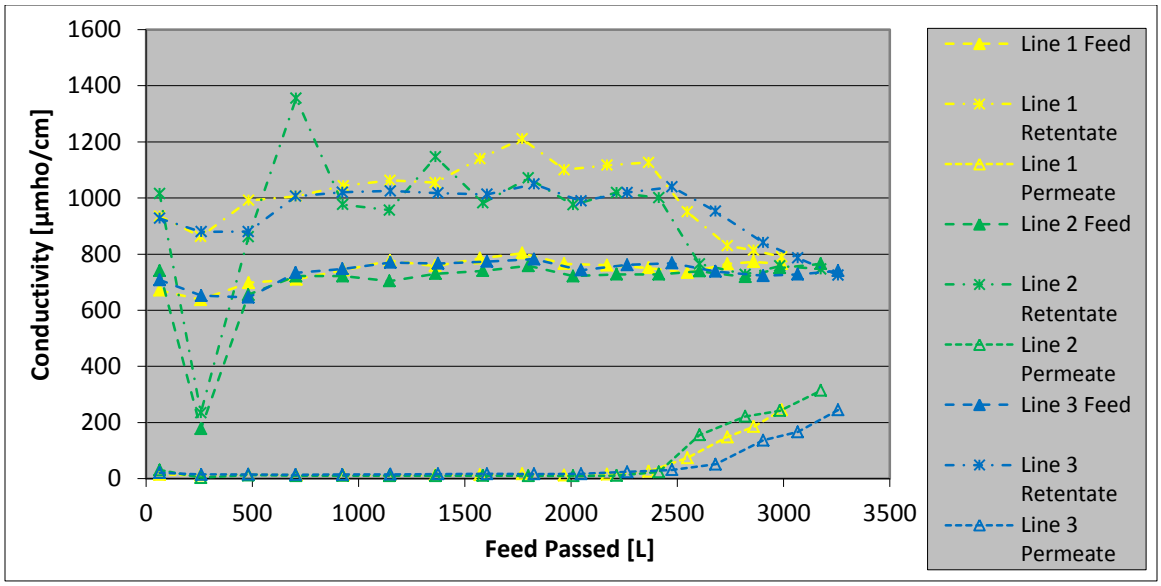

Figure 10: Change in conductivity throughout the progression of Phase I.

Phase I Autopsy Data

Phase I consisted of running three parallel RO lines until failure. Upon membrane failure, the membranes were autopsied to determine the type and extent of fouling. Results from all membrane autopsy analysis are shown below in Table 6. The results of the analysis indicate variability across the membrane. This variability can also be seen directly from the samples themselves as seen in Figure 11.

Table 6: Summary of Phase I autopsy data. Sample nomenclature is as follows (line # - sample location). Sample location 1 was at the beginning of the feed channel where feed water entered the membrane. Sample location 2 was at the center of the membrane. Sample location 3 was at the extreme end of the feed channel where retentate water exited the membrane.

Sample	Day Sacrificed	Analysis				
		ATP [µmol/cm^2]	HPC [CFU/cm^2]	Direct Counts [Cells/cm^2]	Carbo-hydrates [mg/cm^2]	Protein [µg/cm^2]
1-1	107	6.42E-05	7.12E+07	2.43E+07	4.66E-02	1.54E+01
1-2	107	3.90E-05	1.24E+07	2.84E+07	5.18E-02	2.06E+01
1-3	107	5.09E-05	1.33E+06	4.69E+07	N/A	2.41E+01
2-1	107	1.97E-05	2.76E+06	1.26E+07	3.94E-02	1.79E+01
2-2	107	6.70E-05	9.52E+06	1.73E+07	6.07E-02	2.81E+01
2-3	107	1.03E-04	5.16E+07	1.57E+07	N/A	2.38E+01
3-1	107	6.96E-05	3.77E+07	9.71E+07	3.81E-02	1.84E+01
3-2	107	9.43E-05	6.86E+07	9.40E+07	8.43E-02	2.19E+01
3-3	107	1.03E-04	7.63E+07	3.99E+07	N/A	3.60E+01

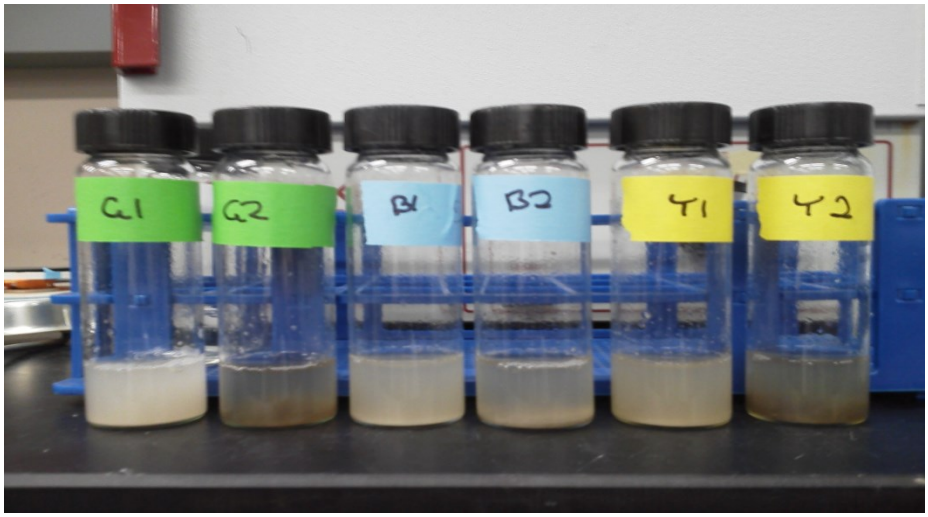

Figure 11: Scraped samples from the Phase I autopsies. A great deal of sample variance was observed across different locations on the same membranes.

Results from the autopsy analysis revealed that similar quantities of the analyzed parameters existed on all three experimental membranes. The membrane of line 3 had the highest amounts of sessile materials (ATP, HPCs, direct counts, carbohydrates and protein), though these amounts remained in the same order of magnitude as those observed on the other membranes (line 1 and 2).

Biofilm Indicators. Membrane surfaces had a high degree of sessile protein, and carbohydrates, averaging 2.29E+01 μg/cm^2 and 5.35E-02 mg/cm^2, respectively. This is indicative of bacteria and extra polymeric substance (EPS) from biofilm formation. Biofilm was also clearly visible on the membrane surface as seen in Figure 12.

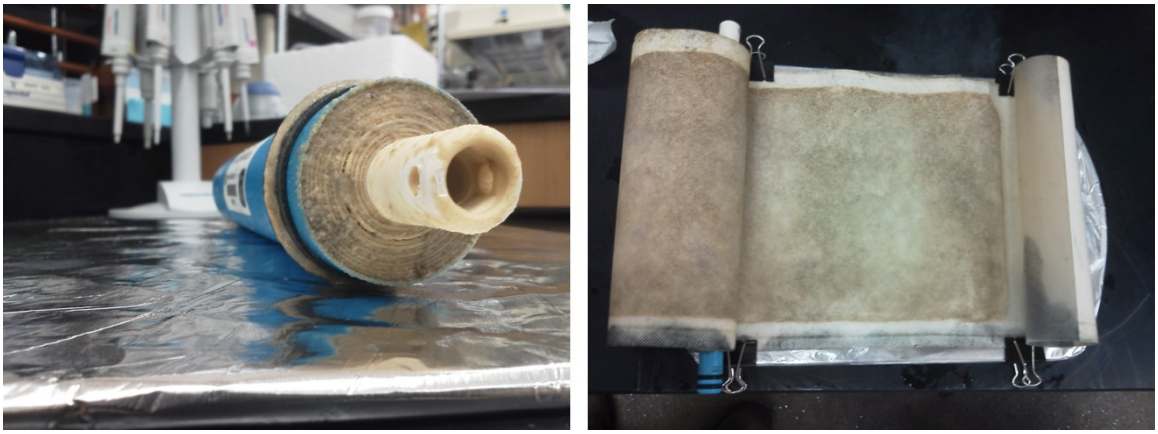

Figure 12: Phase I final autopsy images. Left – The lead face of the membrane element. Biomass is clearly visible on the brine seal and forward faces of the element. Right – Fouling on the membrane surface is clearly visible. The lighter areas along the edges are areas where no flux occurs. Flow direction is downward on the page.

Sessile ATP in Phase I had an average value of 6.79E-05 μmol/cm^2. This is the lowest value out of all the other membrane autopsies that occurred upon membrane failure for membranes that were fed a feed solution with 10 ppm organics. However, this

was still 10 times greater than the highest average sessile ATP value achieved at membrane failure from a membrane fed a feed solution with only inorganics (Phases III and IV).

FESEM. During Phase I, FESEM images were taken of the unused membrane control (Figure 13 and Figure 14) and the fouled membranes of all three lines after failure. FESEM images clearly showed large crystalline deposits on the membrane surface (Figure 15). In fact, Phase I had the largest crystalline deposits out of all the phases. Evidence of biofilm formation can also be seen in the FESEM images as string-like formations draped across the crystalline deposits. Individual cells can be seen upon closer inspection of Figure 16.

Autopsy Summary. Autopsy evidence suggests that combined inorganic fouling and biofouling was achieved during Phase I. This conclusion is supported through the FESEM images, the high sessile ATP values and the presence of sessile protein and carbohydrates.

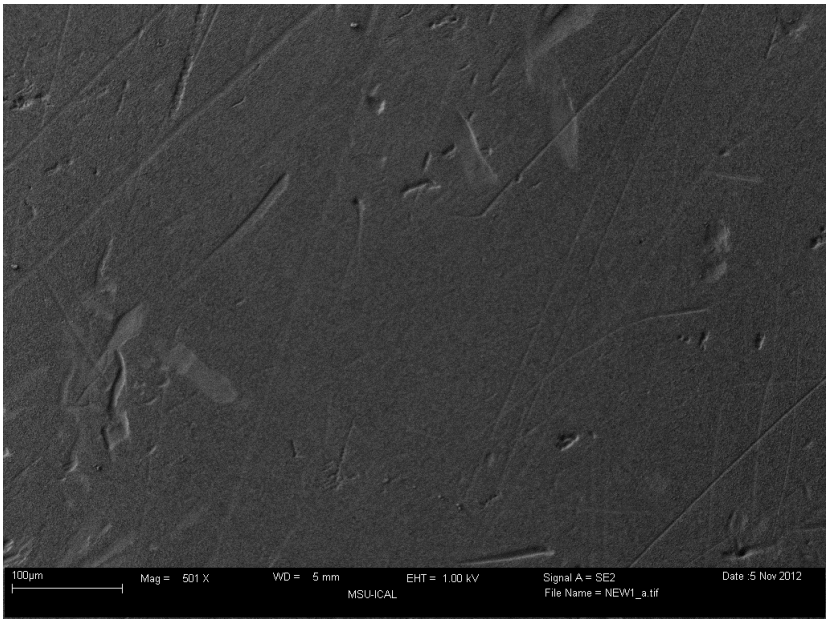

Figure 13: FESEM image of an unused membrane at 501 X magnification.

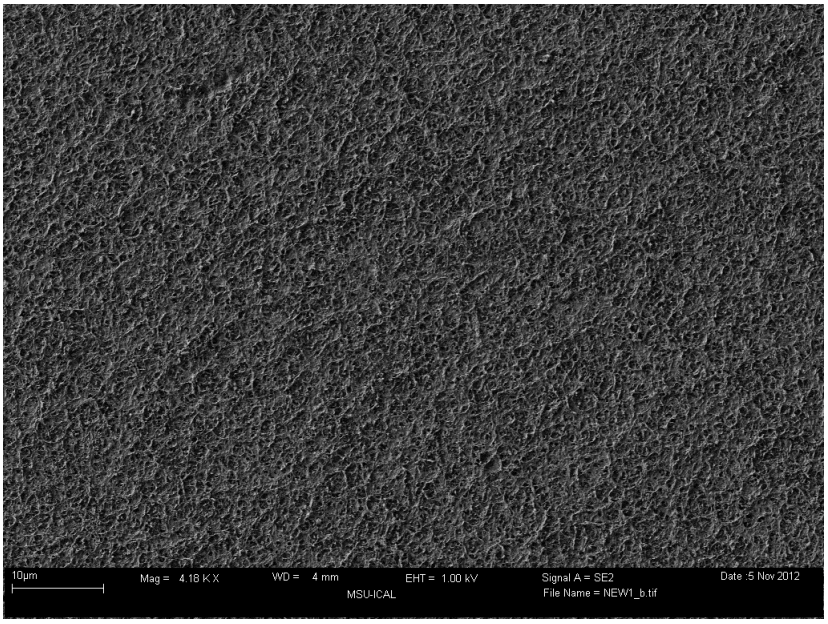

Figure 14: FESEM image of an unused membrane at 4.18 kX magnification taken during Phase I.

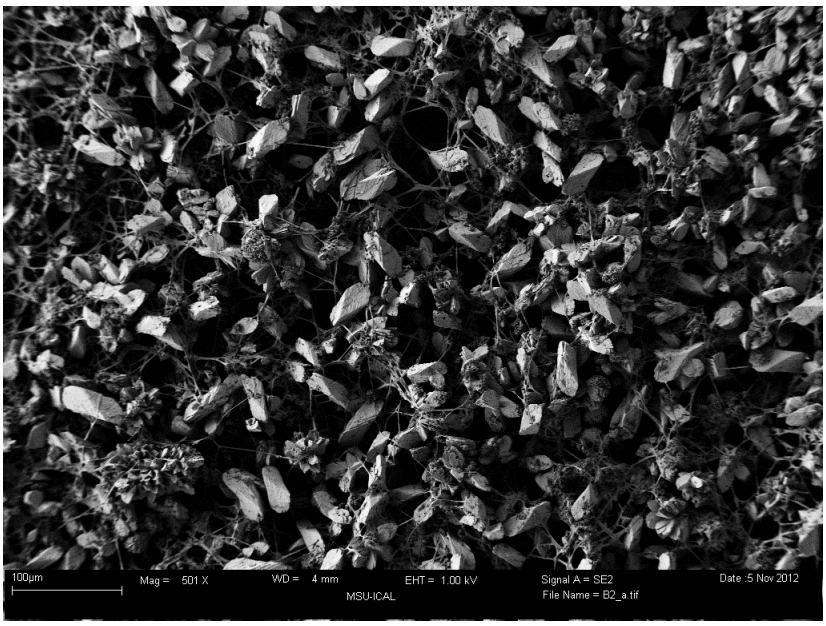

Figure 15: FESEM at 501 X magnification of the line 3 membrane after failure. Note the degree of scaling in the image which was the most severe out of all the other phases.

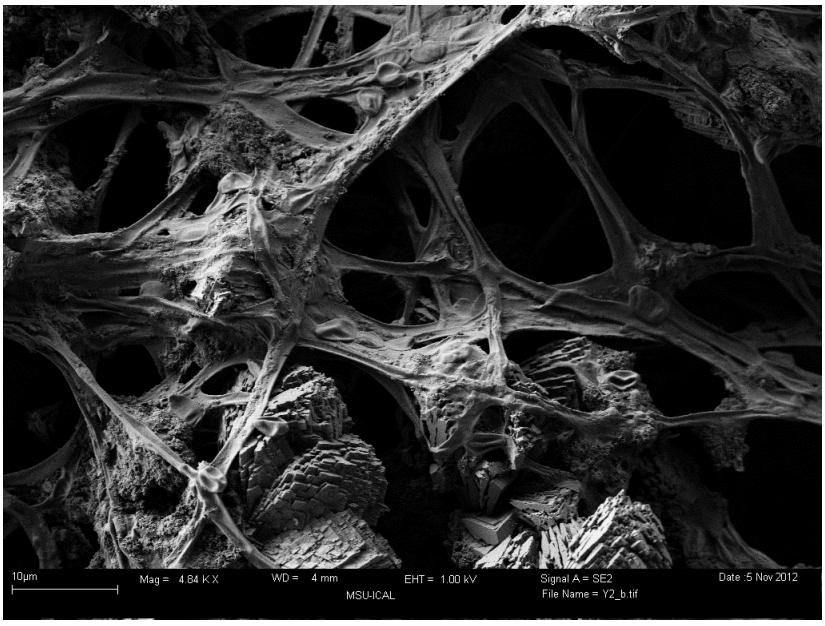

Figure 16: FESEM at 4.84 kX magnification of the line 3 membrane after failure. Biofilm can be seen draped over the scale.

Phase II Results

Phase II began by loading three parallel membrane units with a feed water that contained 10 ppm organics and approximately 150 ppm inorganics (background inorganic concentration of the BAC water) with no added inorganics for the goal of promoting mainly biofouling. Membrane autopsies in Phase II were staggered throughout the operational lifespan of the system. Line 1 was autopsied at 1/3 of the predicted maximum increase in trans-membrane pressure, line 2 at 2/3 the predicted maximum increase in trans-membrane pressure and line 3 at membrane failure. Maximum increase of trans-membrane pressure was predicted by subtracting the initial trans-membrane pressure from the maximum pressure of the RO booster pump. Membrane failure was defined as the time point when TDS removal dropped below ~75% and/or a ~50% reduction in permeate flow was seen. Failure occurred after 88 days of operation and 2,600 L of feed water passed as seen in Figure 17.

Phase II Operational Data

All results are normalized by an accumulated volume of feed water passed through the membrane. This volume was found by taking the run time and multiplying it by the measured flow rate. On days when flow rates were not measured (weekends and holidays), the measured flow rates from the day prior and the day after the break were averaged. That averaged value was then used to calculate a volume of feed water.

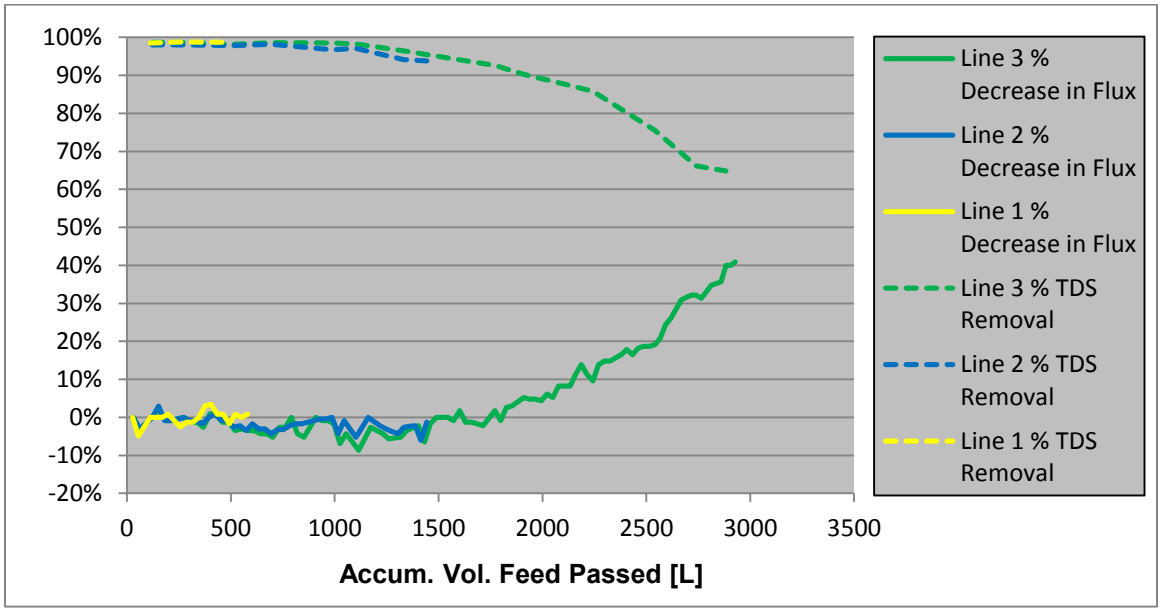

Figure 17: Progression of Phase II failure indicators.

System Operation. Phase II was affected by the worst membrane component malfunction experienced in any of the phases. In the final membrane replicate, the brine seal, a gasket between the membrane unit and membrane housing forcing water to flow through the membrane, was damaged during operation. This allowed for preferential flow around the outside of the membrane unit causing a complete lack of a feed channel pressure drop.

Pressure and Flow. Trans-membrane pressure drop, the change of pressure from the feed line to the permeate line, was very similar for all three membrane lines and increased linearly throughout the experiment. Very early in the phase, the RO booster pump for line 3 was replaced so that all lines would operate under similar pressure conditions resulting in a jump in trans-membrane pressure in line 3.

Feed channel pressure drop is the drop of pressure over the feed channel (feed to retentate). Line 1 was autopsied before an increase of feed channel pressure drop could be detected in that line. The feed channel pressure drop increased to a maximum of 3 psi in line 2 by the time of autopsy which occurred at 2/3 the maximum trans-membrane pressure drop. Unfortunately, feed channel pressure drop did not increase in line 3. This was most likely due to a failure of the brine seal which allowed preferential flow between the membrane and the membrane housing. Feed channel pressure trends are displayed in Figure 18.

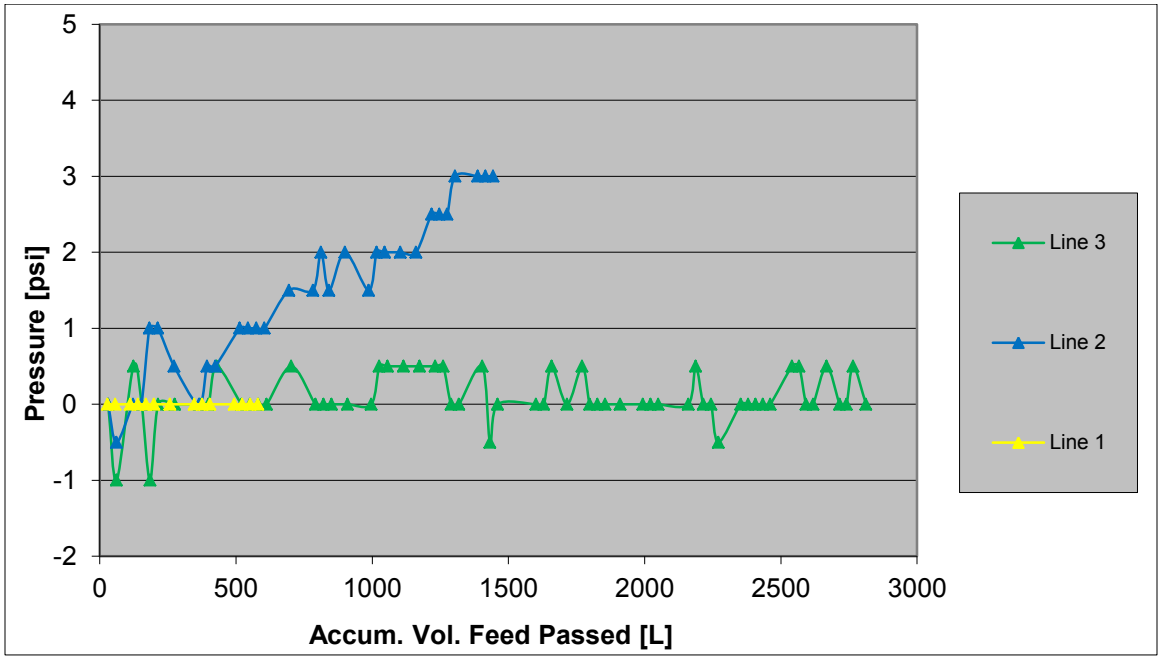

Figure 18: The increase in the feed channel pressure drop over the duration of Phase II.

Permeate flows remained constant until about 1,500 L of feed water passed. At this point, they began to steadily decrease. Retentate flows began at around 500 mL/min and gradually decreased to 420 mL/min by 1,500 L of feed water passed. By this point,

only line 3 remained operational. In line 3 after 1,500 L of feed water passed, the remaining retentate flow began to slowly increase to 450 mL/min. After 2,500 L of feed water passed, the retentate flow decreased to 400 mL/min. Phase II flow data is displayed in Figure 19.

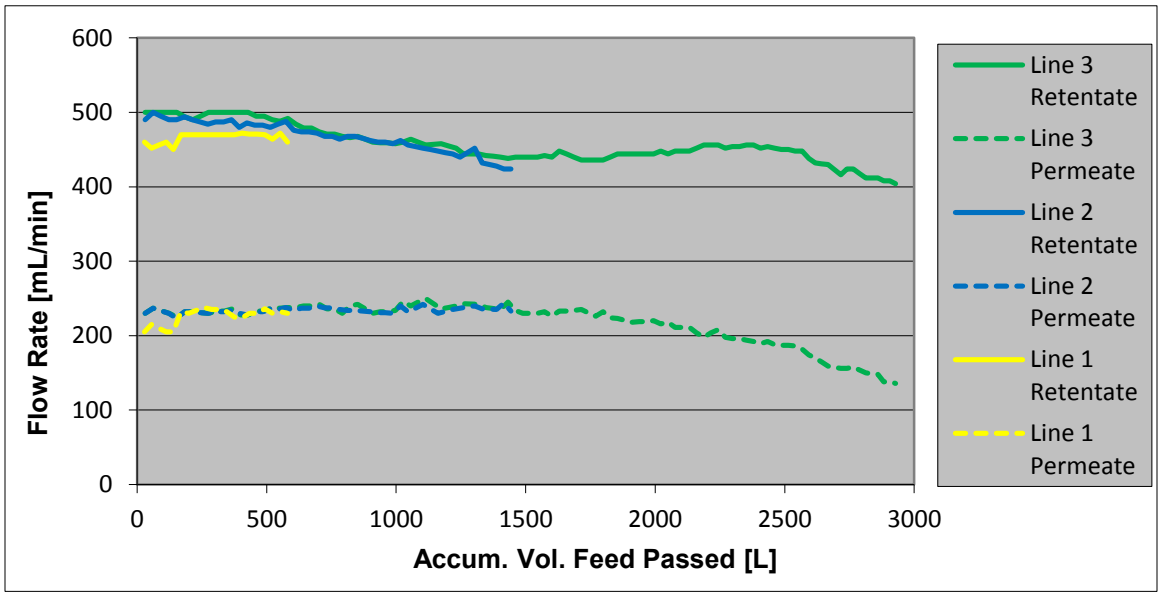

Figure 19: Retentate and permeate flow rates during Phase II.

ATP. The difference between the measured values obtained for retentate and feed waters (adjusted retentate ATP – feed ATP) is displayed in Figure 20. The data exhibits a reasonable amount of scatter. The difference between adjusted retentate ATP – feed ATP at the beginning and end of the experiment was approximately equal but quantity of retentate ATP usually surpassed that of the feed throughout Phase II.

Permeate ATP remained around the limits of detection until the about halfway through the experiment and then increased rapidly in line 3. Lines 1 and 2 were autopsied before an increase in ATP was observed.

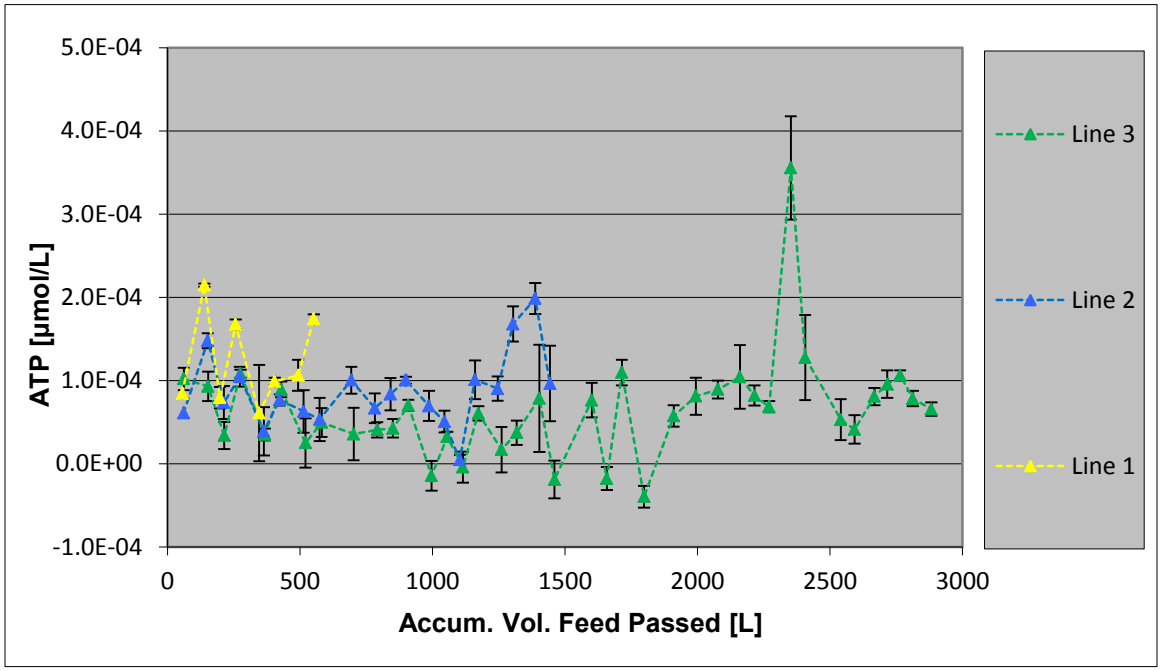

Figure 20: Difference between retentate and feed ATP (adjusted retentate ATP – feed ATP) during Phase II.

HPCs. The difference between the retentate and feed HPCs (adjusted retentate HPCs – feed HPCs) is displayed in Figure 21. This difference remained fairly constant throughout the experiment at around 0.75 Log_{10} (CFU/mL). Only once around 1500 L of feed water passed were the adjusted retentate HPCs less than the feed HPCs. Unadjusted retentate counts remained consistently around 5.0 Log_{10} (CFU/mL) whereas the feed counts remained consistently at 4.0 Log_{10} (CFU/mL) throughout the phase.

Trends in HPCs in the permeate for each line were very consistent between lines. An initial rapid increase to a value of 3.0 Log_{10} (CFU/mL) observed which then plateaued until around 800L of feed passed. After this point, permeate counts began to increase again. By 6,500 L feed water passed, permeate counts had increased to a value of 5.0 Log_{10} (CFU/mL) where they plateaued for the remainder of the phase.

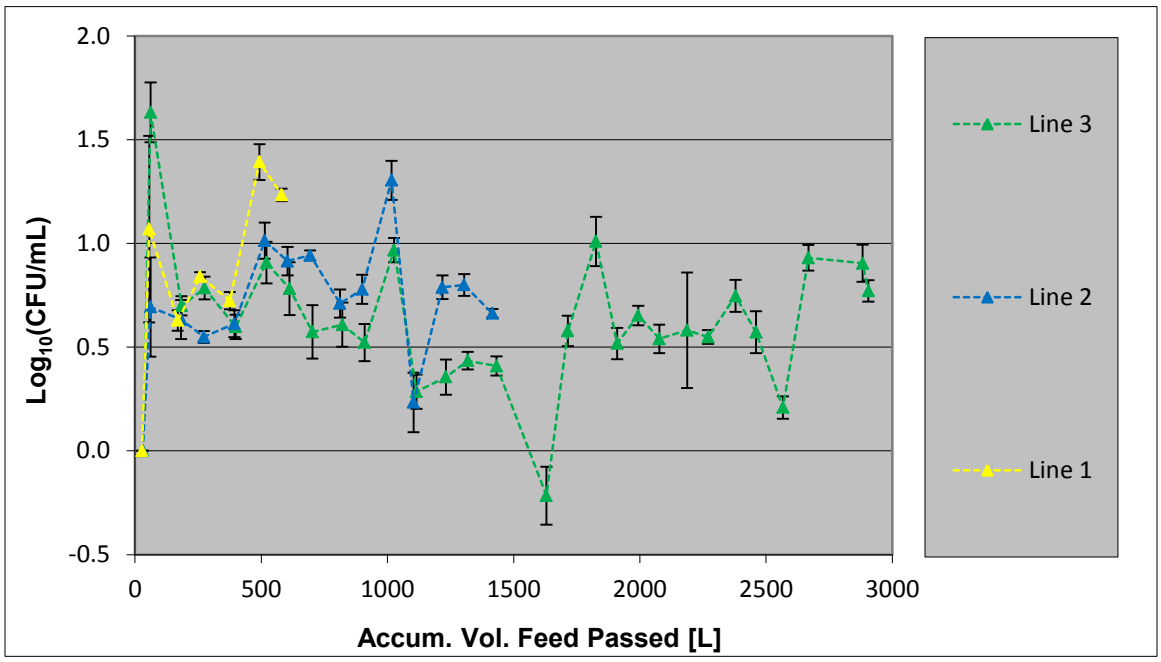

Figure 21: Difference between retentate and feed HPCs (adjusted retentate HPCs – feed HPCs) during Phase II.

The proportions of different colony types also changed as the system aged. Most notable was the appearance of black fuzzy colonies (most likely mold) that appeared near the end of Phase II and became more numerous at the time of shut-down.

Direct Counts. Direct microscopy counts in the feed remained fairly constant at around 1.00E+05 cells/mL for all three lines. Retentate direct counts began at 1.00E+05 cells/mL and slowly increased towards 1.00E+06 cells/mL. Retentate direct counts were generally more numerous than those of the feed. Only once at 1,000 L of feed water passed were the adjusted retentate direct counts less than the feed direct counts.

Cell Clumping. Cell clumping analysis was performed in the retentate streams of each RO line. Three types of clumping analyses were performed: clumping based on

percent total occurrences, clumping based on percent of total cells and concentration of clumps greater than 5 cells. No increases were observed based on percent occurrences. Single cells were around 77% of total occurrences while clumps between 2 to 10 cells and clumps >10 cells remained around 21% and 2%, respectively. Distributions based on percent total cells exhibited a great deal of variation. In general no increasing trend was noticed. Single cells made up about 38% of total cells on average. However, the concentration of clumps > 5 cells began an increasing trend around 1,500 L feed water passed. Maximum clump concentration occurred in line 3 (membrane replicate run to failure) with a value of 25,000 clumps/mL. Clump concentration data is displayed in Figure 22.

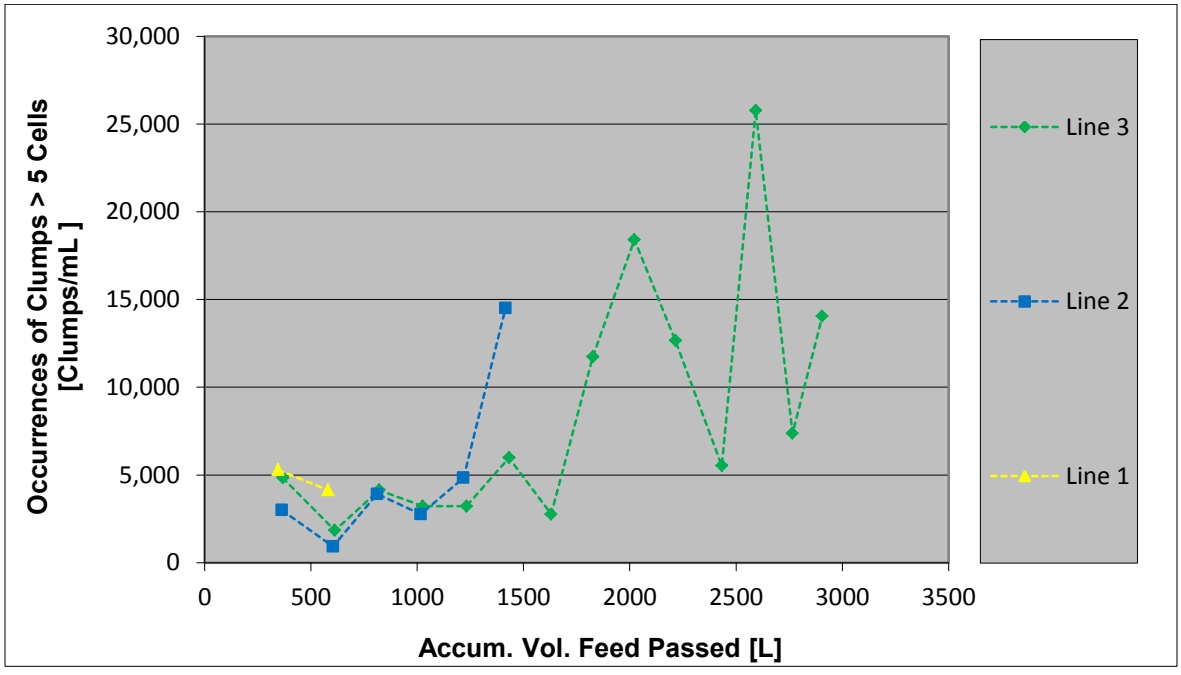

Figure 22: Retentate cell clumping throughout the duration of Phase II.

Conductivity. The measured conductivity in the feed water was consistent throughout the experiment. Retentate conductivity remained constant until the membranes began to fail. Conductivity in the permeate remained constant until around 1,500 L of feed water passed and then began to increase slowly. At 2,250 L of feed water passed, retentate conductivity decreased rapidly until it equaled the feed conductivity. Results from the conductivity analysis are displayed in Figure 23.

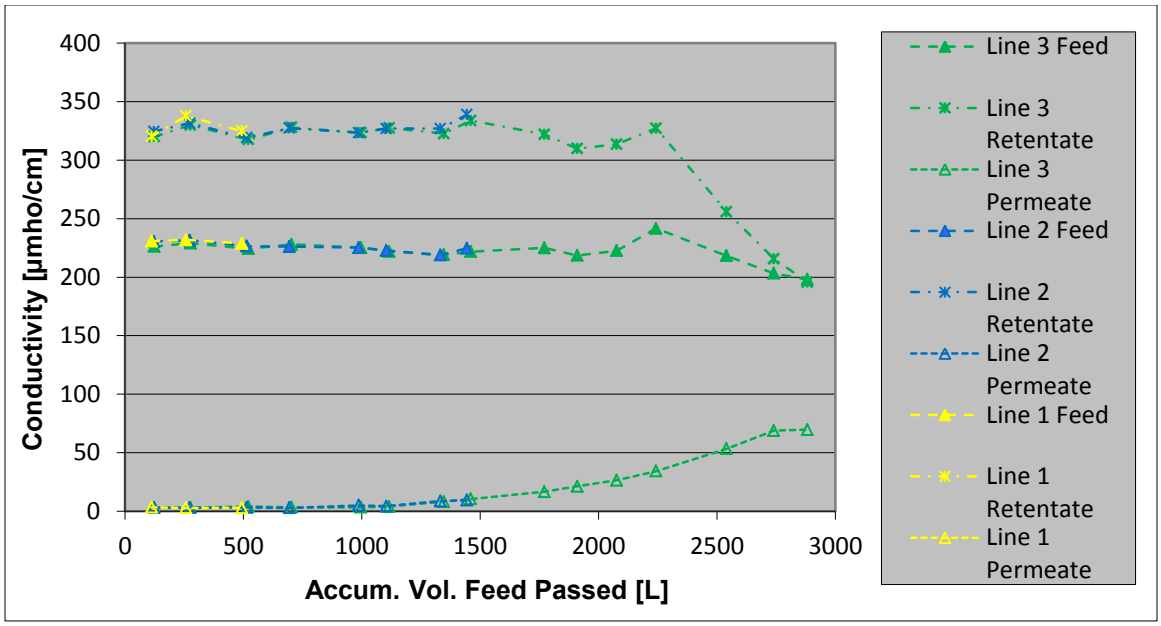

Figure 23: Change in conductivity throughout the progression of Phase II.

Phase II Autopsy Data

Results from all membrane autopsy analyses are shown below in Table 7. The results of the analyses indicate variability across the membrane. In all measurements displayed in Table 7 except for ATP, sessile amounts increased with increasing feed passed. Data did not show any clear trends based on membrane sample location.

Table 7: Summary of Phase II autopsy data. Sample nomenclature is as follows (line # - sample location). Sample location 1 was at the beginning of the feed channel where feed water entered the membrane. Sample location 2 was at the center of the membrane. Sample location 3 was at the extreme end of the feed channel where retentate water exited the membrane.

Sample	Day Sacrificed	Analysis				
		ATP [μmol/cm^2]	HPC [CFU/cm^2]	Direct Counts [Cells/cm^2]	Carbo-hydrates [mg/cm^2]	Protein [μg/cm^2]
1-1	20	6.65E-06	5.68E+05	5.84E+06	2.63E-03	7.80E-01
1-2	20	2.05E-06	1.09E+06	2.79E+06	8.59E-04	2.99E-01
1-3	20	4.25E-06	2.01E+06	4.21E+06	1.51E-03	4.76E-01
Control	N/A	N/A	N/A	N/A	1.84E-03	0.00
2-1	49	1.52E-04	5.04E+06	7.84E+06	1.53E-02	2.99E+00
2-2	49	2.63E-04	7.46E+06	2.46E+07	4.87E-02	1.20E+01
2-3	49	3.80E-04	7.76E+06	2.02E+07	5.62E-02	1.46E+01
Control	N/A	N/A	N/A	N/A	5.70E-04	5.46E-03
3-1	104	1.85E-04	4.53E+07	5.69E+07	9.19E-02	1.77E+01
3-2	104	2.03E-04	6.01E+07	1.12E+08	1.02E-01	2.16E+01
3-3	104	1.35E-04	7.91E+06	2.27E+07	7.83E-02	2.37E+01
Control	N/A	N/A	N/A	N/A	9.37E-05	0.00

Biofilm Indicators. Sessile protein and carbohydrates increased throughout the system's lifespan. Upon membrane failure sessile protein and carbohydrates values averaged 2.10E+01 μg/cm^2 and 9.06E-02 mg/cm^2, respectively. This is indicative of an increase in bacterial accumulation and EPS from biofilm formation. Biofilm was also clearly visible on the membrane surface as seen in Figure 24.

Average sessile ATP at failure was 2.03E-04 μmol/cm^2. An increase in sessile ATP was not observed between the second and final autopsies. This is in direct contrast to the increasing trends observed in sessile HPCs and sessile direct counts which both increased by an order of magnitude between the second and last autopsies. The observed

stagnation with sessile ATP may be related to discrepancies between the standard curves of each autopsy.

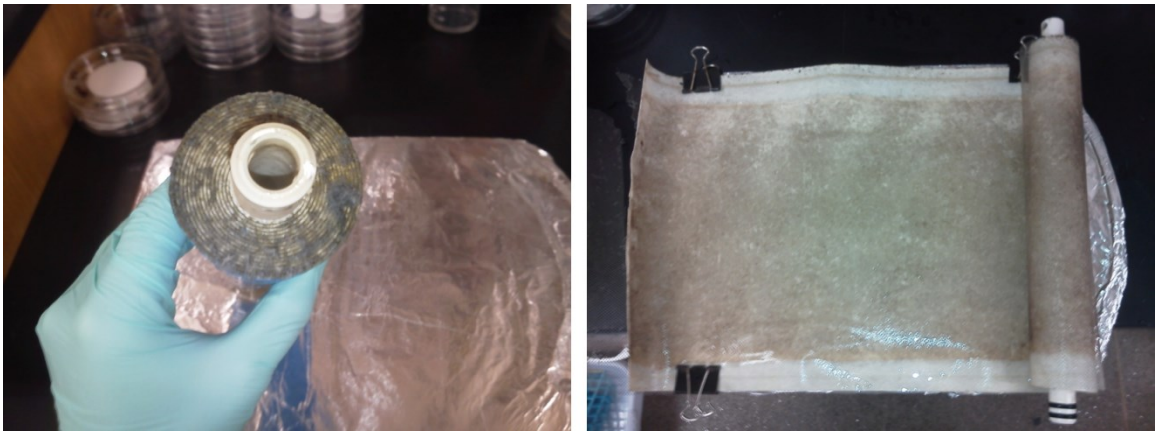

Figure 24: Phase II final autopsy images (Line 3). Left – The lead face of the membrane element. Large amounts of biomass are clearly visible. Right – Fouling on the membrane surface is clearly visible. The lighter areas along the edges are areas where no flux occurs. The flow direction is downward on the page.

FESEM. Phase II FESEM images showed the progression of biofouling across the membrane surface over the lifespan of the system. In the initial membrane autopsy images (line 1), small groups of attached cells can be seen (Figure 25 and Figure 26). By the second autopsy (line 2), these groups have begun to combine, but small amounts of membrane surface can still be seen (Figure 27 and Figure 28). By membrane failure, a confluent biofilm had completely inundated the membrane surface of line 3 (Figure 29 and Figure 30). The observed biofilm was much different than the biofilm in Phase I and lacked the strand-like formations (Figure 15 and Figure 16).

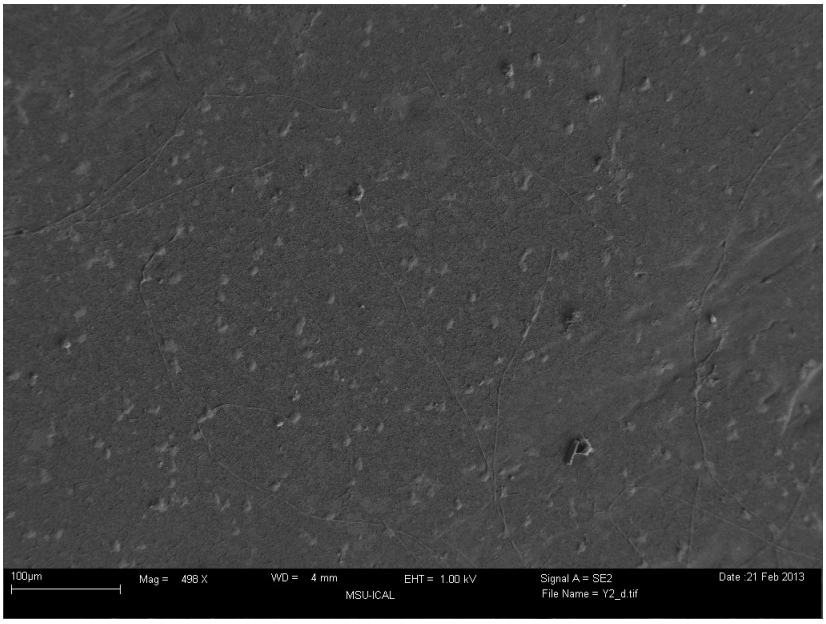

Figure 25: Phase II FESEM image of the line 1 membrane at 500 X magnification. The membrane autopsy was performed at day 20 and after 600 L of feed water was passed. Adhesion of cells to the membrane surface has already begun.

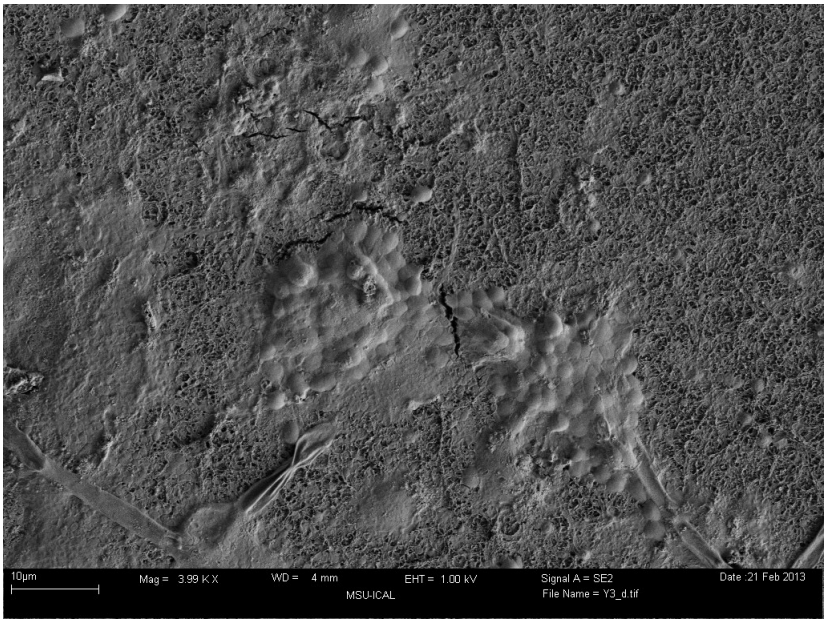

Figure 26: Phase II FESEM image of the line 1 membrane at 4.00 kX magnification. The membrane autopsy was performed at day 20 and after 600 L of feed water was passed. Small clusters of cells can be seen on the membrane surface.

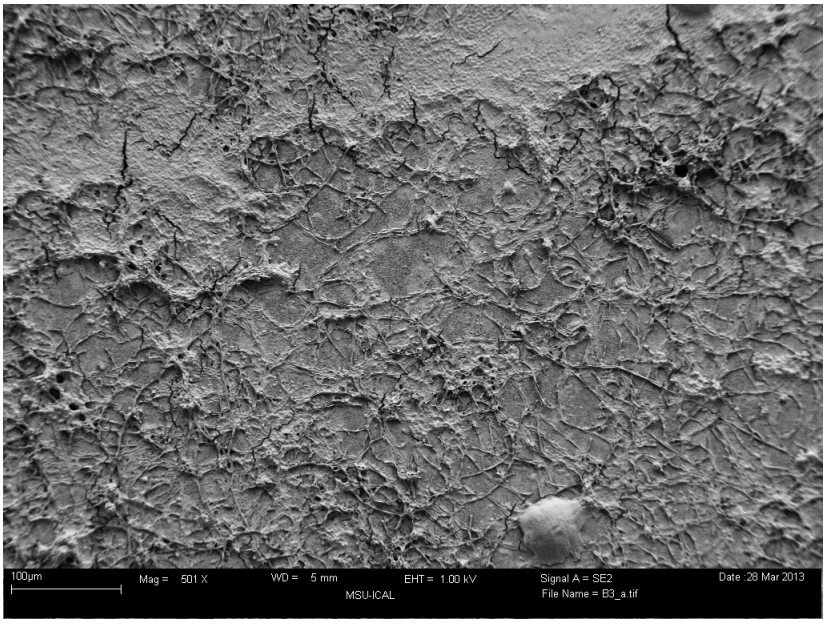

Figure 27: Phase II FESEM image of the line 2 membrane at 500 X magnification. The membrane autopsy was performed at day 49 and after 1400 L of feed water was passed. Further adhesion and growth has almost completely inundated the membrane surface.

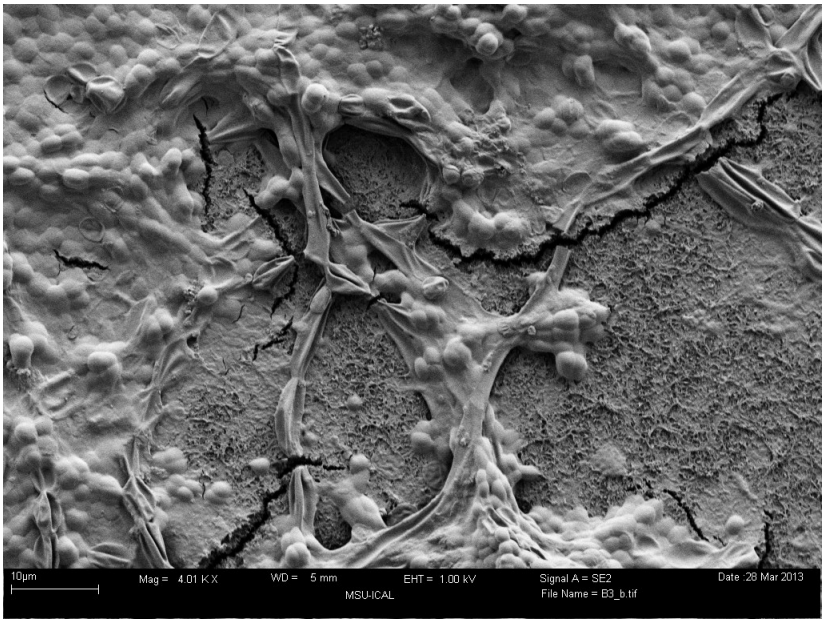

Figure 28: Phase II FESEM image of the line 2 membrane at 4.00 kX magnification. The membrane autopsy was performed at day 49 and after 1400 L of feed water was passed.

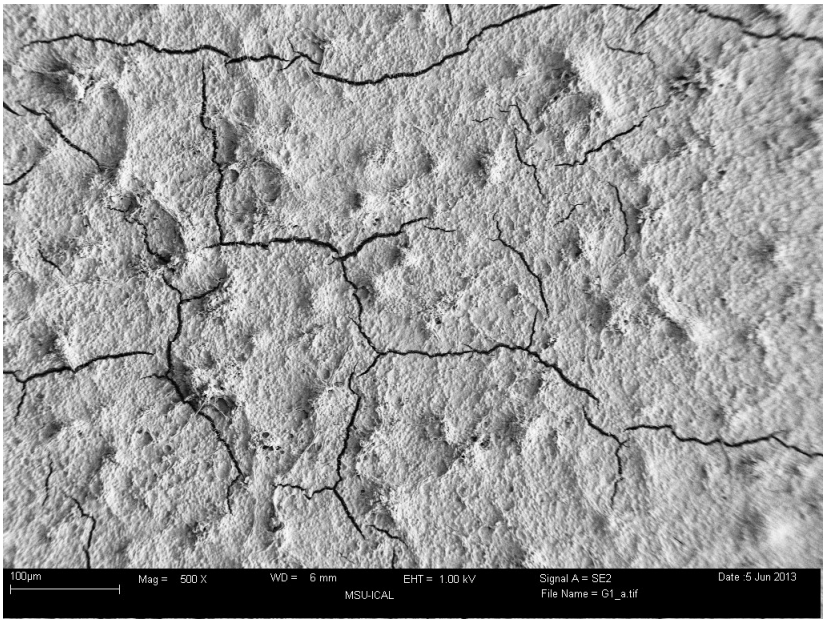

Figure 29: Phase II FESEM image of the line 3 membrane at 500 X magnification. The membrane autopsy was performed after membrane failure. The cracks are from the sample drying process.

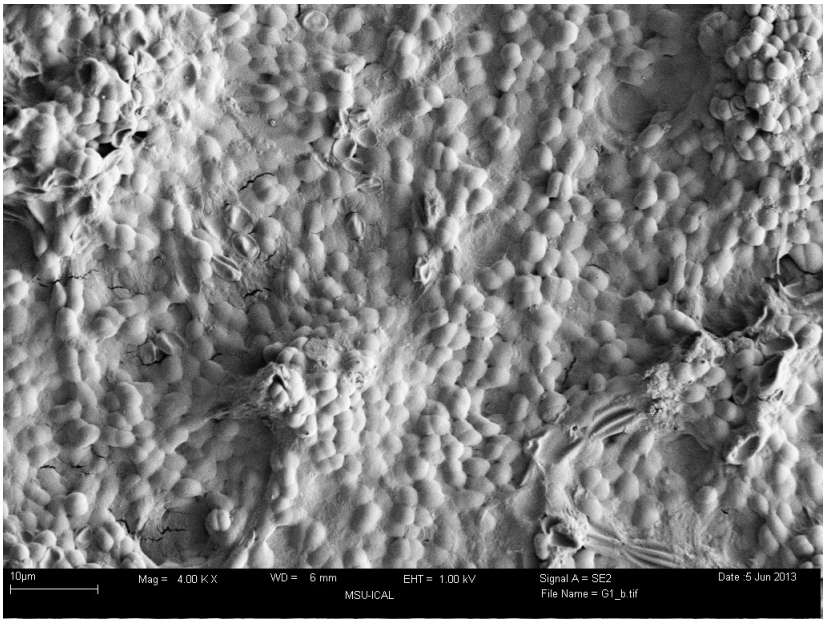

Figure 30: Phase II FESEM image of the line 3 membrane at 4.00 kX magnification. The membrane autopsy was performed after membrane failure. Individual cells imbedded in an EPS matrix are clearly visible.

Autopsy Summary. Overall, the initial goal of biofouling was achieved in Phase II. Sessile protein and carbohydrates were very similar to those observed in Phase I indicating similar amounts of EPS throughout the membrane surface. Sessile ATP was two times greater by failure in Phase II than in Phase I. This could be indicative of a more active and robust biofilm.

Phase III Results

Phase III began by loading three parallel membrane units with feed water that contained 0 ppm added organics and 500 ppm inorganics with the goal of promoting mainly inorganic fouling. Membrane autopsies in Phase III were staggered throughout the operational lifespan of the system. Line 1 was autopsied at 1/3 of the predicted maximum increase in trans-membrane pressure, line 2 at 2/3 the predicted maximum increase in trans-membrane pressure and line 3 after membrane failure. Maximum increase of trans-membrane pressure was predicted by subtracting the initial trans-membrane pressure from the maximum pressure of the RO booster pump. Membrane failure was defined as the time point when TDS removal dropped below ~75% and/or a ~50% reduction in permeate flow was seen. Failure occurred after 173 days of operation and 5,100 L of feed water passed as seen in Figure 31.

Phase III Operational Data

All results are normalized by an accumulated volume of feed water passed through the membrane. This volume was found by taking the run time and multiplying it by the measured flow rate. On days when flow rates were not measured (weekends and

holidays), the measured flow rates from the day prior and the day after the break were averaged. That averaged value was then used to calculate a volume of feed water.

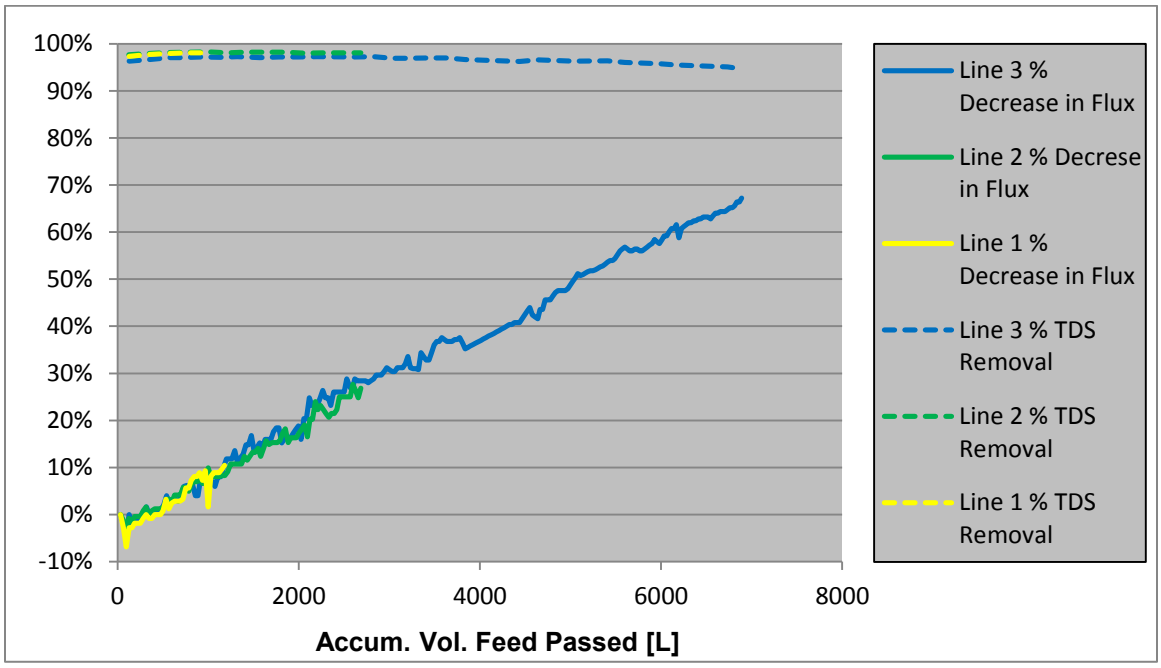

Figure 31: Progression of Phase III fouling indicators

System Operation. During Phase III, a BAC water line was damaged over the weekend resulting in the feed tank for one of the membrane lines (line 3) not filling with water. This problem persisted unknown for 2 days. The issue was immediately rectified. The highest value of retentate cell clumping was recorded from this line in the sample taken after the failure. This is most likely due to not allowing enough time for the system to flush all the biomass growth from the extended stagnation period.

Pressure and Flow. Trans-membrane pressure drop, the change of pressure from the feed line to the permeate line, was very similar for all three membrane lines and increased linearly throughout the experiment. The rate of increase for the trans-

membrane pressure for Phase III was the slowest observed in all four phases since it had the longest operation time until failure.

Feed channel pressure drop is the drop of pressure over the feed channel (feed to retentate). Line 1 was autopsied before an increase of feed channel pressure drop could be detected. The feed channel pressure drop increased to a maximum of 3 psi in line 2 by the time of autopsy which occurred at 2/3 the maximum trans-membrane pressure drop. In line 3, the line that ran until failure, feed channel pressure drop increased to 5 psi where it plateaued until failure. Feed channel pressure trends are displayed in Figure 32.

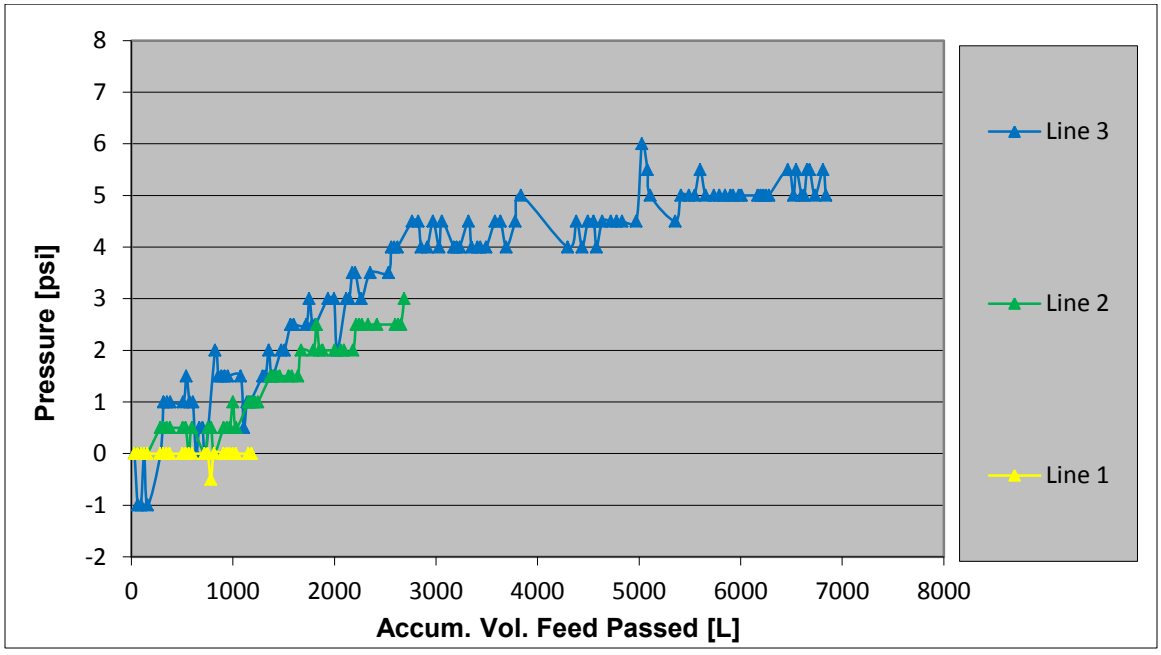

Figure 32: The increase in the feed channel pressure drop over the duration of Phase III.

Permeate flows steadily and consistently decreased from the beginning of this experiment while retentate flows gradually increased. These trends can be observed in Figure 33.

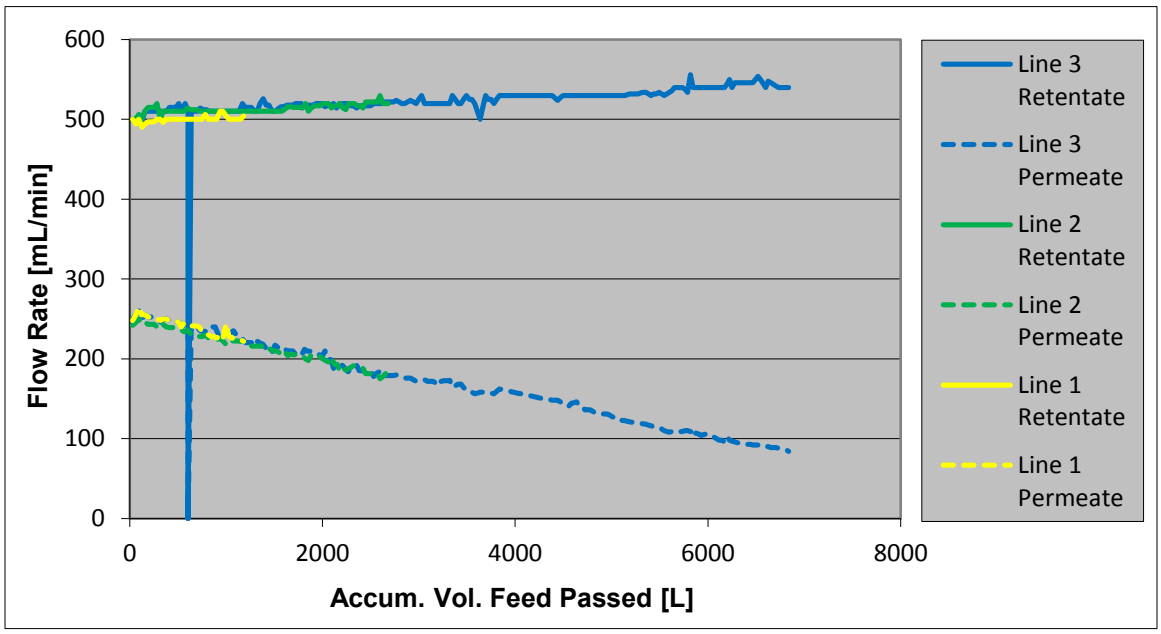

Figure 33: Retentate and permeate flow rates during Phase III.

ATP. The difference between the values obtained for retentate and feed waters (adjusted retentate ATP – feed ATP) is displayed in Figure 34. Feed ATP values were always greater or equal to adjusted retentate values throughout the phase. Permeate ATP remained near the limit of detection throughout most of the experiment. No rapid increase in permeate ATP was detected.

HPCs. The difference between the retentate and feed HPCs (adjusted retentate HPCs – feed HPCs) is displayed in Figure 35. Retentate and feed counts were generally very similar. Feed HPCs were either greater than or equal to the adjusted retentate HPCs for the duration of the phase except at the initial startup when adjusted retentate HPCs surpassed the feed HPCs.

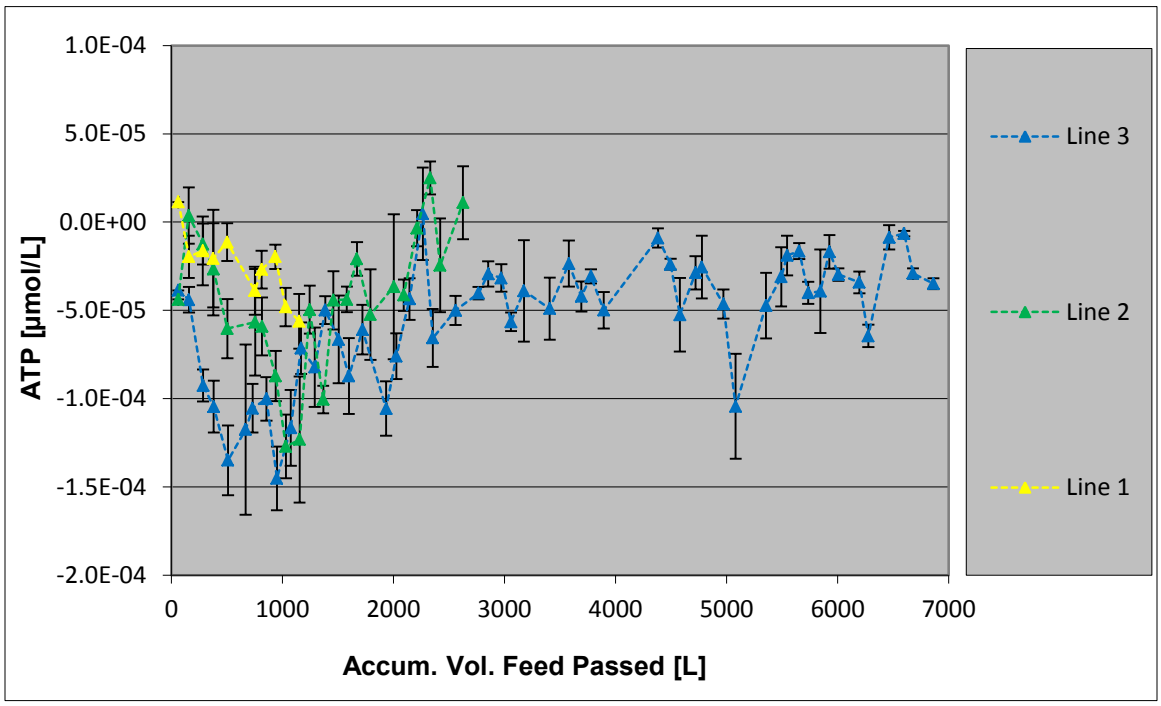

Figure 34: Difference between retentate and feed ATP (adjusted retentate ATP – feed ATP) during Phase III.

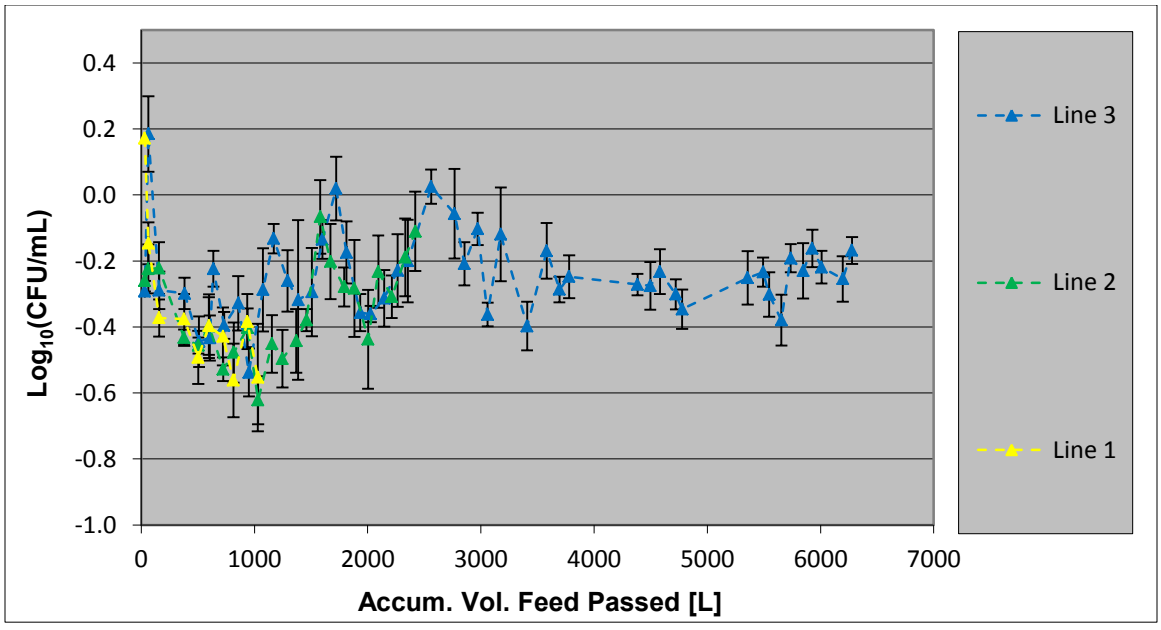

Figure 35: Difference between retentate and feed HPCs (adjusted retentate HPCs – feed HPCs) during Phase III.

Trends in HPCs in the permeate for each line were very consistent. An initial rapid increase of counts was observed during the first 600 L of feed passed. After the increase, permeate counts plateaued and remained relatively constant at a value of 3.0 Log_{10}(CFU/mL).

The proportions of different colony types also changed as the system aged. Most notable was the appearance of black fuzzy colonies (most likely mold) near the end of Phase III that became more numerous with time.

Direct Counts. Direct microscopy counts were performed on the feed and retentate waters. Counts in both the retentate and feed lines remained consistently near 1.00E+05 cells/mL.

Cell Clumping. Cell clumping analysis was performed in the retentate streams of each RO line. Three types of clumping analyses were performed: clumping based on percent total occurrences, clumping based on percent of total cells and concentration of clumps greater than 5 cells. No increases were observed based on percent occurrences. Single cells were around 80% of total occurrences while clumps between 2 to 10 cells and clumps >10 cells remained around 18% and 2%, respectively. Distributions based on percent total cells exhibited a great deal of variation. In general no increasing trend was noticed. Single cells made up about 38% of total cells on average. Overall, the concentration of clumps > 5 cells did not increase throughout the duration of the phase and remained around 2,500 clumps/mL. A large spike in clump concentration was observed at 650 L of feed water passed in line 3. This spike is most likely due from a prolonged stagnation period due to a pump failure. Outside of the outlier due to the

pump failure, the maximum observed clump concentration was 14,000 clumps/mL and it was observed right before line 2 was autopsied. Clump concentration data is displayed in Figure 36.

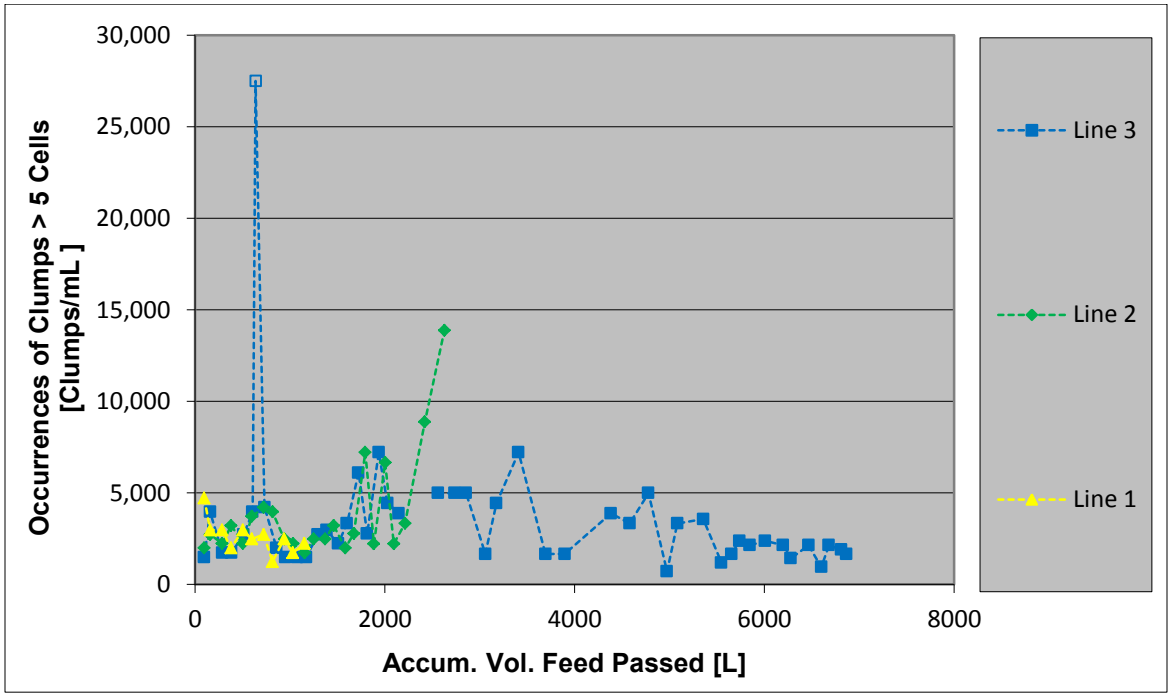

Figure 36: Retentate cell clumping throughout the duration of Phase III.

Conductivity. The measured conductivity in the feed water was consistent throughout the experiment and no significant changes were observed in any of the lines. A very gradual increase in permeate conductivity was observed, whereas the retentate conductivity gradually decreased as the experiment progressed. Results from the conductivity analysis are displayed in Figure 37.

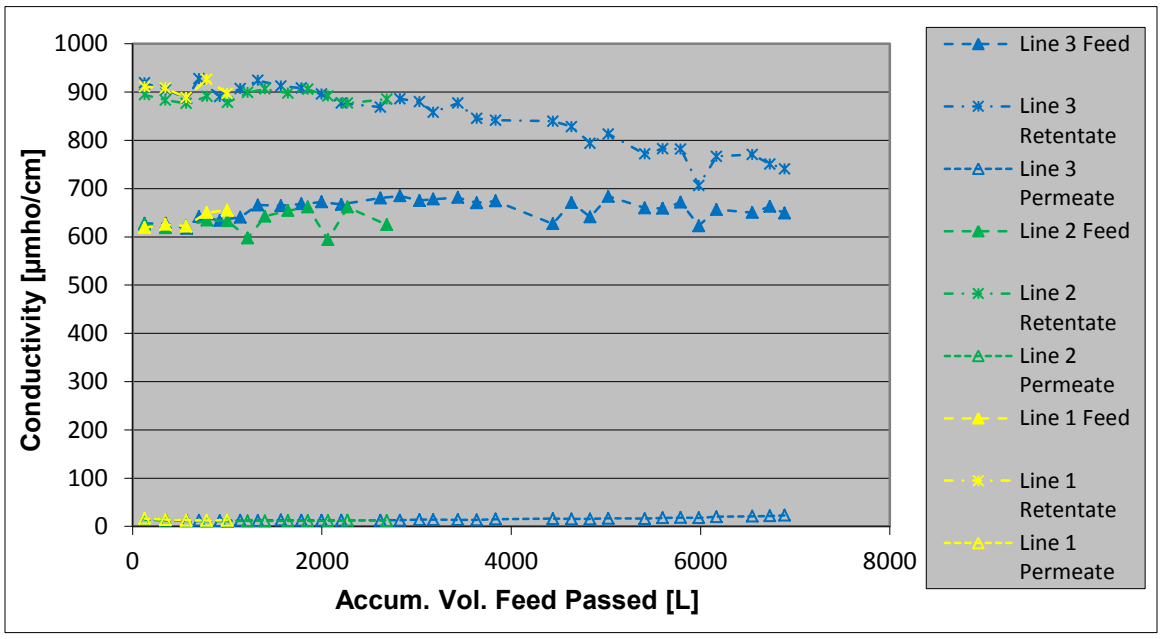

Figure 37: Change in conductivity throughout the progression of Phase III.

Phase III Autopsy Data

Results from the completed membrane autopsy analyses indicate variability across the membrane and are shown below in Table 8. Sessile amounts remained fairly consistent over the duration of the experiment. Figure 38 shows the membrane surface upon autopsy.

Biofilm Indicators. Sessile protein and carbohydrates did not increase throughout the system's lifespan. Upon membrane failure sessile protein and carbohydrates values averaged 5.36E-01 µg/cm^2 and 1.72E-03 mg/cm^2, respectively. This is indicative of a lack in biofilm formation. Average sessile ATP at failure was 2.07E-06 µmol/cm^2. Sessile ATP did not increase throughout the system's lifespan. This trend is further reinforced by trends observed in sessile HPCs and sessile direct counts which remained around the same order of magnitude throughout Phase III.

Table 8: Summary of Phase III autopsy data. Sample nomenclature is as follows (line # - sample location). Sample location 1 was at the beginning of the feed channel where feed water entered the membrane. Sample location 2 was at the center of the membrane. Sample location 3 was at the extreme end of the feed channel where retentate water exited the membrane.

Sample	Day Sacrificed	Analysis				
		ATP [µmol/cm^2]	HPC [CFU/cm^2]	Direct Counts [Cells/cm^2]	Carbo-hydrates [mg/cm^2]	Protein [µg/cm^2]
1-1	38	4.85E-06	6.97E+05	1.68E+06	4.40E-04	4.16E-01
1-2	38	1.15E-06	4.07E+04	5.03E+04	3.93E-05	2.34E-02
1-3	38	3.53E-06	6.37E+05	1.88E+06	3.06E-04	2.99E-01
Control	N/A	N/A	N/A	N/A	N/A	0.00
2-1	88	8.47E-06	N/A	9.84E+06	1.78E-03	6.34E-01
2-2	88	6.43E-06	4.30E+06	5.95E+06	1.30E-03	4.78E-01
2-3	88	4.15E-06	3.10E+06	1.58E+06	1.26E-03	3.55E-01
Control	N/A	N/A	N/A	N/A	3.38E-04	0.00
3-1	241	1.92E-06	5.51E+05	3.90E+06	2.03E-03	5.92E-01
3-2	241	2.07E-06	5.65E+05	3.04E+06	1.72E-03	5.36E-01
3-3	241	4.77E-07	2.07E+05	1.05E+06	4.95E-04	1.70E-01
Control	N/A	N/A	N/A	N/A	3.22E-04	6.67E-04

Figure 38: Phase III final autopsy images (Line 3). Left – The lead face of the membrane element. Chunks of solids and some biomass can be observed. Right – The membrane surface is visibly much cleaner than in combined and organics loading cases. Upon closer inspection lighter areas along the edges can be seen which indicates areas where no flux occurred. Flow direction is downward on the page.

Sessile Spacer ATP. Sessile spacer ATP for Phase III increased over the experiment. Values from the first autopsy (1/3 maximum increase in trans-membrane pressure) were around 1.9E-06 μmol/cm^2. Maximum measured sessile spacer ATP occurred at membrane failure at a value of 1.2E-04 μmol/cm^2. These values are displayed along with Phase IV sessile spacer ATP values in Figure 56.

FESEM. Phase III images indicated a clear increase in inorganic fouling over the course of the experiment. In the initial membrane autopsy images (line 1), small clusters of scale can be seen (Figure 39 and Figure 40). By the second autopsy (line 2), scale clusters grew and became more prevalent, but clean membrane surfaces can still be seen (Figure 41 and Figure 42). Images from the final autopsy (line 3) revealed wide spread scaling across the imaged membrane surface (Figure 43 and Figure 44). It was also observed that the deposition became more severe as distance along the feed channel increased. This is evidence of the effects of concentration polarization.

Autopsy Summary. Overall, the initial goal of inorganic fouling was achieved in Phase III. Comparing FESEM images, the degree of inorganic fouling upon failure did not look as severe as the inorganic fouling observed in Phase I (combined fouling). Sessile protein, sessile carbohydrates, and sessile ATP at failure were the lowest values observed in any of the experimental phases indicating very limited biofilm growth on the membrane surface. Furthermore, sessile spacer ATP values indicated very limited biofilm growth on the feed spacer.

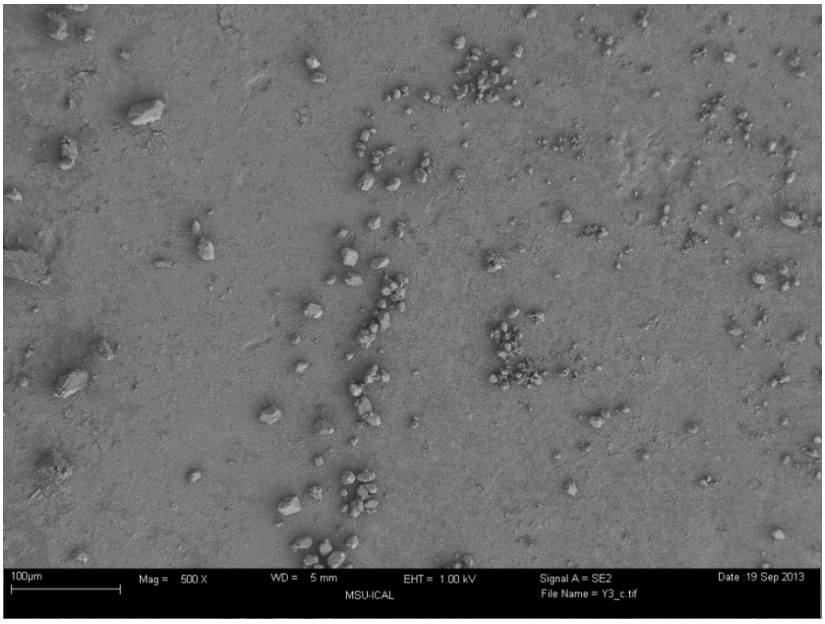

Figure 39: Phase III FESEM image of the line 1 membrane at 500 X magnification. The membrane autopsy was performed on day 39 and after 1200 L of feed water was passed. Small crystalline deposits can be seen on the membrane surface.

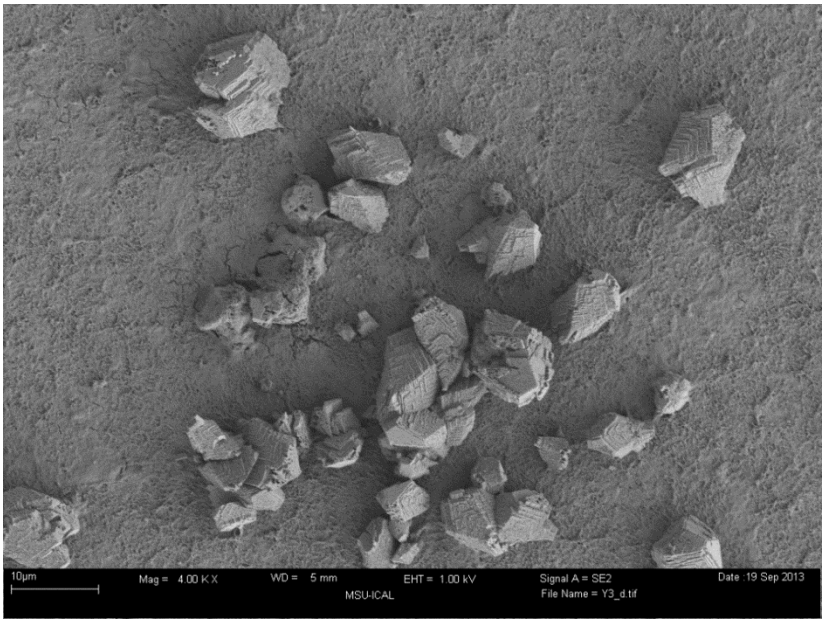

Figure 40: Phase III FESEM image of the line 1 membrane at 4.00 kX magnification. The membrane autopsy was performed on day 39 and after 1200 L of feed water was passed.

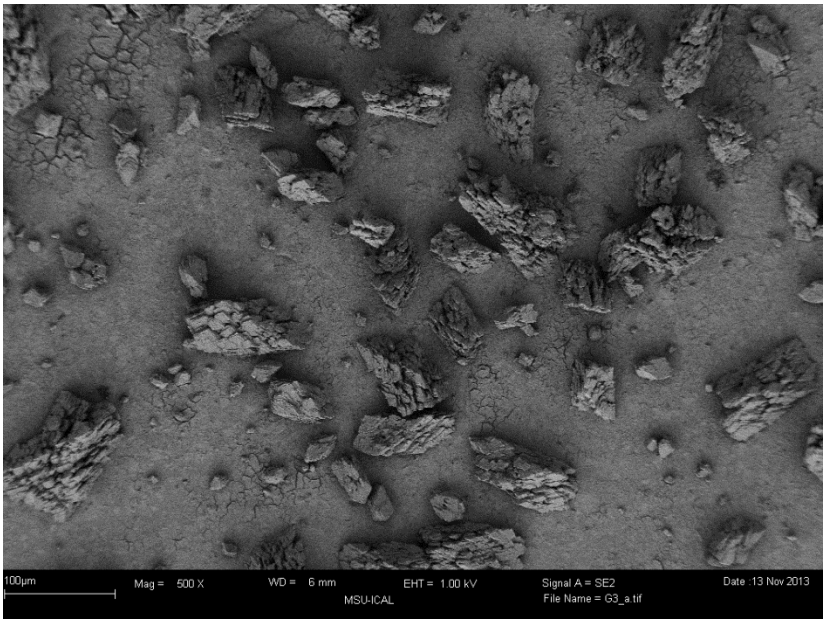

Figure 41: Phase III FESEM image of the line 2 membrane at 500 X magnification. The membrane autopsy was performed on day 89 and after 2700 L of feed water was passed. Deposits have grown larger and more numerous.

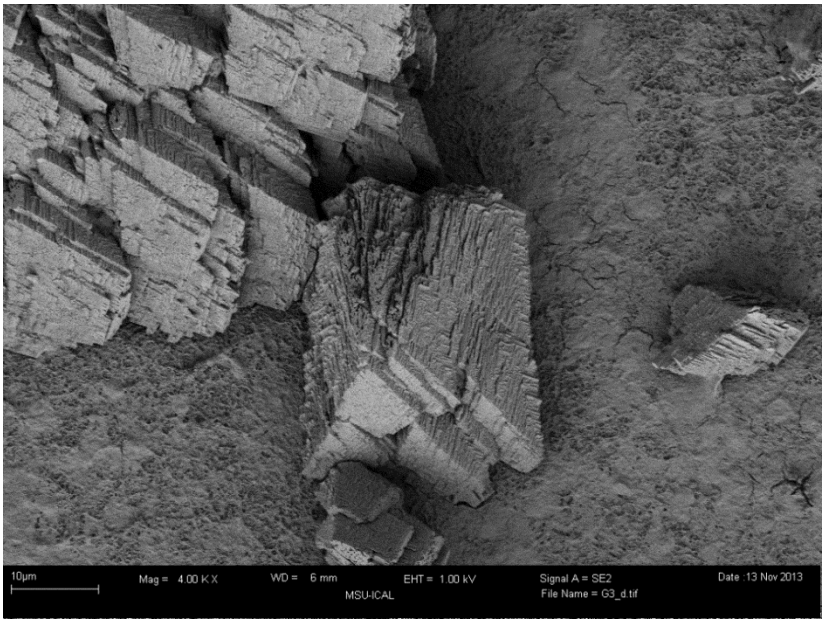

Figure 42: Phase III FESEM image of the line 2 membrane at 4.00 kX magnification. The membrane autopsy was performed on day 89 and after 2700 L of feed water was passed. The very abrupt edges of the deposits can be clearly seen.

Figure 43: Phase III FESEM image of the line 3 membrane at 500 X magnification. The membrane autopsy was performed after membrane failure. At this point, the membrane surface has been covered with scale.

Figure 44: Phase III FESEM image of the line 3 membrane at 4.00 kX magnification. The membrane autopsy was performed after membrane failure. The structure of the scale can be seen clearly.

Phase IV Results

The goal of Phase IV was to run one membrane replicate to failure with each of the aforementioned fouling types (combined inorganic fouling and biofouling, biofouling, and inorganic fouling) with the same feedwater concentrations used previously for each fouling type. Biofouling was promoted using a feed solution with 10 ppm organics and 150 ppm inorganics (background inorganics from the BAC water). A feed solution of 500 ppm inorganics and no added organics was used to promote inorganic fouling. Combined fouling was promoted by using a feed solution containing 500 ppm inorganics and 10 ppm organics. All membrane lines were run until membrane failure which was indicated by the time point when TDS removal dropped below ~75% or a ~50% reduction in permeate flow was seen. Upon failure, membranes were autopsied. The combine loaded membrane failed after 56 days of operation and 1700 L of feed water passed. The organics only membrane reached failure after 81 days of operation and 2,400 L of feed water passed. The inorganics only membrane ran for 110 days and passed 3,400 L before membrane failure was achieved. These trends are displayed in Figure 45.

Phase IV Operational Data

All results are normalized to an accumulated volume of feed water passed through the membrane. This volume was found by taking the run time and multiplying it by the measured flow rate. On days when flow rates were not measured (weekends and holidays), the measured flow rates from the day prior and the day after the break were averaged. That averaged value was then used to calculate a volume of feed water.

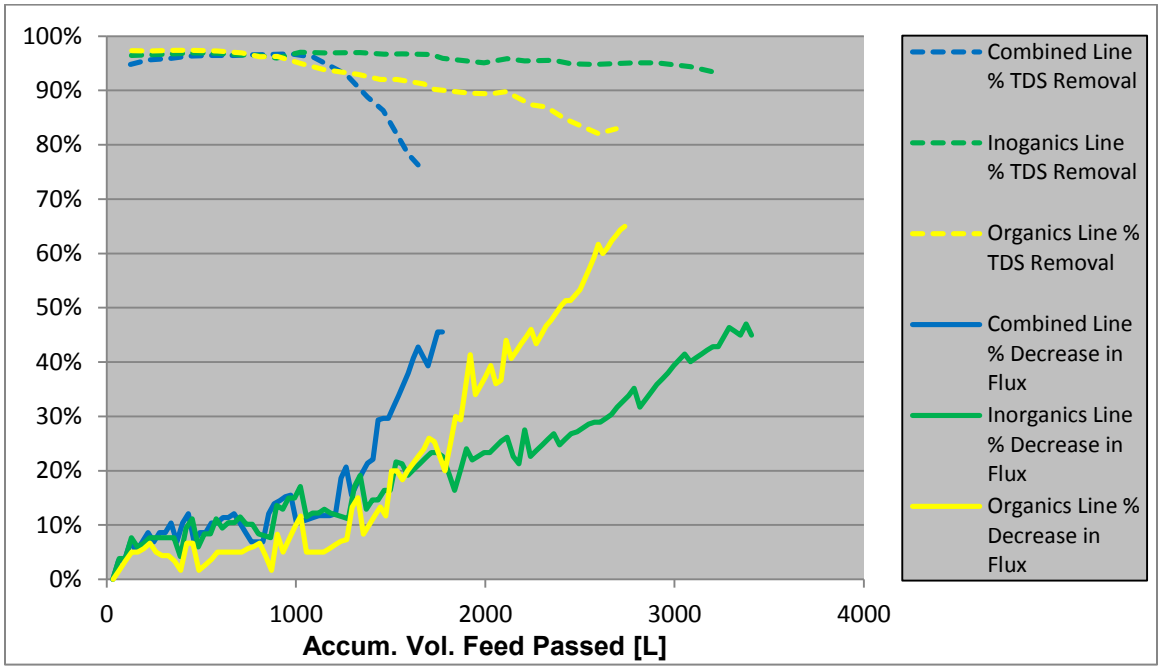

Figure 45: Progression of Phase IV failure indicators.

System Operation. During the end of this phase, the BAC pump failed. This problem was noticed almost immediately, with the membrane only missing one run out of the three that occur daily. Data trends were not affected by this failure nor were any of the other membrane lines since they had already been autopsied.

Pressure and Flow. Trans-membrane pressure drop is the change of pressure from the feed line to the permeate line. In the combined line, trans-membrane pressure drop increased by 6 psi over the first 1,000 L of feed water passed. After this point, the rate increased by increasing 15 psi over the last 700 L of feed water passed. In the organics line, a trend comparable to the combined line was observed, though the final rate of increase was not as high. Initially, the organics line trans-membrane pressure drop increased 10 psi over 1,400 L feed water passed. After this point, a 20 psi increase was

observed over 1,100 L of feed water passed. The inorganics line trans-membrane pressure drop increased linearly by 13 psi over 3,100 L of feed water passed and it had the slowest rate of increase of the phase.

Feed channel pressure drop is the drop of pressure over the feed channel (feed to retentate). In the combined line, feed channel pressure drop increased consistently to a value of 14 psi by 1,500 L of feed water passed. Feed channel pressure drop increased linearly to a maximum value of 13 psi by 2,000 L of feed water passed in the organics line. The pressure drop then decreased to a value of 9 psi by 2,500 L of feed water passed. These two lines had the greatest feed channel pressure drop of all the phases and it was noted upon autopsy that the membranes had begun to telescope. The inorganics line achieved a maximum feed channel pressure drop of 3 psi after 3,000 L of feed water was passed. The increase was linear over the duration of the phase. Feed channel pressure trends are displayed in Figure 46.

Retentate flows remained fairly constant throughout Phase IV. In the inorganics line, retentate flow started at 500 mL/min and gradually increased to 540 mL/min throughout the operational timeframe. The combined and organics lines started at 460 mL/min and 490 mL/min, respectively. Retentate flows in both lines fluctuated throughout the experiments but ended at a value of 440 mL/min. Permeate flows for all three lines were initially 300 mL/min. The flow rates began to decline at the same rate. This rate increased for the combined and organics lines at 1,300 L feed water passed with the combined line having the greatest rate. The inorganics line permeate flow rate decreased at a constant rate throughout Phase IV. Flow data can be viewed in Figure 47.

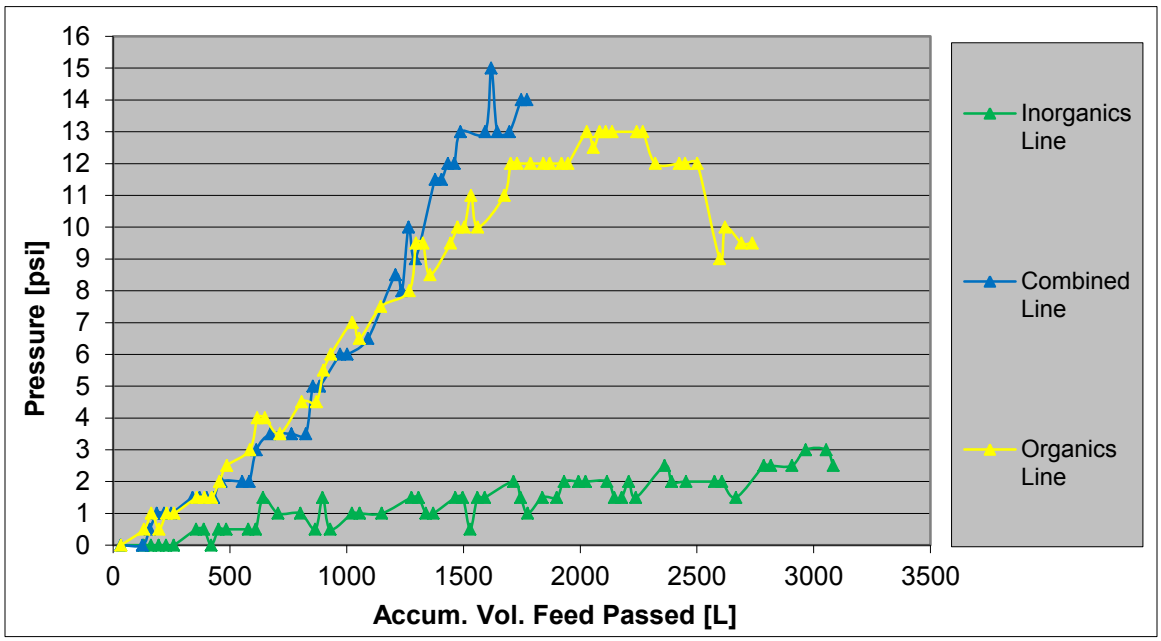

Figure 46: The increase in the feed channel pressure drop over the duration of Phase IV.

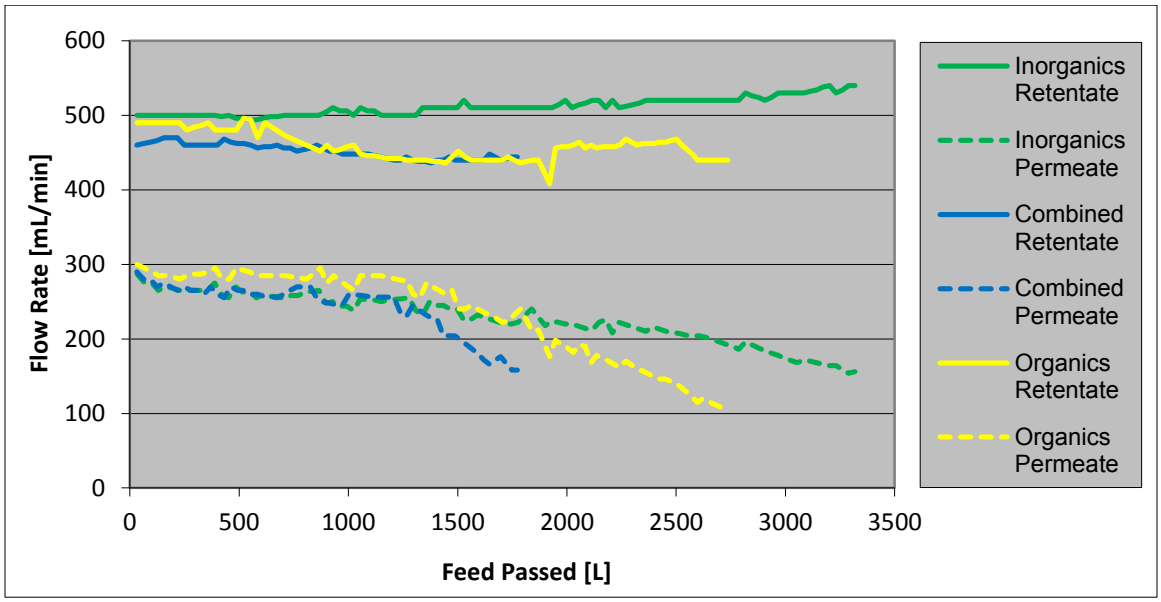

Figure 47: Retentate and permeate flow rates during Phase IV.

ATP Luminescence. Feed ATP values and trends were similar in all three lines except for a single spike in the combined line feed at 600 L of feed water passed. The difference between adjusted retentate ATP and feed ATP were equal in the inorganics line for the entire phase with only two minor exceptions. Adjusted retentate ATP began to surpass feed ATP after 1,000 L of feed water passed in the organics line. The ATP data in the combined line showed more fluctuation than the other two lines. Outside of the large spike in feed ATP, generally more ATP could be detected in the retentate than the feed for the combined line. Phase IV ATP data is displayed in Figure 48.

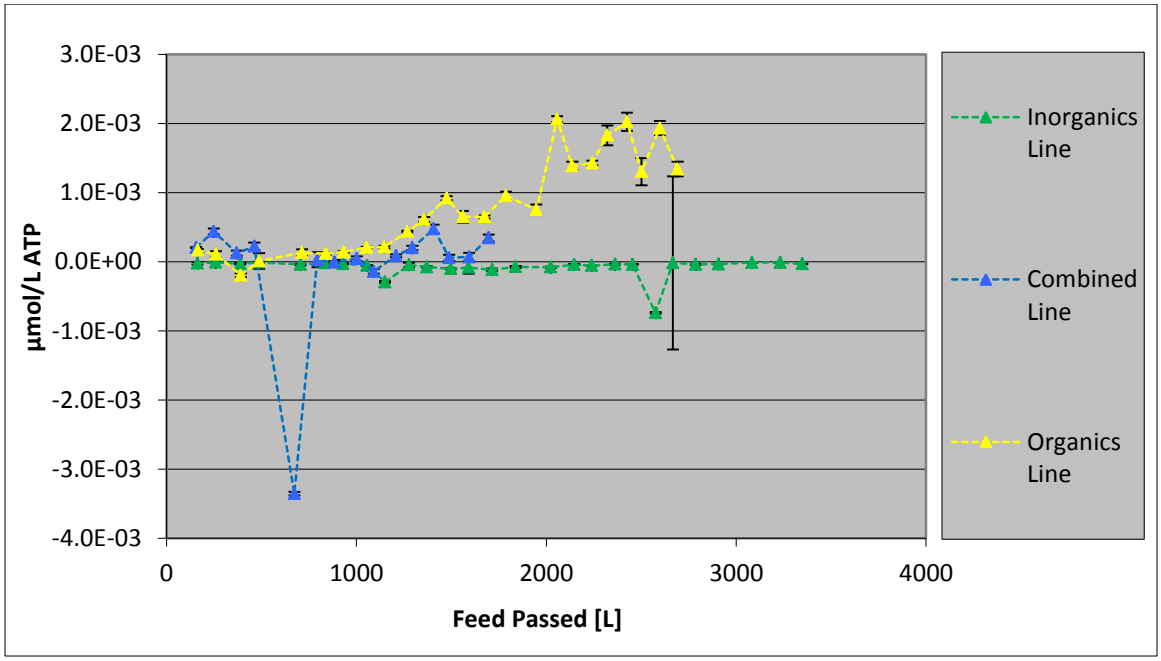

Figure 48: Difference between retentate and feed ATP (adjusted retentate ATP – feed ATP) during Phase IV.

Permeate ATP remained around the limit of detection for the inorganics line for most of the phase. Permeate ATP for the organics line began to increase at around 1,100 L feed water passed. The combined line had the highest permeate ATP during the first

1,000 L of feed water passed. As with the organics line, permeate ATP followed the same increasing trend at around 1,100 L of feed water passed.

HPCs. The difference between adjusted retentate HPCs and feed HPCs for the inorganics and combined lines were in the same order of magnitude for the duration of Phase IV. The opposite can be seen in the organics line. In this case, the adjusted retentate HPCs were an order of magnitude greater than the feed HPCs by 1,000 L of feed water passed. By 2,000 L of feed water passed, adjusted retentate HPCs had become two orders of magnitude greater than the feed water. Phase IV HPC data is displayed in Figure 49.

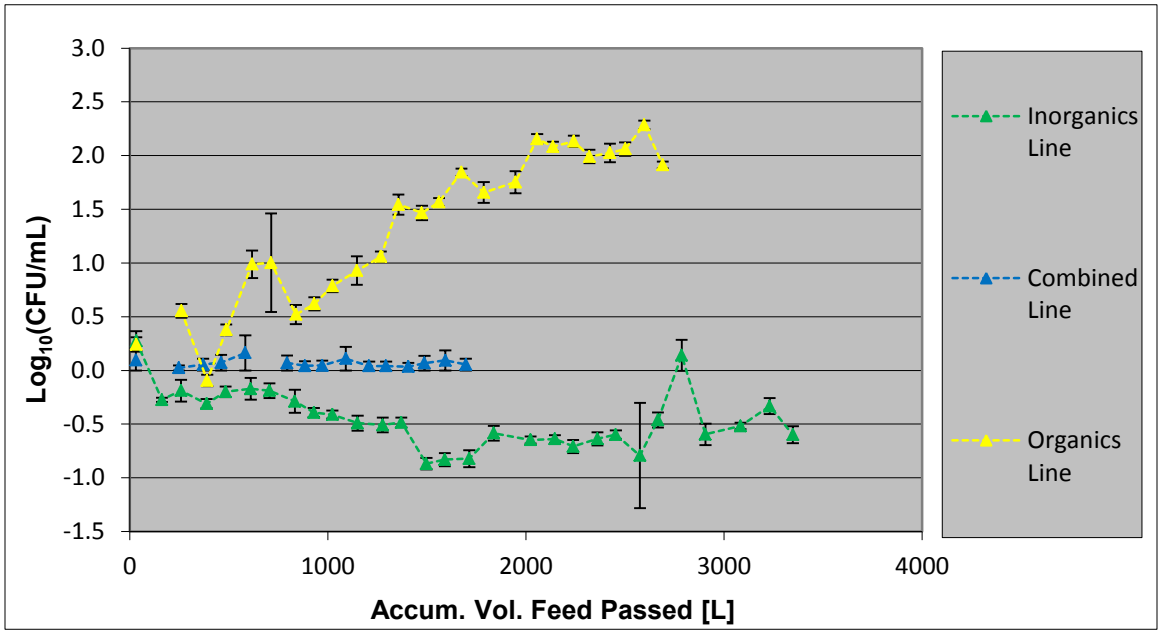

Figure 49: Difference between retentate and feed HPCs (adjusted retentate HPCs – feed HPCs) during Phase IV.

Combined and organics line permeate HPCs increased following the same trend. In these lines, permeate counts rapidly increased to 4.0 Log_{10}(CFU/mL). A plateau period was observed from 200 L to 1,200 L of feed water passed. After this point, permeate HPCs increased an order of magnitude to 5.0 Log_{10}(CFU/mL) by 1,700 L of feed water passed. Inorganic line permeate HPCs increased exponentially by two orders of magnitude (from 1.0 Log_{10}(CFU/mL) to 3.0 Log_{10}(CFU/mL) over the duration of the phase.

Direct Counts. Feed direct counts started between 1.00E+04 cells/mL and 5.00E+04 cells/mL for all lines. Feed counts gradually increased and plateaued at around 1.00E+05 cells/mL.The direct counts of the retentate for the inorganics line remained constant just short of 1.00E+05 cells/mL. Retentate direct counts for the combined and organics lines started at 1.00E+05 cells/mL. Around 800 L of feed water passed the retentate direct counts for these two lines began to increase. Counts in the organics line surpassed 1.00E+06 cells/mL while counts in the combined line approached 1.00E+06 cells/mL. Direct counts in the retentate of the combined line showed the most variability, often oscillating between 1.00E+05 and 1.00E+06 cells/mL.

Cell Clumping. Cell clumping analysis was performed in the retentate streams of each RO line. Three types of clumping analyses were performed: clumping based on percent total occurrences, clumping based on percent of total cells and concentration of clumps greater than 5 cells. In the combined line, no increases were observed based on percent occurrences. Single cells were around 83% of total occurrences while clumps between 2 to 10 cells and clumps >10 cells remained around 16% and 1%, respectively.

Distributions based on percent total cells exhibited a great deal of variation. In general no increasing trend was noticed. Single cells made up about 55% of total cells on average. Overall, the concentration of clumps > 5 cells did not increase in the combined line throughout the duration of the phase and remained around 2,500 clumps/mL. The maximum observed clump concentration was 7,500 clumps/mL and it was observed at 1,400 L of feed water passed.

No increases were observed based on percent occurrences in the organics line. Single cells were around 81% of total occurrences while clumps between 2 to 10 cells and clumps >10 cells remained around 18% and 1%, respectively. Distributions based on percent total cells exhibited a great deal of variation. In general no increasing trend was noticed. Single cells made up about 58% of total cells on average. The concentration of clumps > 5 cells in the organics line began to increase at around 1,000 L of feed water passed. The maximum observed clump concentration was 47,000 clumps/mL and it was observed at 2,400 L of feed water passed.

In the inorganics line, no increases were observed based on percent occurrences. Single cells were around 83% of total occurrences while clumps between 2 to 10 cells and clumps >10 cells remained around 16% and 1%, respectively. Distributions based on percent total cells exhibited a great deal of variation. In general no increasing trend was noticed. Single cells made up about 47% of total cells on average. Overall, the concentration of clumps > 5 cells did not increase throughout the duration of the phase and remained around 2,500 clumps/mL. Clump concentration data is displayed in Figure 50.

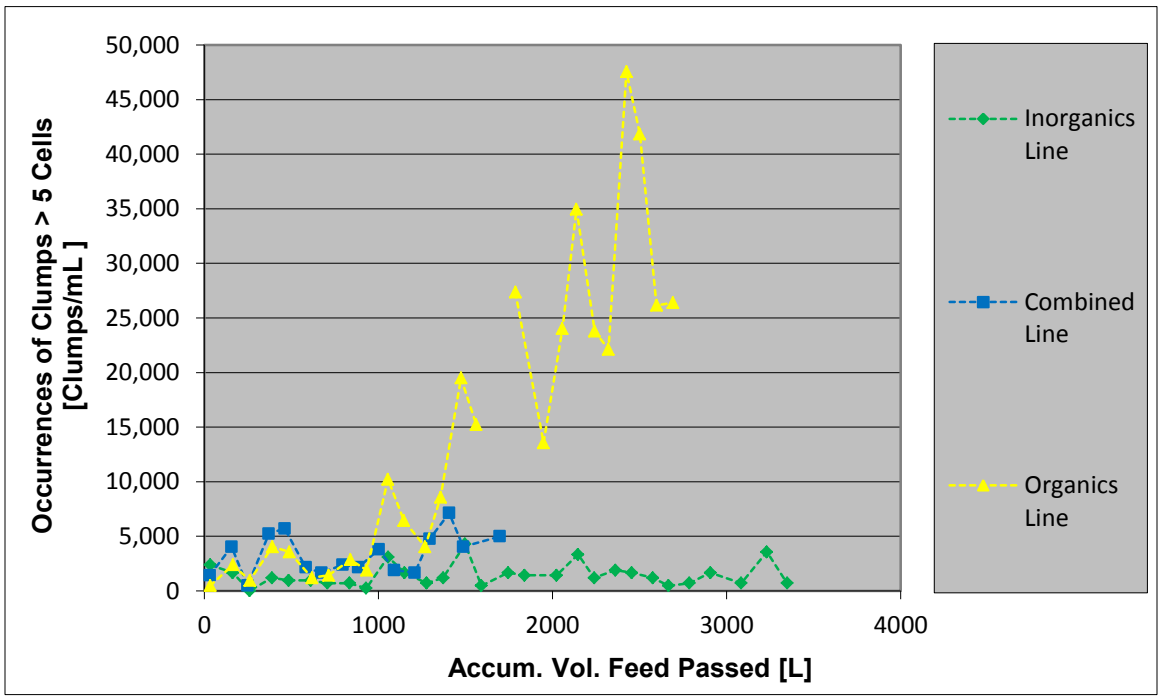

Figure 50: Retentate cell clumping throughout the progression of Phase IV.

Conductivity. Feed conductivity for the combined and organics lines remained consistent throughout the duration of Phase IV at values of 650 µmho/cm and 190 µmho/cm, respectively. Feed conductivity for the inorganics line displayed slight oscillation. The average value for the inorganics line was at 650 µmho/cm with minimum and maximum values at 600 µmho/cm and 700 µmho/cm, respectively

Retentate conductivity for the combined and inorganics lines was initially 970 µmho/cm. Conductivity in the combined line's retentate began to decrease at 1,000 L feed water passed. A decrease in the retentate conductivity of the inorganic line was noticed at around 2,000 L of feed water passed. The retentate conductivity on the organics line remained constant at 240 µmho/cm for the duration of the phase.

In the combined line, permeate conductivity began to increase at around 1,000 L feed water passed. Permeate conductivity began to gradually increase at around 1,500 L of feed water passed in the organics and inorganics lines. Phase IV conductivity data is displayed in Figure 51.

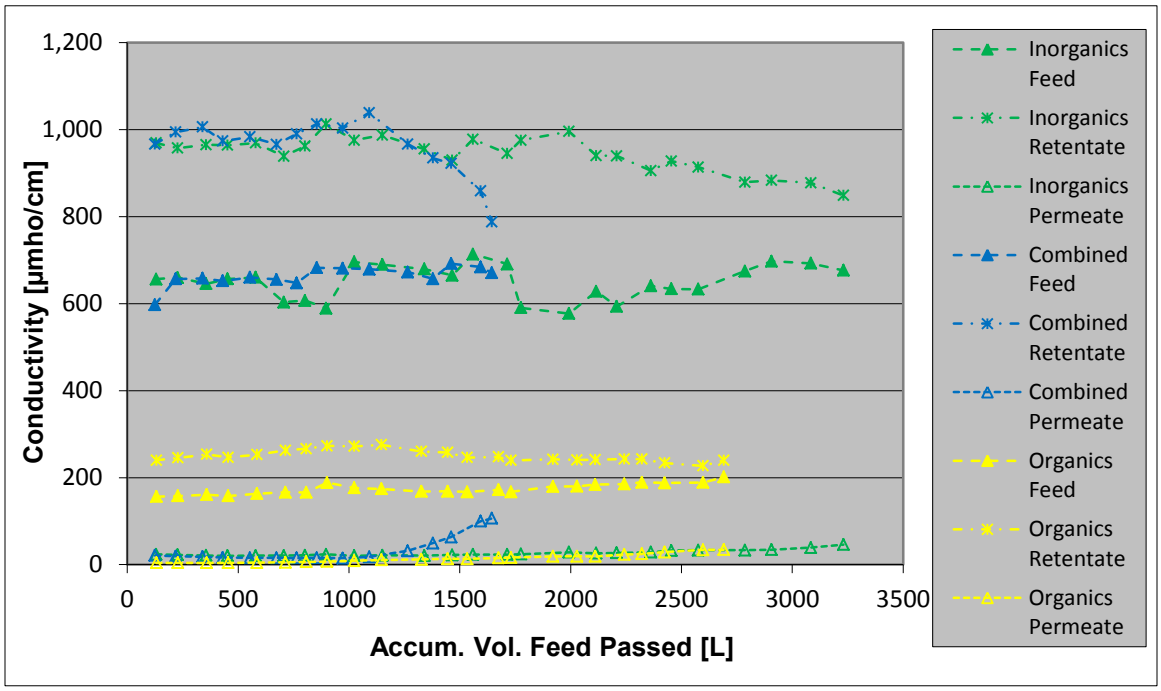

Figure 51: Change in conductivity throughout the progression of Phase IV.

Phase IV Autopsy Data

Results from all membrane autopsy analysis are shown below in Table 9. The results of the analyses indicate variability across the membrane. Visual observation of the combined and organics loaded membrane elements showed a marked difference from the inorganics loaded membrane element as seen in Figure 52 and Figure 53, respectfully.

Table 9: Summary of Phase IV autopsy data. Sample nomenclature is as follows (line # - sample location). Sample location 1 was at the beginning of the feed channel where feed water entered the membrane. Sample location 2 was at the center of the membrane. Sample location 3 was at the extreme end of the feed channel where retentate water exited the membrane.

Sample	Day Sacrificed	Analysis			
		ATP [µmol/cm^2]	HPC [CFU/cm^2]	Direct Counts [Cells/cm^2]	Protein [µg/cm^2]
Inorganics-1	110	6.50E-06	1.39E+06	2.06E+06	1.77E+00
Inorganics-2	110	8.14E-06	1.41E+06	4.07E+06	1.69E+00
Inorganics-3	110	6.45E-06	1.22E+06	8.22E+06	1.26E+00
Control	N/A	N/A	N/A	N/A	0.00
Combined-1	61	1.94E-04	6.76E+06	2.84E+07	3.32E+00
Combined-2	61	6.69E-05	3.24E+07	8.91E+07	8.93E+00
Combined-3	61	1.68E-04	4.29E+07	7.32E+07	1.33E+01
Control	N/A	N/A	N/A	N/A	1.90E-02
Organics-1	95	3.21E-04	3.59E+08	2.11E+08	4.26E+01
Organics-2	95	2.81E-04	3.74E+08	1.01E+08	4.62E+01
Organics-3	95	4.34E-04	2.64E+08	1.52E+08	4.33E+01
Control	N/A	N/A	N/A	N/A	2.96E-02

Figure 52: Phase IV combined and organics line autopsy photos. Left – Membrane telescoping observed in the combined line. Center – Membrane telescoping observed in the organics line and a great quantity of biomass on the front of the element and brine seal. Right – Fouling on the membrane surface of the organics line. The lighter colored areas along the edges are where flux does not occur. Flow direction is downward on the page.

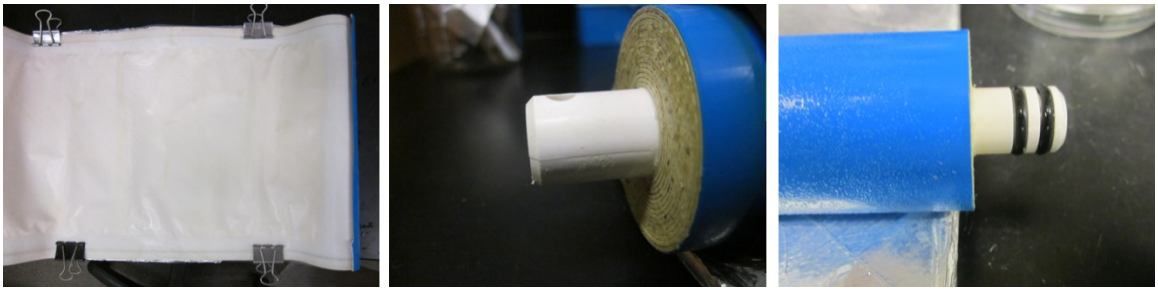

Figure 53: Phase IV inorganics line autopsy photos. Left – Fouling on the membrane surface which is notably much cleaner than those observed in the combined and organics line. Flow direction is downward on the page. Center – Feed side of the membrane element. Only minor quantities of biomass were observed. Right – Retentate end of the membrane. Deposits can be seen on the outside of the membrane.

Combined Loading. Images acquired from FESEM indicated biofilm growth on the membrane surface (Figure 54 and Figure 55). Almost no inorganic scalants could be seen. This was further validated by tests for calcium carbonate. Calcium carbonate only tested positive at the very end of the feed channel flow path where the effects of concentration polarization would be greatest. These results are in stark contrast to what was observed in Phase I (combined loading) where significant scaling was observed. This may be due to the fact that in Phase I the system ran 49 days with only a 2 ppm organics and 500 ppm inorganics concentrations in the feed water which may have allowed for significant scale formation during this timeframe.

The membrane had an average sessile ATP value of 1.43E-04 $\mu g/cm^2$. This value is comparable to the average observed in Phase II (organics loading). Sessile HPCs and sessile direct counts were also in the same order of magnitude as those observed in Phase II. This is indicative of a similar degree of biofouling or at least biological activity. Average sessile protein, on the other hand, was half of the value observed in Phase II. Sessile spacer ATP value averaged at 5.40E-05 $\mu g/cm^2$ and can be seen in Figure 56.

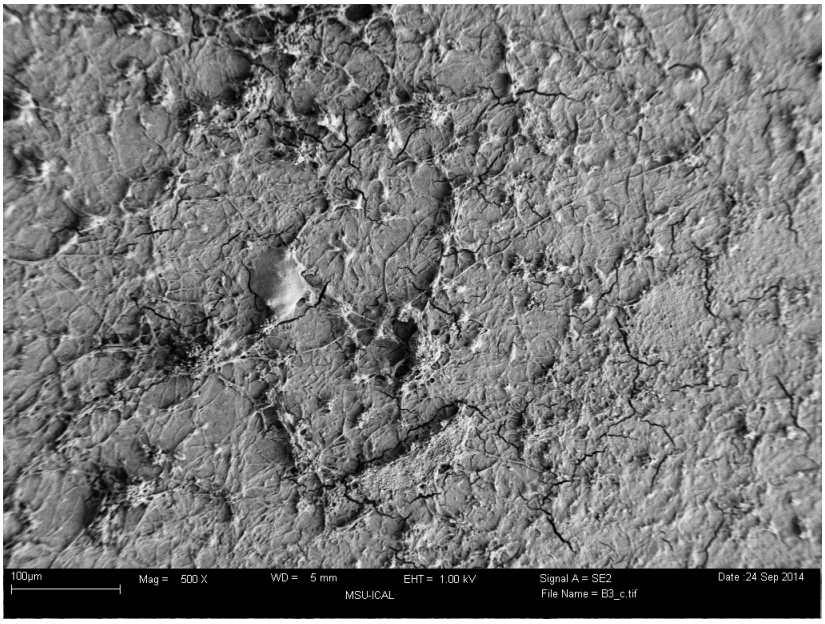

Figure 54: Fouling after membrane failure of the combined line at 500 X magnification. Note the absence of any crystalline deposits which is in stark contrast to what was observed in Phase I

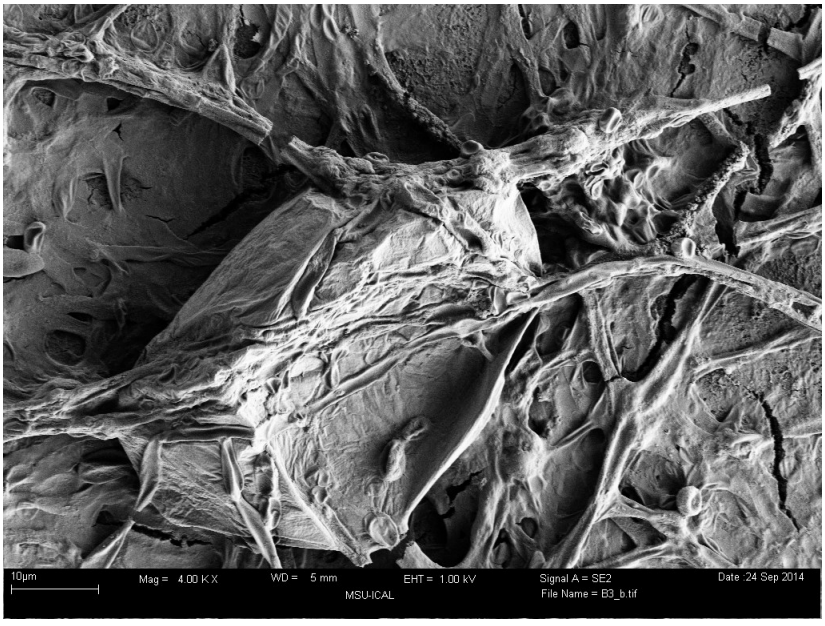

Figure 55: Fouling after membrane failure of the combined line at 4.00 kX magnification. Biofilm has covered the membrane surface and what appears to be an inorganic deposit.

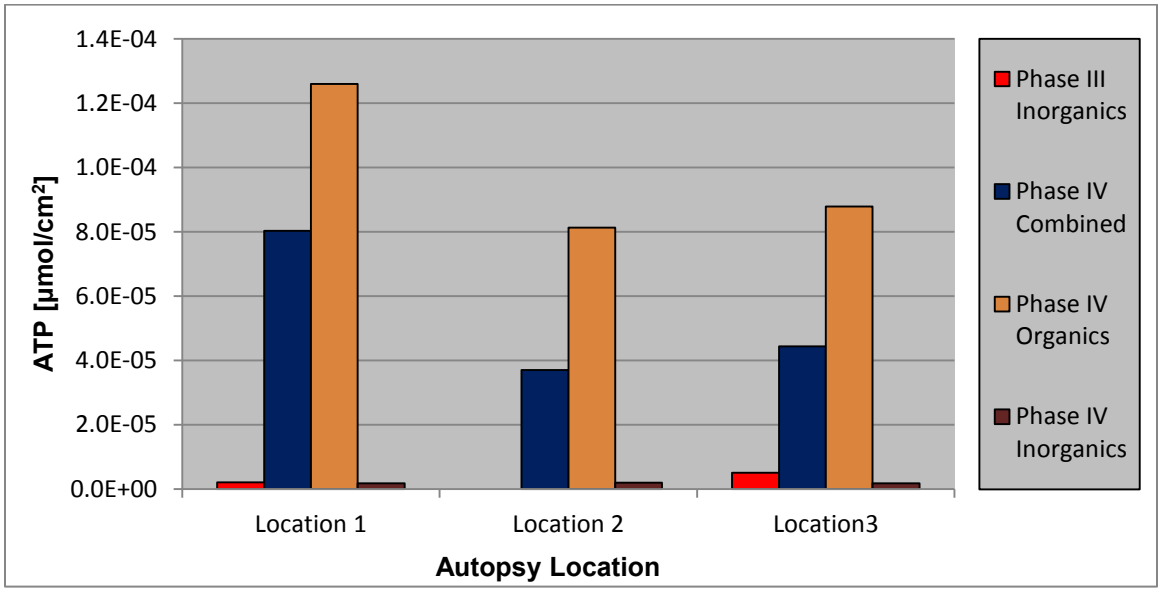

Figure 56: Sessile spacer ATP after membrane failure. Sample location 1 was at the beginning of the feed channel where feed water entered the membrane. Sample location 2 was at the center of the membrane. Sample location 3 was at the extreme end of the feed channel where retentate water exited the membrane.

This value is thirty times greater than the values observed in membranes with inorganic fouling. This is indicative of biofilm growth on the feed channel spacer.

Autopsy evidence suggests that biofouling was the primary mechanism of membrane failure and that inorganic scaling was not widespread enough to be a significant detriment to membrane performance.

Organic Loading. Images acquired from FESEM indicated biofilm growth on the membrane surface (Figure 57 and Figure 58). No inorganic scalants could be seen. This was further validated by tests for calcium carbonate, where no positive tests were observed on any of the membrane samples. Biofilm morphology was significantly different from the morphology displayed in Phase II. Images from this phase indicated an elaborate biofilm consisting of layer upon layer of strand-like structures. The images

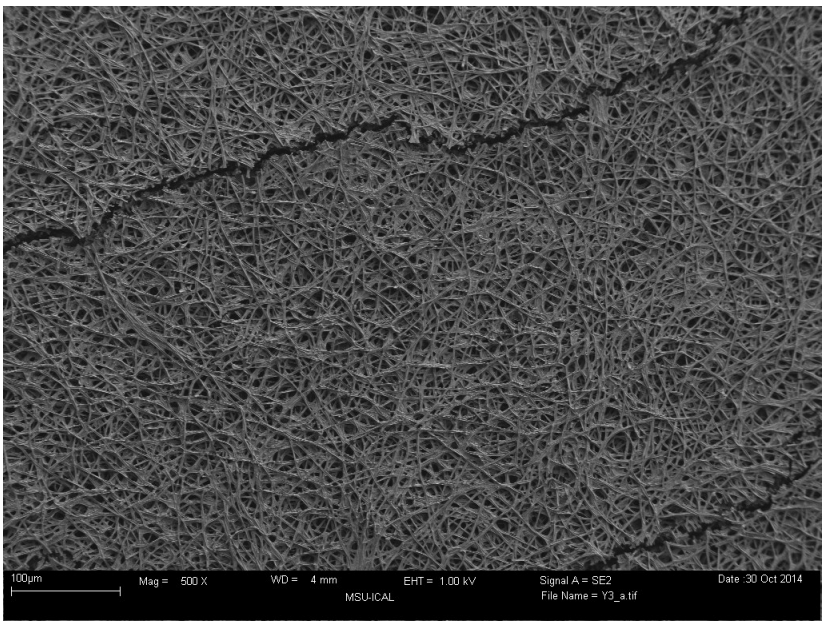

Figure 57: Fouling after membrane failure of the organics line at 500 X magnification. Layers of the strand like biofilm can be seen. The cracks are due from the drying process.

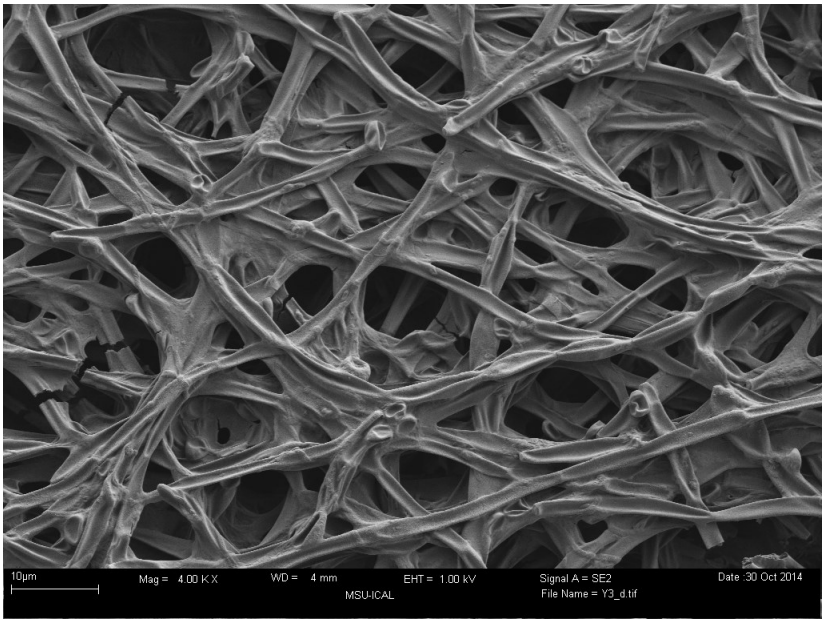

Figure 58: Fouling after membrane failure of the organics line at 4.00 kX magnification. More detailed view of the biofilm can be seen in this image.

from Phase II indicated a biofilm consisting of fluffy pillows of cells embedded in EPS. Difference in morphology may be related to the conditions in which the biofilm developed. In the final membrane replicate of Phase II, the brine seal was damaged during operation. This allowed for preferential flow around the outside of the membrane thus reducing the shear force experienced by the biofilm on the membrane surface.

The membrane had an average sessile ATP value of 3.45E-04 $\mu g/cm^2$. This is the highest value observed on any membrane throughout the project. Sessile HPCs and sessile direct counts further support the ATP data since they are also the greatest values measured on any membrane. Furthermore, sessile spacer ATP values were the greatest observed at a value of 9.84E-05 $\mu g/cm^2$ indicating the most severe biofilm growth on the feed channel spacer.

Autopsy results strongly suggest that biofouling was the predominant contributing factor to membrane fouling. Inorganic scalants could not be found in any FESEM image nor were they detected in the tests for calcium carbonate indicating no significant role in membrane failure.

Inorganic Loading. Images acquired from FESEM indicated inorganic fouling on the membrane surface (Figure 59 and Figure 60). This was further validated by tests for calcium carbonate in which every membrane sample tested positive. The degree of inorganic fouling was comparable to that seen on the final membrane of Phase III.

The membrane had an average sessile ATP value of 7.03E-06 $\mu g/cm^2$. This value is comparable and in the same order of magnitude to the average observed in Phase III (inorganic fouling). Sessile HPCs and sessile direct counts were also comparable to the

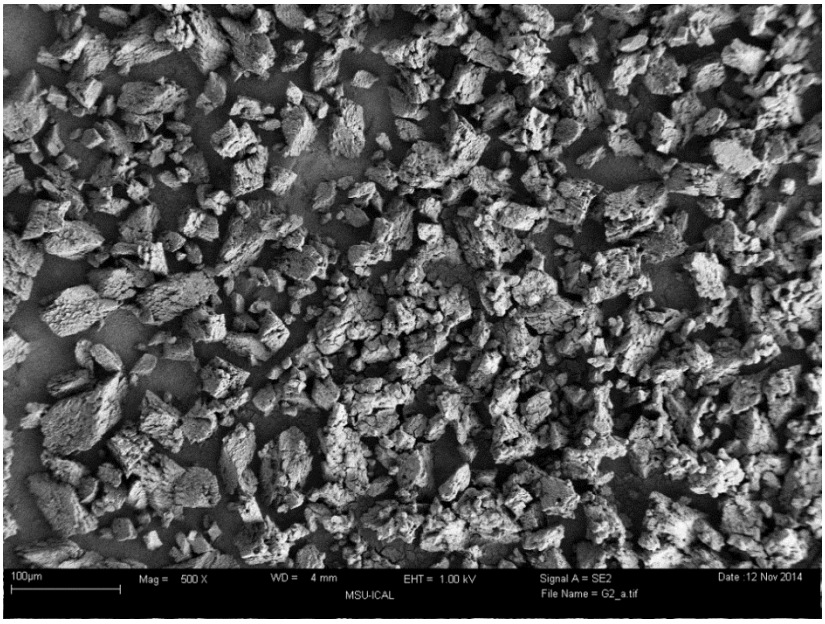

Figure 59: Fouling after membrane failure of the inorganics line at 500 X magnification. The membrane surface has been covered in scale much like that observed at Phase III failure.

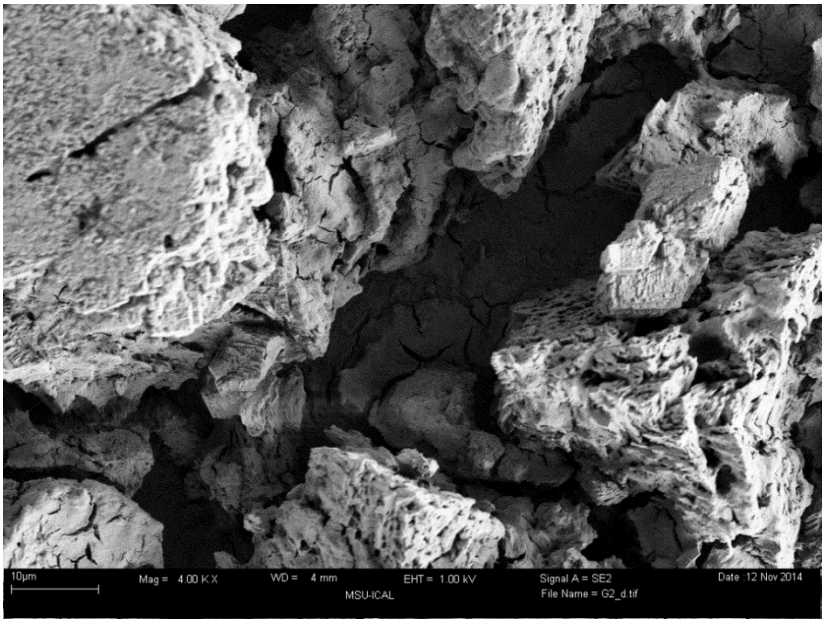

Figure 60: Fouling after membrane failure of the inorganics line at 4.00 kX magnification. This image displays a more detailed view of the scale on the surface.

values observed in Phase III. However, average sessile protein was twice the value observed at membrane failure in Phase III. Observed sessile spacer ATP had an average value of 1.90E-06 μg/cm^2 which was as less than value in Phase III indicating limited biofilm growth on the feed channel spacer.

Autopsy results suggest that biofouling was not a significant contributing factor to membrane fouling. The primary cause of membrane failure was inorganic fouling. This is apparent from the FESEM images and the very low quantities of the measured parameters that reflect biofouling.

Cryo Sections. Phase IV provided the unique opportunity to compare cryo sections for all three feed loading types. Cryo sections were taken from membranes that had reached failure. Interestingly, nothing could be seen except a clean membrane surface with the cryo sections taken from the combined loaded membrane. Luckily, cryo sections from both the organics and inorganics membrane provided results. On the organics loaded membrane, a biofilm can be seen. The average thickness of the biofilm was determined to be 40 μm with a standard deviation of 14 μm. On the inorganics loaded membrane, scale is visible. The average thickness of the scale was determined to be 23 μm with a standard deviation of 6 μm. Cryo section images for both the organics and inorganics lines are displayed in Figure 61.

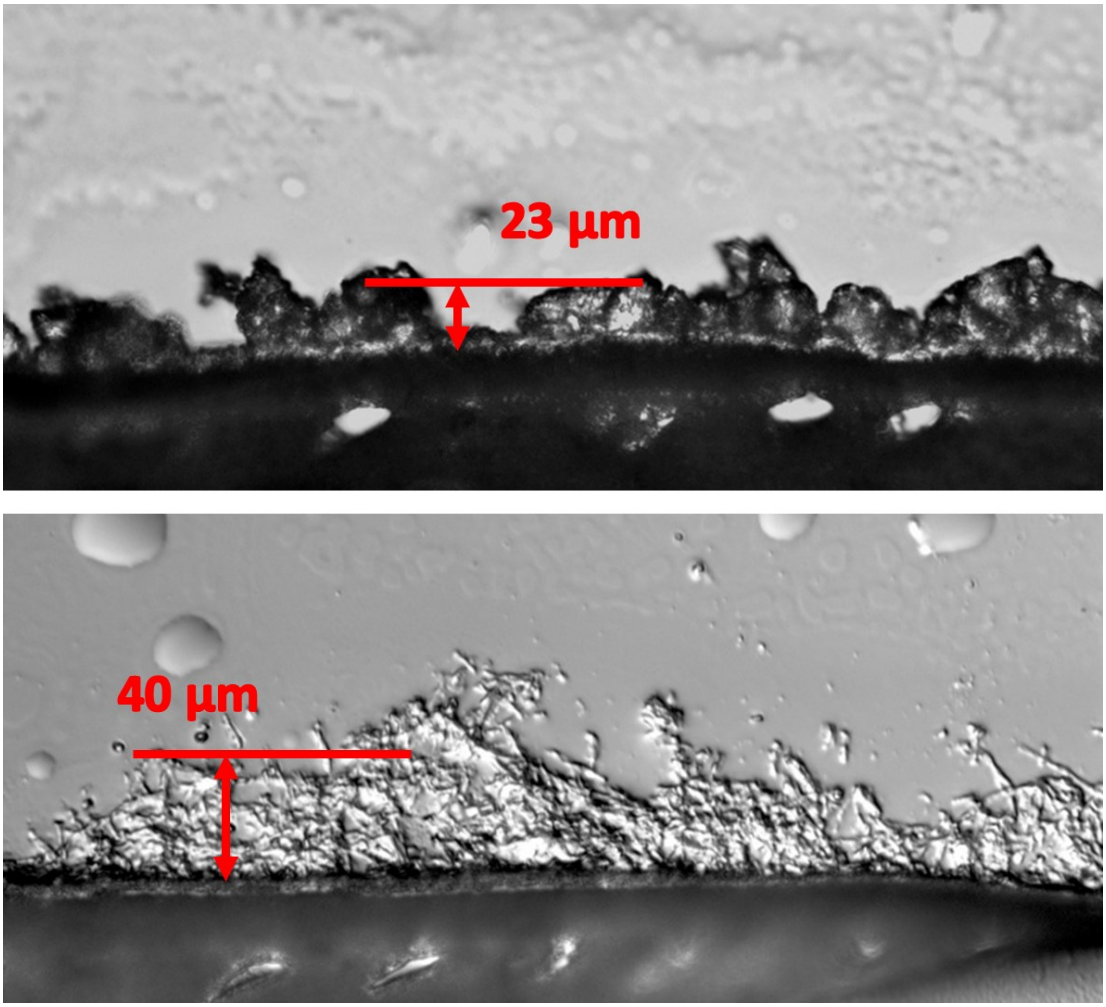

Figure 61: Cryo section images. Top – Inorganics loaded membrane experiencing inorganic fouling had an average foulant thickness of 23 µm. Bottom – Organics loaded membrane experiencing biofouling had an average biofilm thickness of 40 µm.

Autopsy Summary. Autopsies confirmed the degree and type of fouling in each membrane. In Phase IV, it was found that an organics only loading caused biofouling, and an inorganics only loading caused inorganic fouling. The exception was the combined loading in Phase IV, where the autopsy data suggested minimal inorganic fouling. This is in direct contrast to what was observed in the combined loading experiment in Phase I.

Statistical Analysis Results

Operational data for all the phases was combined and graphed so promising parameters for the non-destructive assessment of biofouling could be determined. Using Minitab v. 17, general linear models and ANOVAs were performed to determine if each parameter was statistically significantly different with respect to feed type. To determine if fundamental model assumptions were met, a Q-Q plot and a residuals plot were created. Unless noted otherwise in the following sections, all model assumptions were met.

Permeate F/F0

ANOVA analysis concluded that the ratio of permeate flow over the initial permeate flow (F/F0) and feed type interaction (slopes of the regression lines) was significantly different from each other based on feed type. Permeate flow rate ratio was determined to be a valid non-destructive parameter for determining the presence of biofouling. Figure 62 displays raw data analyzed with this model.

Permeate C/C0

Statistical analysis on the permeate conductivity indicated that the interaction between the ratio permeate conductivity to initial permeate conductivity (C/C0) and feed type (slope of the regression line) was significantly different between the combined and inorganic feed types and the organic and inorganic feed types. No significance was noted between the combined and organics feed types. Permeate conductivity ratio was determined to be a valid non-destructive assessment method since autopsy data indicated

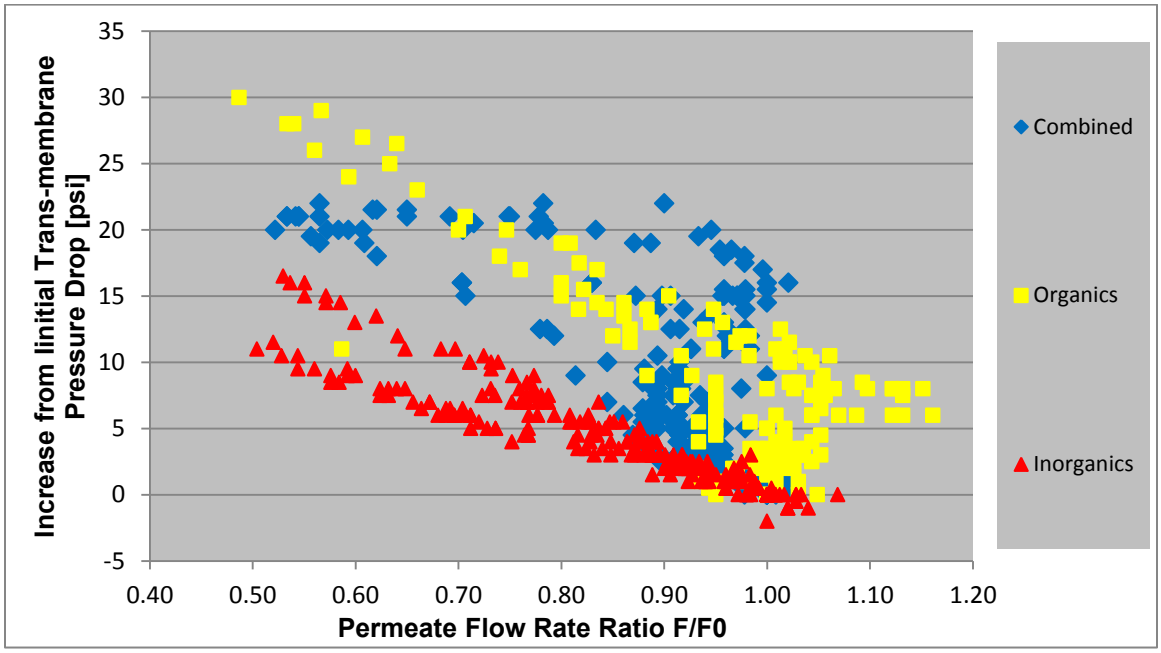

Figure 62: Increase in trans-membrane pressure drop vs. permeate flow rate ratio. Membranes loaded with inorganics only had a very linear decline in flux unlike the membranes suffering from biofouling (combined and organics loaded).

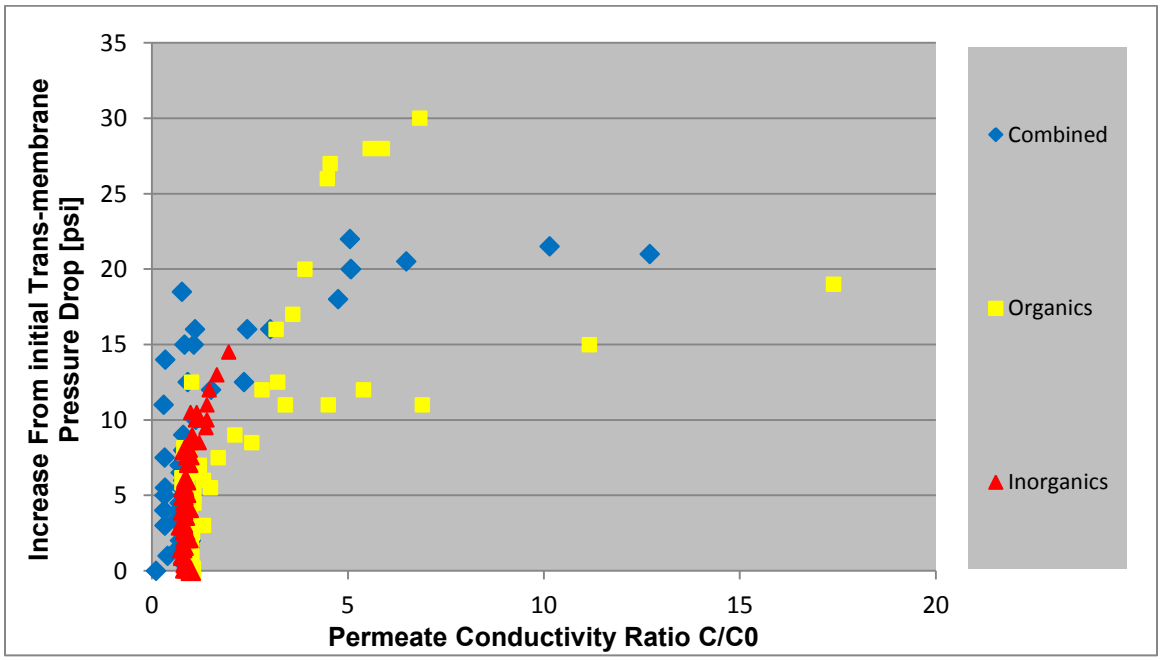

Figure 63: Increase in trans-membrane pressure vs. permeate conductivity ratio. Membranes suffering from biofouling experienced large increases in permeate conductivity compared to membranes that were inorganically fouled.

that biofouling occurred in both the combined and organics loading cases. Figure 63 displays raw data analyzed with this model.

Permeate F/F0 vs. Permeate C/C0

Statistical models were also performed on Permeate F/F0 vs Permeate C/C0. This was done by using the same type of model with the same fixed and nested random effects. The covariate was Permeate C/C0 and the interaction between covariate and feed type was still treated as the most important parameter of the model. The only difference was that Permeate F/F0 was the response instead of the increase in trans-membrane pressure drop.

Analysis results indicated that the interactions between Permeate C/C0 and feed type (the slope of the regression line) were all significantly different based on feed type. Permeate F/F0 vs Permeate C/C0 was determined to be a valid non-destructive method to assess the presence of biofouling. Figure 64 displays raw data analyzed with this model.

Retentate Cell Clumping > 5 Cells/clump

The Log_{10} transform of the retentate cell clumping data was taken to properly linearize the data. Once linearized, a statistical model was applied to the data set.

Statistical analysis indicated that the interaction between Log_{10} retentate cell clumping > 5 cells/clump and feed type (slope of the regression line) was significantly different between the combined and inorganic feed types and the organic and inorganic feed types. No significance was noted between the combined and organics feed types. The concentration of retentate cell clumps > 5 cells/clump was determined to be a valid non-destructive assessment method for biofouling since autopsy data indicated that

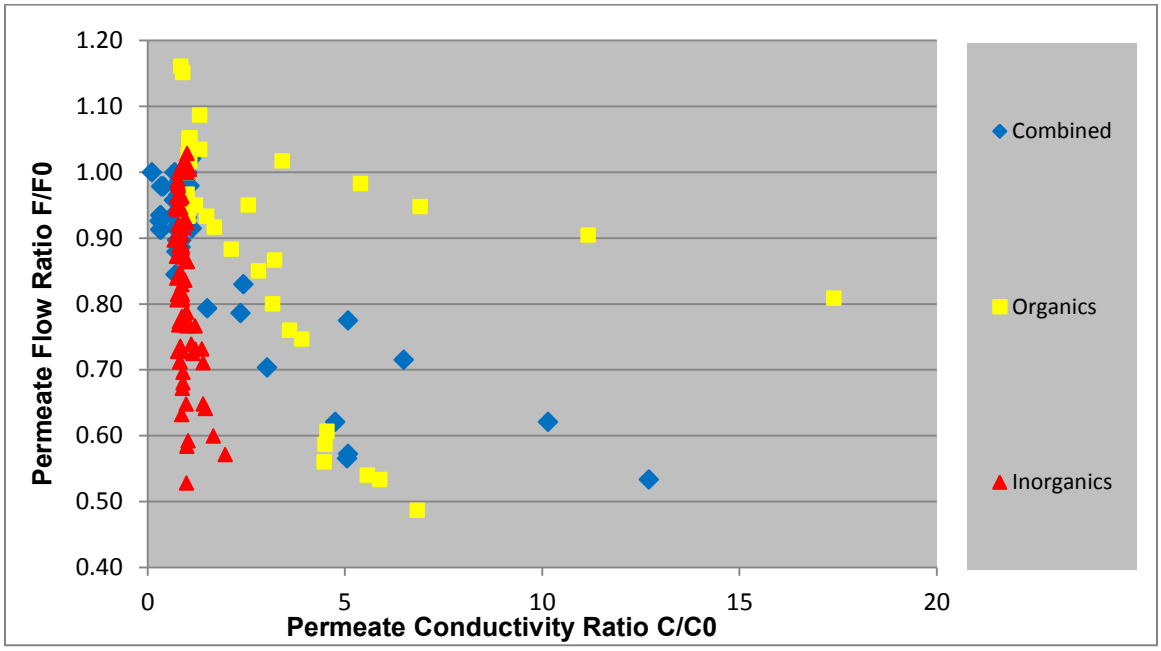

Figure 64: Permeate flow ratio vs. Permeate conductivity ratio. Membranes suffering from biofouling experienced a rise in permeate conductivity as flux decreased.

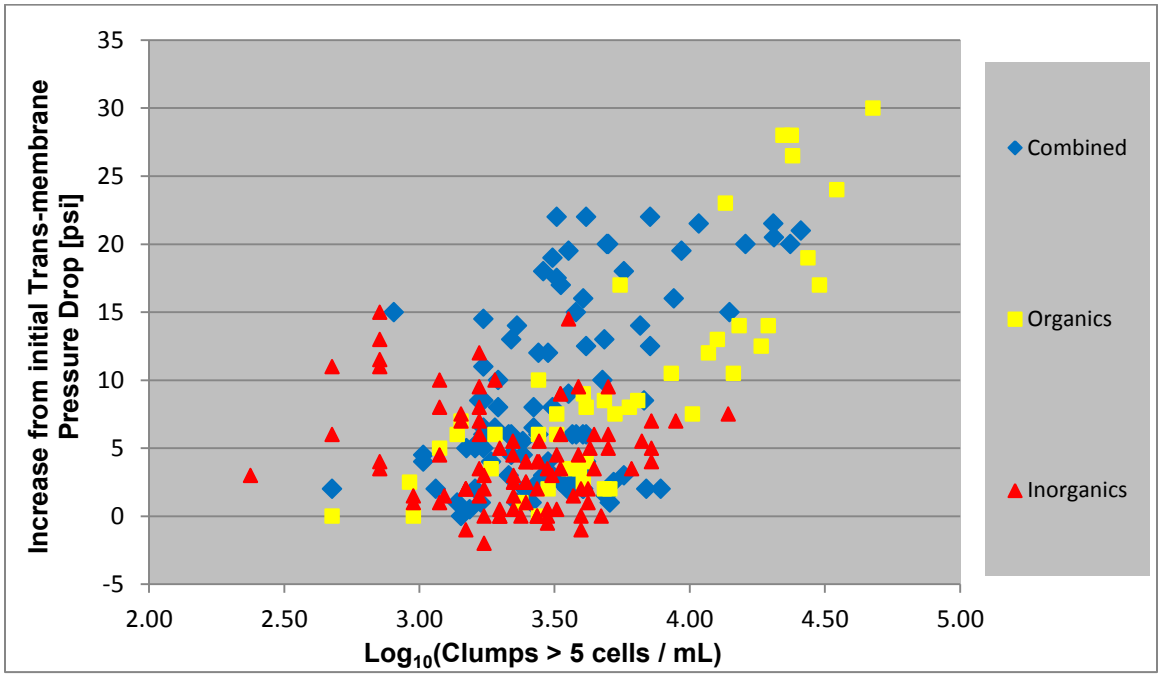

Figure 65: Increase in trans-membrane pressure vs. retentate cell clumping. In membranes suffering from biofouling, large retentate cell clumping values are observed at high trans-membrane pressures.

biofouling occurred in both the combined and organics loading cases. Figure 65 displays raw data analyzed with this model.

Feed Channel Pressure Drop

Statistical analysis indicated that the interactions between the increase in feed channel pressure drop and feed type (slope of the regression line) were not significant. This is understandable because similar feed channel pressure drop values were observed at similar increase in trans-membrane pressure drop values in all the explored fouling cases. However, this doesn't necessarily mean that it cannot be an indicator of biofouling. During Phase IV, the combined and organics loaded membranes experience feed channel pressure drops greater than 10 psi. The inorganic loaded membranes of Phase III and IV had a maximum feed channel pressure drop of 5 psi and 3 psi, respectively. Therefore, the magnitude of the feed channel pressure drop is more indicatory of biofouling than the interaction between the increase in feed channel pressure drop and feed type.

Change of Concentration from
Adjusted Retentate ATP to Feed ATP

Statistical analysis indicated that the interaction between the ATP difference and feed type (slope of the regression line) was only significantly different between the organics and combined feed types. No significance was determined between the inorganics and combined feed types and the inorganics and organics feed types. The change in concentration from the adjusted retentate ATP to feed ATP was determined not to be a reliable non-destructive assessment of biofouling.

Change of Concentration from Adjusted Retentate HPCs to Feed HPCs

Statistical analysis indicated that the interaction between the HPC difference and feed type (slope of the regression line) was significantly different between the combined and inorganic feed types and the organic and inorganic feed types. No significance was noted between the combined and organics feed types. The change of concentration from the adjusted retentate HPCs to the feed HPCs was shown to be a statistically valid method to non-destructively assess membrane biofouling since autopsy data indicated that biofouling occurred in both the combined and organics loading cases. However, this method is not viewed as practical because of the scatter in the data.

Change in Concentration from Adjusted Retentate to Feed Direct Counts

Statistical analysis indicated that the interaction between the direct count difference and feed type (slope of the regression line) was not significantly different between any of the feed types. The change in concentration from the adjusted retentate direct counts to feed direct counts was determined not to be a reliable non-destructive assessment of biofouling.

CHAPTER 5

DISCUSSION

System Operation Discussion

Combined Loading

The experimental design necessitated the replication of feed water characteristics either within or between phases. Of interest was knowing if similar feed waters led to reproducible operating conditions. The operational timeframe of the combined loaded membranes was different between Phases I and IV most likely due to the fact that Phase I employed a lower organics loading rate during the initial 49 days of operation. During Phase I, the membranes ran roughly 94 days passing around 2,800 L of feed water. Of that time, the system only operated at a loading of 10 ppm organics and 500 ppm inorganics for 45 days passing an average of 1,300 L of feed water. The initial 49 days, the system was processing feed water with 2 ppm organics and 500 ppm inorganics. The combined line of Phase IV operated at a consistent loading of 10 ppm organics and 500 ppm inorganics for its entire operational life of 56 days passing 1,700 L of feed water. The shorter operating time of Phase I at 10 ppm organics and 500 ppm inorganics is most likely due to fouling that occurred during the initial 49 days at lower organics loading.

Interestingly, the initial organics concentration in Phase I was a fifth of the final organics concentration. One fifth the operational time under the lower organics concentration is 10 days and 300 L of feed water passed. Adding these calculated values to the operational time at 10 ppm organics results in an operational timeframe of 55 days

and 1,600 L of feed water passed which is remarkably similar to the combined loading line of Phase IV.

Organic Loading

The final membrane replicate of Phase II operated for 88 days and passed 2,600 L of feed water at 10 ppm organics and 150 ppm inorganics (background TDS from BAC water). This is very comparable to the operational life of the organics loaded membrane in Phase IV which ran 81 days and passed 2,400 L of feed water. This indicates that the general rate of fouling was very similar between the phases.

Inorganic Loading

The similarities between operation lifespans in the combined and organics loading cases were not observed with the inorganics only loaded membranes. The final membrane replicate of Phase III (inorganics only) operated 173 days and passed 5,100 L of feed water before failure was achieved. The inorganics loaded line of Phase IV operated for a shorter time, running 110 days and passing 3,400 L of feed water before membrane failure was achieved.

System Operation Conclusions

Overall, the membrane units performed remarkably similar in respect to the types of feed water loadings they received. Membranes with combined loading had the shortest lifespans. Lifespans are also comparable between phases in the combined loaded cases if only the time Phase I operated at 10 ppm organics in the feed water is considered. Membranes experiencing only organic loading had very comparable lifespans between

the phases. Unfortunately, lifespans cannot be compared between the phases for membranes experiencing inorganics only loading. Here the difference in time between failures was around 60 days.

Review of the operational data suggests that pump failure events did not have an overall long lasting negative effect on system performance or alter the general trends of the data. These types of failures were often caught quickly, the longest being two days due to a holiday. The only failure to have significantly impacted the performance of the system was the brine seal failure in Phase II. This failure is most unfortunate, but also indicates that many of the following methods can still be applicable under extraneous circumstances. Ideally, more replicates should be run so better feed channel pressure drop data can be acquired.

Autopsy Discussion

Autopsy analysis can be broken into biological indicators and scaling indicators. Biological indicators consisted of sessile ATP, spacer ATP, HPCs, direct counts, protein, carbohydrates, TOC and volatile solids. Scaling indicators consisted of sessile total solids, inorganic carbon, and calcium carbonate. Significant problems were encountered with the sessile total and volatile solids and the sessile organic and inorganic carbon which are detailed in Appendix E and Appendix G, respectively. FESEM and cryo sectioning were performed to visualize the fouling layers.

Because of experimental design, it is only possible to compare autopsy results for all three feed loading conditions at the final autopsy point (after membrane failure); combined loaded autopsy data exists only at membrane failure. Autopsy data confirms

that biofouling was present in the combined and organics loaded membranes. No clear trends between the biological indicators on individual membranes could be determined. That is to say, if one membrane had the highest recorded sessile ATP at a certain sample location; it did not necessarily have the highest sessile protein, HPCs, or direct counts at that location. One trend was very clear throughout the autopsy data at membrane failure. The measured quantities of the biological indicators were at least an order of magnitude greater in membranes subjected to combined and organics loading than those subjected to an inorganics only loading. This is strong evidence that supports the statistical models using feed type to differentiate between biofouling and inorganic fouling. Autopsy analyses also indicate that each feed loading condition resulted in the desired fouling type in all cases except for one. The exception was the combined loading in Phase IV were inorganic fouling was just not obvious.

The progression of fouling can be viewed with autopsy data obtained in Phases II and III since autopsies were staggered throughout the systems lifespan. The biological parameters in Phase III remain virtually constant throughout the progression of the experiment. Of more interest is the progression of the biological indicators in Phase II. Between the first autopsy time point (~1/3 system life span) and the second autopsy time point (~2/3 system life span), sessile ATP, protein, and carbohydrates increased by two orders of magnitude. FESEM images taken during the second autopsy also show that at this point, the majority of the membrane surface has been colonized by biofilm. Most of the analyzed parameters did not show divergent trends between feed loading types until 2/3 the maximum trans-membrane pressure drop was achieved. This means that these

methods are not sensitive enough to be used for predicting biofouling since biofouling was well established by the time divergent trends were noted. However, they are more than adequate to assess if it is biofouling that is negatively impacting the system.

Operational Data Discussion

Pressure

Two types of pressure were measured in all of the experimental phases. Trans-membrane pressure drop was the pressure drop from the feed line to the permeate line caused by the resistance of the membrane and the presence of fouling layers. Feed channel pressure drop is the pressure drop along the feed channel due to fictional resistance of the feed channel spacer combined with fouling layers (Vrouwenvelder et al., 2011a).

Trans-membrane Pressure Drop. Trans-membrane pressure drop was observed for all membranes. As mentioned in Chapter 2, trans-membrane pressure drop can assess the severity of fouling, but it cannot determine the type of fouling. Given that it can be used to assess the degree of fouling, it was chosen to be the response in the statistical models.

Of all the pressure measurements, trans-membrane pressure was the most accurate since it did not involve compounding errors from subtracting pressure measurements. This was possible since the permeate discharged at atmospheric pressure, which would not be the case if the permeate line was plumbed into a pressure vessel like in many other systems.

Feed Channel Pressure Drop. It was originally thought that feed channel pressure drop would be a key indicator of biofouling since extensive research by Vrouwenvelder et al. (2011a) has linked the growth of biofilm on the membrane's feed channel spacer to increased feed channel pressure drop. However, they also noted that feed channel pressure drop is not entirely exclusive to biofouling and can be seen in other fouling cases. The presence of an increase in feed channel pressure drop was also noted for all fouling cases in this experiment.

In the statistical analysis, interactions between the feed type and feed channel pressure drop were not significantly different between the feed types. This means that at similar trans-membrane pressure drops, the feed channel pressure drops were also similar making it independent of the type of fouling. However, experimental results indicated the real difference may not be in the degree to which the feed channel pressure drop increased with respect to trans-membrane pressure drop but in the magnitude of the feed channel pressure drop. Phase IV combined and organics loading feed channel pressure drops had a maximum value of 14 psi and 13 psi, respectively. This is 3 times greater than the maximum observed feed channel pressure drop (5 psi) associated with inorganics only loading.

Results from the experimental phases also showed that feed channel pressure drop was variable between phases given similar feed types. Phase I (combined loading) maximum feed channel pressure drop was 7 psi while the combined line of Phase IV had a maximum value at 14 psi. The inorganics loaded membranes had the most consistent feed channel pressure drops at maximum values of 5 psi and 3 psi for Phases III and IV,

respectively. Due to a brine gasket failure in the final membrane replicate of Phase II (organics loaded), no maximum feed channel pressure drop value could be recorded.

Large variability in feed channel pressure drop values may be due to the way they were measured and calculated. This was done by subtracting the retentate pressure from the feed pressure which was measured from separate gauges. This compounds any associated measurement errors or gauge calibration errors. Ideally, differential pressure gauges should be used for this type of measurement as recommended by Vrouwenvelder et al. (2011a). However, advanced instrumentation on these types of household membrane systems are not economical.

Feed channel pressure drop is also not sensitive enough to be used as an early warning for biofouling and cannot be exclusively linked to biofouling (Vrouwenvelder et al., 2011a). This is adequately reflected in the data collected during this experiment given that the inorganically fouled membranes had a maximum feed channel pressure drop of 5 psi. Furthermore, feed channel pressure drop greatly depends on the proper seating and performance of the brine seal. This was observed in the last membrane replicate of Phase II, since no feed channel pressure drop was observed when this gasket malfunctioned.

Other Pressure Consideration. Other inherent difficulties of pressure measurement must be noted. Foremost is that the stock pressure gauges that are packaged with these household systems are of low quality and suffer from severe calibration errors which will be detrimental when it comes to measuring feed channel pressure drop. The stock gauges also do not handle pressure pulsations well which will make them useless in household

systems that employ a RO booster pump. During initial setup, rapid oscillations in the pressure gauges (upwards of 20 psi) were observed during pump operations, which would make any pressure measurement a guess at best. This problem was overcome by using liquid filled gauges and pulsation dampening snubbers to mitigate the pressure pulsations from pump operations. Changes in these components may not be economical for field systems. At current stock configuration, calculating pressure differentials is not a viable option for monitoring or assessing fouling.

Permeate ATP

In membranes with biofouling, ATP was detected in the permeate after 1,000 L of feed water had been passed. In membranes experiencing inorganic fouling, ATP remained around the limit of detection. Unfortunately, it is doubtful that this is indicative of biofouling because it might be more directly related to the type of feed water being treated. It was not possible to sterilize or keep the permeate lines sterile since the line discharged into the atmosphere. It is highly likely that detectable ATP resulted from the growth from either indigenous bacteria or contaminating bacteria on the downstream side of the membrane that were metabolizing organics that were able to pass through the membrane.

ATP, HPCs and Direct Counts

The difference between the adjusted retentate concentration and feed concentration of these three operational parameters was monitored. Retentate concentrations were adjusted to account for the calculated concentration of these constituents due to permeate production. It was hoped that a significant increase could be

observed in the retentate stream indicating growth or production of biomass across the membrane unit.

Collected data showed a great deal of scatter. Statistical analysis performed on the ATP and direct count data revealed no significance between feed types. Results for the HPCs indicated a significant difference between the inorganics feed type and the combined and organics feed types. All three of these parameters measure essentially the same thing and having one out of three parameters being statistically significant is not convincing. Experimental evidence strongly suggests that taking the difference between the influent and retentate numbers is too variable to be reliable. Variable data trends were also seen with research applied to full scale RO treatment plants were bacterial numbers were measured using flow cytometry (Dixon et al., 2012).

Flow Rates

Two flow rates, retentate and permeate, were measured throughout all the phases. Retentate flow rate was the flow rate of the concentrate or water that did not flux through the membrane. The permeate flow rate was the rate at which water fluxed through the membrane.

Retentate Flow Rates. Retentate flow rates were variable in all membrane lines with biofouling. In lines with inorganic fouling, retentate flows consistently and slowly increased over the duration of membrane operation. Given the lack of consistency in the lines with biofouling, retentate flow rates do not warrant additional discussion.

Permeate Flow Rates. Permeate flow rates decreased throughout system lifespan differently depending on the type of fouling. Membrane lines suffering from inorganic fouling had a gradual and linear decrease in flux over their lifespans. These inorganic fouling operational results are consistent with observations from another experiment where a very linear flux decline with respect to surface coverage of scale was seen during the development of the ex situ scale observation detector (EXSOD) (Uchymiak et al., 2009). Comparing FESEM images taken during Phase III with the measured flux, a clear and linear decline in flux can be seen as inorganic foulants become more predominant on the membrane surface. It also should be noted that inorganically fouled membranes reached failure due to the inability to meet permeate production thresholds.

A far different trend was observed with membranes experiencing biofouling (Phase I, Phase II, Phase IV combined, and Phase IV organics) than for those with inorganic fouling. In these cases, permeate production remained constant for the initial 2/3 of the membranes lifespan. Sometime afterwards, a breakpoint where the flux decreased dramatically was observed, although the time at which this occurred varied with individual lines. Similar operational characteristics were noted in studies done by Vrouwenvelder et al. (2011a) where they observed that biomass accumulation in membrane modules increased feed channel pressure drop before flux declined.

Phase I (combined loading) presented a unique case for monitoring membrane flux given that two different loading strategies were employed. During the initial 49 days of operation, feed loading was 2 ppm organics and 500 ppm inorganics. Given the similarity to the loading in Phase III (inorganics) it is strange that no linear decrease in

flux was observed over that period. Further differences can be seen when the feed loading was increased to 10 ppm organics and the 500 ppm inorganics remained constant. The lines still operated at constant flux until maximum trans-membrane pressure was achieved. This is unlike the performance characteristics observed in the other membrane lines experiencing biofouling (Phase II, Phase IV combined, and Phase IV organics) where flux began to drastically decrease before reaching maximum trans-membrane pressure.

It is difficult to determine why the permeate flux characteristics varied between inorganic fouling and biofouling situations. One hypothesis considers the performance of the flow restrictor. As the feed pressure in the system increases, the output flow rate of the booster pump decreases. In inorganic fouling cases, the retentate flow rate either gradually increased or remained constant. This resulted in the same rate of water leaving the membrane as concentrate throughout the life of the system but a decrease in the rate water was being delivered to the system as trans-membrane pressure increased. The mass balance on the system dictates that the permeate production is the variable that must give.

In biofouling cases, a decrease in retentate flow rates was usually observed as trans-membrane pressure increased. These decreases would enable permeate production to remain constant since the decrease in feed flow rate is being compensated by a decrease in retentate flow rate. Perhaps biofouling in the flow restrictor itself increased the degree at which it reduced the retentate flow. An unfouled flow restrictor (most likely seen in the inorganics only lines) appears to only restrict the retentate at a set limit. However, a flow restrictor that is being plugged with biomass ads an increasing degree of

retentate flow reduction allowing for the system to compensate against the decreased feed flow rate.

The dramatic decrease in flux may also be explained by increased biofouling of the feed channel spacer and membrane surface. Research has found that biofilm EPS increases hydraulic resistance and therefore decreases flux (Herzberg and Elimelech, 2007). Sessile feed spacer ATP data taken during Phase IV indicates a high level of ATP on the feed channel spacers of the combined and organics lines. Research with NMR has shown that biofilm growth on the feed channel spacer results in a multitude of negative operating consequences such as disruption of flow field homogeneity, dead zones (no fluid flow) in certain areas, development of preferential flow paths and back flow (Graf von der Schulenburg et al., 2008; Pintelon et al., 2010; van Loosdrecht et al., 2012; Vrouwenvelder et al., 2011a). These problems were most likely experienced as seen by the large feed channel pressure drops in the combined and organics lines of Phase IV. Due to the brine gasket failure, Phase II most likely saw back flow and dead spaces due to the preferential flow around the outside of the membrane element. Simulations have shown that dead zones and preferential flow paths increase the solute residence time leading to local accumulation of water with higher total dissolved solids (TDS) (Picioreanu et al., 2009). A substantial rise in salt concentration increases the trans-membrane osmotic pressure and consequently decreases flux (Herzberg and Elimelech, 2007).

Other Flow Rate Considerations. Statistical models indicated a significant difference in how the ratio of permeate flow to initial permeate flow changed based on

feed loading type as trans-membrane pressure drop increased. This makes this parameter a good non-destructive assessment of biofouling when it is coupled with trans-membrane pressure measurements. Furthermore, permeate production is also very easy and inexpensive to measure. A graduated cylinder and an accurate stopwatch is all that is needed making these measurements extremely economical.

Permeate Conductivity

In membranes with biofouling, significantly greater increases in permeate conductivity were observed than in membranes suffering from inorganic fouling only. Membranes afflicted with biofouling reached failure due to the inability to meet permeate quality thresholds in all cases except for one, the organics line in Phase IV. In this case, reduction in permeate production reached the experimental failure condition first, but by this time, TDS removal was very near 75%.

As noted earlier, autopsy analysis of the membranes with advanced biofouling (Phase I (combined), Phase II (organics), the combined line of Phase IV and the organics line of Phase IV) show that membrane surfaces had at least an order of magnitude more sessile ATP than membranes experiencing inorganic fouling. Research has shown that upon the development of a biofilm, an increase in salt concentration near the membrane surface led to increased salt transport across the membrane (Herzberg and Elimelech, 2007). They also found that the increase in salt concentration elevates the trans-membrane osmotic pressure which consequently decreases fluid flux. A decrease in permeate flux further increases the permeate salt concentration. This is because salt passage is a function of the salt concentration and the membrane salt permeability

constant which is dependent on the type of salt and the membrane's chemical makeup. If the salt concentration was to remain constant but H_2O flux decreased, an increase in salt concentration would be noted in the permeate. In essence, biofouling has a two pronged negative effect on permeate conductivity. It increases the salt concentration near the membrane surface which increases salt transport across the membrane and it reduces permeate flux which decreases the degree of which the passed salt in the permeate gets "diluted."

Retentate Cell Clumping

An increase in the concentration of cell clumps in the retentate stream was noticed in all membranes experiencing biofouling except for the combined loaded membrane of Phase IV. Outside of the exception, membranes experiencing biofouling had the highest observed clumping values. Statistical analysis confirmed that clump data was significantly different between membranes experiencing biofouling compared with those only experiencing inorganic fouling.

With membranes from Phase I and the organically loaded membrane of Phase IV clump values pushed or surpassed 50,000 clumps/mL. In these four lines, the averaged maximum clumping value during advanced biofouling (last 1/3 of system lifespan) was around 40,000 clumps/mL Clump values in Phase II were lower with a maximum observed value of 25,000 clumps/mL. A possible explanation of the lower observed value could be due to the failure of the brine seal which resulted in preferential flow outside of the membrane thus reducing the shear forces any biofilm would experience inside the membrane unit. The reduced shear within the membrane unit may have

resulted in reduced sloughing of biofilm. With the membranes only experiencing inorganic fouling and the combined loaded membrane of Phase IV, clumping values generally were less than 5,000 clumps/mL and only twice was a clumping value of over 10,000 clumps/mL observed. The first instance which happened in Phase III at 650 L feed passed was most likely the result of a pump failure where the system sat stagnant for two days. Not enough time was allowed to flush out all the extra bacterial growth so high clumping values were observed.

Cell clumping may also be applicable in large scale treatment plants. When flow cytometry (FCM) was applied at the Adelaide Desalination Plant, it was noted that FCM was limited if cells where agglomerated (Dixon et al., 2012). This poses problems with the use of FCM in biofouling assessment since Behnke et al. (2011) found that at most, only 33% of the total effluent cells in biofouled tube reactors existed as single cells. In this study, it was found that around 45% of the total cells in the system existed as single cells. Perhaps it would be easier and more beneficial to monitor cell clumping in a full sized system instead.

Hydrogen Sulfide

In membranes that experienced significant biofouling, a "rotten egg" smell could be noticed coming from the initial slug of retentate water upon system startup after stagnation. This smell is indicative of the presence of hydrogen sulfide from the biological reduction of sulfate. This smell was documented in all Phases except for Phase III (inorganic fouling). Also, this smell was not noted in the inorganically fouled membrane of Phase IV.

The smell of hydrogen sulfide was noticed towards the extreme end of the membrane lifespan of membranes experiencing biofouling. In Phase I, it was noted around day 96 of the experiment or around 2,900 L feed water passed. In Phase II the smell was noticed at around 2,400 L of feed passed. Attempts were made in Phase IV to quantify hydrogen sulfide in the retentate but failed. The methodology and discussion of this endeavor can be found in Appendix D.

Sulfate reduction occurs in anaerobic conditions. However, feed water conditions were aerobic. Therefore, for sulfate reduction to occur in these membrane systems, biological activity would be needed to change the redox conditions that existed initially in the feed water. The membrane systems in this experiment were point-of-use systems which generate water on demand. When no water production is demanded, they sit stagnant with a slug of unprocessed feed water inside the membrane units. In the case of this experiment, the stagnation period lasted for eight hours. This is plenty of time, given enough biological activity, to change the redox environment within the system to allow sulfate reduction. In the early stages on the system lifespan and in cases with inorganic fouling only, not enough biomass was present to create favorable redox conditions. However, redox conditions were met for sulfate reduction in systems shown to have significant biofouling and thus the odor of hydrogen sulfide could be detected in the retentate stream. Note that the production of hydrogen sulfide may be different in systems with lower organic loading rates; these experiments were done with 10 ppm, which exceeds normal operating conditions.

Operational Data Conclusions

Analysis of the data collected over the four experimental phases suggests several parameters that can be monitored to non-destructively assess biofouling. Permeate F/F0, permeate C/C0, retentate cell clumping, and the difference from adjusted retentate to feed HPCs were all found to be statistically significant non-destructive indicators of biofouling. The difference from adjusted retentate to feed HPCs was treated with high skepticism since two other similar analyses were found not to be significant and will not be recommended. Feed channel pressure drop was not found to be statistically significant but will be recommended since experimental evidence strongly suggests that there is a large difference in the observed magnitudes between membranes with biofouling and inorganic fouling. However, concerns were raised when calculating pressure differentials given the low quality of the stock pressure gauges of the system. Hydrogen sulfide detection will also be recommended though there are several factors that will severely impact its applicability. A detailed discussion of these methodologies can be found in Chapter 6.

CHAPTER 6

RECOMMENDED METHODS

Overview

The research conducted in the project using feedwater that accelerated fouling has highlighted several promising methods to non-destructively assess reverse osmosis biofouling in household systems. No one method is one hundred percent reliable proof that biofouling is occurring since a great deal of variation will be observed from system to system under field conditions. These methods are best used as a series of checks, the more methods that test positive for biofouling; the more likely it is occurring. It is also extremely important that the collected data for each non-destructive method is paired with an operational measurement that gauges the degree of fouling like trans-membrane pressure drop. For instance, high permeate conductivity was noted only in membranes suffering from biofouling, but monitoring permeate conductivity alone does not provide enough information about the system to reliably assess if the system is biofouled. Perhaps high permeate conductivity is measured, but the increase trans-membrane pressure drop is very low. This would be more indicative of a tear in the membrane envelope or permeate O-rings that have not seated correctly than the presence of biofouling because increased resistance to flux (as measured by the increase in trans-membrane pressure drop and caused by the growth of fouling layers) is not present in the system. These methods are also trend analyses so data must be collected at different operational time points so performance trends can be visualized. Furthermore, these

methods lack the sensitivity to provide early warning for the presence of biofouling. It is unclear whether these methods are warranted for use in full scale RO treatment plants were operational, energy, and other economic considerations are vastly different from the household systems on which these methods were developed. However, these methods could be used to conveniently and economically assess if household RO membrane systems are experiencing biofouling or inorganic fouling.

Permeate Flow Rates

Permeate flux proved to be significantly different between all the feed water types. Initial permeate flux in the combined and organics loading cases remained constant for at least the first 2/3 of the operation time until failure and then began to drastically decrease. Membranes fed with only inorganic constituents displayed a constant and linear decrease of flux throughout membrane operation.

For this method to properly work initial permeate flow rate and trans-membrane pressure drop must be recorded. Recording permeate flow rates becomes more complex if the system uses pressurized permeate storage tanks. It would be either necessary to disconnect the permeate line from the tank and measure flow or completely drain the tank so the permeate is discharging at atmospheric pressure. Measuring output from a full permeate storage tank is not indicative of actual permeate production rates. Once the system is set to measure the actual permeate flow rate, a graduated cylinder and a stop watch are all that are needed. To ensure the system is running at a pseudo steady state, it is best to allow it to operate for at least 2 min before measurements begin. Record the volume of fluid that is dispensed and the time required to dispense that volume. Also

record the trans-membrane pressure at which the system was operating during the measurement. These measurements will need to be repeated periodically over the system's lifespan to track operational trends. Normalize the flow rates by taking a ratio of the current flow rate to the initial flow rate. Normalize the pressure data to the initial observed TMP drop by subtracting the initial observed pressure drop from all subsequent pressure drops

Generally, if a very linear decrease in permeate flux is observed, inorganic fouling is likely to be occurring. If permeate production data displays two very distinct rates of decrease over the membrane lifespan, biofouling is likely present.

Permeate Conductivity

Permeate conductivity proved to be significantly different between biofouling (combined and organics loading) and inorganic fouling (inorganics only). Permeate conductivity drastically increased in the combined and organics loading cases as fouling progressed. No drastic increases were observed in the inorganic feed type.

For this method to properly work initial permeate conductivity and trans-membrane pressure drop must be recorded. Permeate conductivity is easily measured with the use of a conductivity meter following the recommended procedures outlined in the meter's manual. To ensure the system is running at a pseudo steady state, it is best to allow it to operate for at least 2 min before measurements begin. Record the permeate conductivity and the trans-membrane pressure at which the system was operating at during the measurement. These measurements will need to be repeated periodically over the system's lifespan to track operational trends. Normalize the permeate conductivity by

taking a ratio of the current conductivity to the initial conductivity. Normalize the pressure data to the initial observed TMP drop by subtracting the initial observed pressure drop from all subsequent pressure drops

Generally, if no increase or only a very minor increase in permeate conductivity is observed, inorganic fouling is likely to be occurring. If permeate conductivity drastically increases, biofouling is likely present.

Permeate F/F0 vs. Permeate C/C0

Alternatively, the two prior methods can be combined into an interesting graphical presentation. Plot the permeate flow ratio to the permeate conductivity ratio. The more vertical the line, the more likely inorganic fouling is occurring. The less vertical the line, the more likely biofouling is taking place.

Retentate Cell Clumping

Retentate cell clumping was significantly different between biofouling (combined and organics loading) and inorganic fouling (inorganics only). Retentate cell clumping drastically increased in the combined and organics loading cases as fouling progressed. No drastic increases were observed with the inorganic feed type.

Microscopy facilities and an image capture and analysis software package are essential for this method. In the case of this experiment, Nikon Eclipse E800 and a 100x Nikon oil emersion lens were used in conjunction with MetaVue® and MetaMorph® image capture and analysis software packages.

Proper bacterial staining and dilutions are also required for this method to work. Initially, DAPI stain was tried but only subpar results were obtained. The stains in the LIVE/DEAD® BacLight™ Bacterial Viability Kit were tried and worked extremely well. When sampling, it best to allow the system to operate for at least 2 min before samples are taken. This will give enough time to remove planktonic cells that have reproduced over the stagnation period. It is also very important to minimize sample disturbances since they might break apart any clumps that are present. This means slow pipetting and other transfers to minimize turbulence and shear. Samples during this experiment were never diluted and it was found that staining and filtering 5 mL of sample using 500 µL of a 1:150 stain solution worked best. Ultimately, the sample volume is totally dependent on the amount of cells present in the sample and needs to be adjusted so microscope images are of high quality. This means that the filtered volume should result in sufficient cells on the filter to be visible in most frames of reference but not so many that counting is impeded by excessive cell numbers.

Clumping analysis will be more consistent if the same area of filter is analyzed for every sample. Ultimately this area is accounted for when clump concentrations are calculated, but it is best to remain consistent. Once images are taken they need to be combined and thresholded. The pixel area of all the thresholded objects must be measured and exported to a spread sheet application like Excel®. To maintain consistency, thresholding ranges were kept constant throughout the experiment. In this case all areas that were brighter than 55 on a scale from 0 – 255 were defined as cells.

Since the samples will be environmental, a large variety of bacteria of different shapes and sizes will be present. It will be necessary to determine the average bacterial size for the analysis to be performed. This was done by finding the average pixel area of thresholded objects within a defined pixel area range. Pixel areas are highly dependent on magnification and camera resolution. The greater the magnification and resolution, the more pixel area a thresholded single cell will occupy; therefore, a reasonable size range must be determined based on the specifications of the microscope setup that will be used. In the case of this experiment, a size range between 5 and 350 pixels was used to determine the average cell pixel area. This value was later adjusted to account for upgraded imaging equipment to keep the analysis consistent. The 350 pixel value may have been on the larger end of the spectrum for single cells but once these ranges are determined, it is important that they remain consistent so results are comparable.

Three methods to display clumping data were examined. One method was based comparing clumps sizes based on % occurrences. Another method was based on comparing clump sizes based on % total cells. The final method was just monitoring the concentration of all clumps > 5 cells. A more detailed description of these methods can be found in Chapter 3. Of all the methods, the final concentration method worked the best.

Feed Channel Pressure Drop

Feed channel pressure drop was not significantly different between the feed loading types. These results indicate that the slope of the regression line was similar throughout the various feed types. While a feed channel pressure drop is strong indicator

of biofouling, a scientific literature also notes its presence in inorganic fouling cases (Vrouwenvelder et al., 2011a). However, this doesn't mean that the measurement is without merit. Collected data suggests that high feed pressures are indicative of biofouling. Phase IV combined and organics lines had maximum feed channel pressure drops of 14 psi and 13 psi, respectively. The system should be shut down before the feed channel pressure drop reaches this extreme given that membrane telescoping was observed. Telescoping can damage the integrity of the membrane and allow for contaminant passage through tears. Inorganics only loaded membranes had a maximum feed channel pressure drop of 5 psi, three times less than the maximum observed in biofouling cases. Unfortunately, no clear pressure threshold between inorganic and biofouling can be established since many other operational factors can affect the feed channel pressure drop including the integrity of the brine seal (as seen in Phase II). However, if other methods are indicating biofouling and a large feed channel pressure drop is observed, this is extra evidence that suggesting biofouling is occurring.

Feed channel pressure measurements are not without their problems in these systems. Unfortunately, the stock gauges were of poor quality and did not handle pressure pulsations from the RO booster pumps well. On systems with large pressure oscillations, the use of this method would require upgrading the stock pressure gauges to include liquid filled gauges and pulsation dampening snubbers. This setup successfully mitigated the pulsations from the RO booster pump operation throughout the experiment. Furthermore, the stock system uses absolute pressure gauges to monitor the pressures in the different lines. Determining pressure drops requires subtracting two measurements

from each other thus incurring extra error. This error is further compounded by any calibration errors between the gauges. Ideally, a differential pressure gauge would be implemented. This would mitigate gauge calibration errors and allow for the direct measurement of the feed channel pressure drop. Any system upgrades would incur extra costs which may not be desirable.

Hydrogen Sulfide

Hydrogen sulfide was included as another check to see if biofouling is occurring. During experimentation a "rotten egg" smell was detected in the retentate stream on the extreme end of the membrane's lifespan. This method must be taken with extreme scrutiny since many factors are not controllable.

First, sulfate must be present in the water for this reduction to actually occur. Waters with extremely low or no sulfate will most likely not have significant sulfate reduction for this to be noticed. Second, the duration of the stagnation time of the system greatly affects this method. A stagnation period long enough to create a redox environment conducive for sulfate reduction is needed, and that will also depend on the quantity of organic carbon present and the initial amount of oxygen. Microbial activity that utilizes the organic carbon as an energy source and the oxygen as a terminal electron acceptor will create the anaerobic environment conducive for sulfate reduction. Therefore, initial organic carbon and oxygen levels are also crucial. In the lab experiment, the system ran routinely on eight hour intervals. These intervals will most likely be variable in the field. It will therefore be imperative to know how long the system has been stagnant to properly use this method because the longer the system sits

stagnant, the more likely the proper environmental conditions for sulfate reduction will exist. A system that has been stagnant for 2 weeks could undergo sulfate reduction with very little biomass present because the membrane system has been deprived of oxygen for such a long time. The last concern deals with the quantification hydrogen sulfide. If the sample is not collected the instant the system starts up, the hydrogen sulfide will either be significantly diluted or completely flushed out of the system by the time the sample is taken.

Conclusion

Several non-destructive assessment methods have been developed. Future non-destructive biofouling assessments could employ a combination of the research methods described in Chapter 2. Methods will most likely be chosen based on system suitability, economics and operator preference. A combination of these methods will be needed to provide enough insight to non-destructively assess the type of fouling within the membrane.

REFERENCES CITED

Al-Juboori, R. A., and T. Yusaf, 2012, Biofouling in RO system: Mechanisms, monitoring and controlling: Desalination, v. 302, p. 1-23.

Behnke, S., A. E. Parker, D. Woodall, and A. K. Camper, 2011, Comparing the Chlorine Disinfection of Detached Biofilm Clusters with Those of Sessile Biofilms and Planktonic Cells in Single- and Dual-Species Cultures: Applied and Environmental Microbiology, v. 77, p. 7176-7184.

Bouwer, H., 2000, Integrated water management: emerging issues and challenges: Agricultural Water Management, v. 45, p. 217-228.

Dixon, M. B., S. Lasslett, and C. Pelekani, 2012, Destructive and non-destructive methods for biofouling analysis investigated at the Adelaide Desalination Pilot Plant: Desalination, v. 296, p. 61-68.

Eaton, A. D., L. S. Clesceri, A. E. Greenberg, M. A. H. Franson, American Public Health Association., American Water Works Association., and Water Environment Federation., 1998, Standard methods for the examination of water and wastewater: Washington, DC, American Public Health Association.

Escobar, I. C., and A. A. Randall, 2001, Assimilable organic carbon (AOC) and biodegradable dissolved organic carbon (BDOC): Complementary measurements: Water Research, v. 35, p. 4444-4454.

Flemming, H. C., 1997, Reverse osmosis membrane biofouling: Experimental Thermal and Fluid Science, v. 14, p. 382-391.

Flemming, H. C., G. Schaule, T. Griebe, J. Schmitt, and A. Tamachkiarowa, 1997, Biofouling - the Achilles heel of membrane processes: Desalination, v. 113, p. 215-225.

Flemming, H. C., and A. Tamachkiarow, 2003, Monitoring of biofilms in technical systems - a crucial component of advanced anti-fouling strategies: Membranes in Drinking and Industrial Water Production Iii, p. 199-204.

Fritzmann, C., J. Loewenberg, T. Wintgens, and T. Melin, 2007, State-of-the-art of reverse osmosis desalination: Desalination, v. 216, p. 1-76.

Graf von der Schulenburg, D. A., J. S. Vrouwenvelder, S. A. Creber, M. C. M. van Loosdrecht, and M. L. Johns, 2008, Nuclear magnetic resonance microscopy studies of membrane biofouling: Journal of Membrane Science, v. 323, p. 37-44.

Herzberg, M., and M. Elimelech, 2007, Biofouling of reverse osmosis membranes: Role of biofilm-enhanced osmotic pressure: Journal of Membrane Science, v. 295, p. 11-20.

Hwang, S.-N., W. Choi, H. Lim, J. Choi, H. Kim, and I. S. Chang, 2012, Fluorescence spectrum-based biofouling prediction method for RO membrane systems: Desalination and Water Treatment, v. 43, p. 238-245.

Kappelhof, J., H. S. Vrouwenvelder, M. Schaap, J. C. Kruithof, D. van der Kooij, and J. C. Schippers, 2003, An in situ biofouling monitor for membrane systems: Membranes in Drinking and Industrial Water Production Iii, p. 205-210.

Kavanagh, J. M., S. Hussain, T. C. Chilcott, and H. G. L. Coster, 2009, Fouling of reverse osmosis membranes using electrical impedance spectroscopy: Measurements and simulations: Desalination, v. 236, p. 187-193.

Komlenic, R., 2010, Biofouling: Rethinking the causes of membrane biofouling: Filtration & Separation, v. 47, p. 26-28.

Pandey, S. R., V. Jegatheesan, K. Baskaran, and L. Shu, 2012, Fouling in reverse osmosis (RO) membrane in water recovery from secondary effluent: a review: Reviews in Environmental Science and Bio-Technology, v. 11, p. 125-145.

Picioreanu, C., J. S. Vrouwenvelder, and M. C. M. van Loosdrecht, 2009, Three-dimensional modeling of biofouling and fluid dynamics in feed spacer channels of membrane devices: Journal of Membrane Science, v. 345, p. 340-354.

Pintelon, T. R. R., S. A. Creber, D. A. G. von der Schulenburg, and M. L. Johns, 2010, Validation of 3D Simulations of Reverse Osmosis Membrane Biofouling: Biotechnology and Bioengineering, v. 106, p. 677-689.

Sheng, G. P., and H. Q. Yu, 2006, Characterization of extracellular polymeric substances of aerobic and anaerobic sludge using three-dimensional excitation and emission matrix fluorescence spectroscopy: Water Research, v. 40, p. 1233-1239.

Sim, L. N., Z. J. Wang, J. Gu, H. G. L. Coster, and A. G. Fane, 2013, Detection of reverse osmosis membrane fouling with silica, bovine serum albumin and their mixture using in-situ electrical impedance spectroscopy: Journal of Membrane Science, v. 443, p. 45-53.

Tay, K. G., and L. F. Song, 2005, A more effective method for fouling characterization in a full-scale reverse osmosis process: Desalination, v. 177, p. 95-107.

Uchymiak, M., A. R. Bartman, N. Daltrophe, M. Weissman, J. Gilron, P. D. Christofides, W. J. Kaiser, and Y. Cohen, 2009, Brackish water reverse osmosis (BWRO) operation in feed flow reversal mode using an ex situ scale observation detector (EXSOD): Journal of Membrane Science, v. 341, p. 60-66.

van Loosdrecht, M. C. M., L. Bereschenko, A. Radu, J. C. Kruithof, C. Picioreanu, M. L. Johns, and H. S. Vrouwenvelder, 2012, New approaches to characterizing and understanding biofouling of spiral wound membrane systems: Water Science and Technology, v. 66, p. 88-94.

van der Kooij, D., H. R. Veenendaal, C. Baarslorist, D. W. Vanderklift, and Y. C. Drost, 1995, BIOFILM FORMATION ON SURFACES OF GLASS AND TEFLON EXPOSED TO TREATED WATER: Water Research, v. 29, p. 1655-1662.

Vrouwenvelder, H. S., J. A. M. van Paassen, H. C. Folmer, J. Hofman, M. M. Nederlof, and D. van der Kooij, 1998, Biofouling of membranes for drinking water production: Desalination, v. 118, p. 157-166.

Vrouwenvelder, J. S., J. Kruithof, and M. VanLoosdrecht, 2011a, Biofouling of Spiral Wound Membrane Systems: Biofouling of Spiral Wound Membrane Systems, p. 1-334.

Vrouwenvelder, J. S., and D. van der Kooij, 2001, Diagnosis, prediction and prevention of biofouling of NF and RO membranes: Desalination, v. 139, p. 65-71.

Vrouwenvelder, J. S., M. C. M. van Loosdrecht, and J. C. Kruithof, 2011b, Early warning of biofouling in spiral wound nanofiltration and reverse osmosis membranes: Desalination, v. 265, p. 206-212.

Wilson, S., M. A. Hamilton, G. C. Hamilton, M. R. Schumann, and P. Stoodley, 2004, Statistical quantification of detachment rates and size distributions of cell clumps from wild-type (PAO1) and cell signaling mutant (JP1) Pseudomonas aeruginosa biofilms: Applied and Environmental Microbiology, v. 70, p. 5847-5852.

APPENDICES

APPENDIX A

DOSE SOLUTION CONCENTRATIONS

APPENDIX A: Table of Dose Solution Concentrations

Constituent	20x Concentrated Organic Dose Solution [g/L]	Organic Dose Tank [g/L]	Inorganic Dose Tank 1 [g/L]	Inorganic Dose Tank 2 [g/L]
L-Glutamic Acid	-	1.409	-	-
L-Aspartic Acid	-	1.593	-	-
L-Serine	33.542	1.677	-	-
L-Alanine	28.436	1.422	-	-
D(+)Glucose	28.752	1.438	-	-
D(-)Galacturonic Acid Monohydrate	33.857	1.693	-	-
D(+)Galactose	28.752	1.438	-	-
D(-)Arabinose	28.751	1.438	-	-
Monobasic Potassium Phosphate	10.424	0.521	-	-
$CaCl_2$	-	-	8.247	-
$MgCl_2*6H_2O$	-	-	4.821	-
$Al_2(SO_4)_3*16H_2O$	-	-	0.162	-
Na_2SO_4	-	-	-	2.230
$MgSO_4*7H_2O$	-	-	-	3.316
$NaHCO_3$	-	-	-	24.135
$MnSO_4*H_2O$	-	-	-	0.017
pH	-	-	4.41	8.34

APPENDIX B

COMPARISON OF NON-HOMOGINIZED AND HOMOGENIZED DATA

APPENDIX B: Comparison of Non-homogenized and Homogenized Data

Introduction

During Phases III and IV, comparison studies between homogenized and non-homogenized samples were performed. During Phases I and II autopsies, homogenization was not performed on any of the aqueous samples acquired. Concerns were voiced that cell clumping could be detrimental to the accuracy of several analyses, sessile HPC's thought being the biggest impacted.

Materials and Methods

Sampling and Sample Preparation. The procedure used to sample and prepare the membrane swatches is described in detail in the Membrane Autopsy Analytical Methods section of Chapter 3.

Homogenization. Before homogenization, the homogenization probe was sterilized through autoclaving to ensure no microbial contamination of the samples. Samples were prepared using a homogenizer (IKA, Model # T25S1, Staufen im Breisgau, Germany) and homogenized for 30 seconds at 20,500 rpm. To ensure no cross contamination between samples, the homogenization probe was cleaned by homogenizing sterile water for 30 seconds. This was followed by a 15 second homogenization of a 70% ethanol and a 1 min. soak in that solution. Finally the probe was used to homogenize two more vials of sterile water for 30 seconds each. All homogenization was performed at 20,500 rpm.

Heterotrophic Plate Counts (HPC). Samples were serially diluted in autoclaved nano-pure water so that 30-300 colonies would be produced on a single plate from 100 µL of sample. The dilution water was also plated to check for contamination issues. All spread plates were made with DifcoTM R2A agar (Becton, Dickison, and Company, Cat # 218261). All samples were incubated at 28°C for 7 days before being counted on a Leica Colony Counter (Leica Inc., Buffalo, NY, USA).

Results

Homogenized and non-homogenized HPC's were analyzed to determine the extent at which homogenization affected the analysis. Results of the comparisons are displayed in Figure A1. Homogenized and non-homogenized sample were within in the same order of magnitude for the various feed water types.

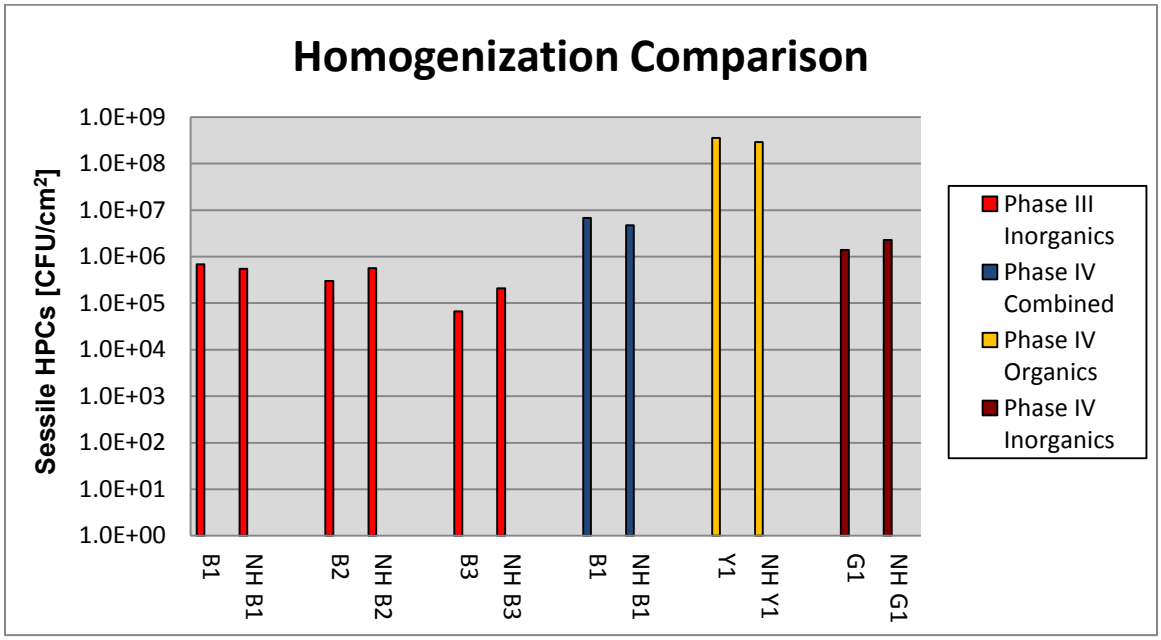

Figure A1: A comparison of homogenized and non-homogenized sessile HPCs. The sample prefix NH denotes non-homogenized samples.

Discussion

Results from the comparison study indicate that homogenization does not significantly affect the results of sessile HPC analysis. Furthermore, the study demonstrates that the difference between homogenized and non-homogenized samples is not significant enough to have any adverse effects when it comes to comparing data across different membrane fouling types.

APPENDIX C

RETENTATE PROTEIN CONCENTRATION AND QUANTIFICATION

APPENDIX C: Retentate Protein Concentration and Quantification

Introduction

The purpose of this experiment was to see if protein from sloughed EPS could be detected in the retentate stream and if it could be used as a non-destructive indicator of membrane biofouling. The microorganisms of a biofilm excrete EPS for a variety of different reason, i.e. adhesion, protection, etc. Invariable, as the biofilm expands, portions of the biofilm and thus EPS will be sloughed and exit the membrane system in the retentate stream. As biofouling becomes more severe, the amount of sloughed EPS in the retentate should also increase. Being able to detect and quantify this increase could be an indicator of biofouling.

Materials and Methods

Sample Collection. Samples of retentate water were collected weekly during Phase II in 50 mL Falcon tubes. The Falcon tubes were rinsed 3 times with nano-pure water and once with sample prior to final sample collection. Once collected, the samples were stored frozen until the protein analysis could be performed.

Protein Concentration. Concentration of the protein in the retentate samples was performed using 9K MWCO 20 mL Pierce Concentrators (Pierce Biotechnology, Cat # 89885, www.thermoscientific.com/pierce). Prior to sample concentration, each concentrator was pre-rinsed using the outlined pre-rinsing procedure. During pre-rinsing, the concentrators were centrifuged at 3000xg for 10 min. with a Sorvall Legend XTR

centrifuge (Thermo Scientific, Cat # 75004521, Madison, WI, USA) using a swinging bucket rotor (Thermo Scientific, Cat # 75003607, Madison, WI, USA).

For sample concentration, the recommend procedure was followed. A 20 mL sample volume was placed in the upper sample chamber of the concentrator. Additionally, 7.2 mL of nano-pure water was placed in the lower concentrator chamber to ensure a 1 mL volume of final concentrate. The concentrators were centrifuged at 3000xg using bucket rotors for 45 min. at room temperature. Once completed, the 1 mL of concentrate was immediately removed for sample analysis.

Protein Concentration Determination. Protein concentrations were determined using a Coomassie Plus (Bradford) Assay Kit (Pierce Biotechnology, Cat # 23236, www.thermoscientific.com/pierce). The kit's Micro Test Tube Protocol was exactly followed. Standards were made following the kit's procedure and using bovine serum albumin (Pierce Biotechnology, Cat # 23209, www.thermoscientific.com/pierce). Mixed samples/standards and reagents were transferred to disposable cuvettes (VWR, Cat # 97000-586, us.vwr.com) and absorbance was read at 595 nm with a Genesys 10uv scanning spectrophotometer (Thermo Scientific, SN 2LGN161001, Madison, WI, USA). All samples and standards were run in triplicate.

Initially, the 1 mL of concentrated retentate sample was diluted to 3 mL so the assay could be run in triplicate. Fully concentrated samples were also tested once it was determined that the assay was not sensitive enough to detect protein in the concentrated samples that were diluted for triplicate analysis.

Results

The results from the protein concentration are shown in Table A1 below. The retentate samples that were analyzed were collected in the 3 weeks prior to failure and membrane autopsy so they should have the greatest amount of sloughed protein due to the advanced stage of biofouling that was present on the membrane surface.

Table A1: A comparison of absorbance readings for protein samples and standards. Results indicate that protein concentration was not successful.

Sample Date	Concentration Factor	Absorbance at 595 nm		
04/25/13	20x	0.319	N/A	N/A
05/02/13	20x	0.317	N/A	N/A
05/08/13	6.2x	0.306	0.307	0.319
05/15/13	6.2x	0.311	0.319	0.320
Blank (0µg/mL BSA)	N/A	0.308	0.310	0.305
2.5µg/mL BSA	N/A	0.412	0.412	0.413

Discussion

The results indicate that protein could not be concentrated enough to be a reliable indicator of biofouling. It was hoped that protein could be detected before 04/25/13. By this date, trans-membrane pressure had reached it maximum and a permeate conductivity had already begun to increase.

Furthermore, performing 20x concentrations becomes a costly endeavor since one concentrator is needed for every measurement. Therefore, in order to perform the

analysis in triplicate on a single sample, which is highly recommended due to the degree of variability in the Coomassie Plus Assay, three protein concentrators are required. When three concentrators are used, assay costs multiply quickly.

APPENDIX D

RETENTATE HYDROGEN SULFIDE CONCENTRATION AND QUANTIFICATION

APPENDIX D: Retentate Hydrogen Sulfide Quantification

Introduction

During Phase I and II, phases which had high levels of bacterial growth on the membrane surface, a rotten egg smell was noticed during the operation of the membrane units as they approached system failure. This smell was not noticed in Phase III where inorganic fouling was the cause of failure. It was hypothesized that high levels of bacterial activity created an environment suitable for sulfate reduction over the period of time when the membrane units were stagnant. During Phase IV, retentate sample were taken to determine if an increase in hydrogen sulfide could be detected and if this increase could indicate the presence of biofouling.

Materials and Methods

Sample Collection. Samples of Phase IV retentate water were collected weekly in 15 mL centrifuge tubes. The centrifuge tubes were rinsed 3 times with nano-pure water. To collect the required retentate sample, sample tubes were held under each retentate line outlet prior to system operation. This was essential to collect the initial slug of water that had been stagnant in the system and should have had the greatest hydrogen sulfide concentration. Sample tubes were filled with retentate sample to the brim to minimize any possible headspace for off gassing. Once collected, the samples were stored frozen until the analysis could be performed.

Hydrogen Sulfide Concentration Determination. Five hundred milliliters of a copper reagent was made using deionized water, 0.624 g of cupric sulfate pentahydrate (Fisher Scientific, Cat # C489-500, www.fishersci.com) and 5 mL of 5 M hydrochloric acid. Four milliliters of the copper reagent was then added to 100 mm x 10 mm Kimex screw top tubes.A standard curve was made by using 7 sealed Hungate tubes filled with 100% prepurified N2. Sodium sulfide nonahydrate (MP Biomedicals, LLC, Cat # 02152580, www.mpbio.com) was mixed with anoxic water creating a 50mM starting solution. A series of half dilutions where performed using a sterile syringe to a final concentration of 1.5625mM. The seventh tube was left with only anoxic water and was used as a blank.

Fifty microliters of sample or standard was added to the Kimex tubes filled with copper reagent. The tubes were mixed and absorbance at 480 nm was measured immediately using a Genesys 10uv scanning spectrophotometer (Thermo Scientific, SN 2LGN161001, Madison, WI, USA). All samples and standards were run in triplicate.

Results

Samples near the end of the operational life of the combined line and the organics line were analyzed. No hydrogen sulfide was detected in any of the samples analyzed.

Discussion

To have enough through put to justify analysis, samples were frozen. This ended up being severely detrimental to hydrogen sulfide detection since it is believed much of the hydrogen sulfide was lost in the freezing process.

Just because this methodology failed, doesn't mean that the overall concept is flawed. Hydrogen Sulfide gas could be smelled during the operation of all combined and organics only lines (lines with the most sessile biomass) as they approached failure. An alternative approach to hydrogen sulfide quantification could be to use a DR 900 Colorimeter (HACH, Cat # 9385160, www.hach.com) in conjunction with the Sulfide Reagent Set (HACH, Cat # 2244500, www.hach.com). It would also be imperative to analyze collected samples as soon as possible, avoiding freezing at all costs.

APPENDIX E

SESSILE TOTAL AND VOLATILE SOLIDS

APPENDIX E: Sessile Total and Volatile Solids

Introduction

Total and volatile solids analyses were performed in an attempt to determine the amount of solids ant thus the amount of fouling on the membrane surface. These analyses were performed in Phases I through III.

Materials and Methods

Membrane swatches that were 4 cm x 4 cm were carefully cut from the unrolled membrane at designated areas using a template to ensure proper sample size. Six samples per membrane were taken. Membrane swatches were then placed in plastic petri plates and stored at room temperature until analysis could be performed later that day.

Analysis began by weighing the empty glass petri plates in which the analyses would be performed. Membrane swatches were then transferred to the glass petri plates and placed in an oven (Thermo Scientific, Model # 664, Madison, WI, USA) overnight at 105°C. After being baked, samples were transferred to a desiccator and then weighed. For total volatile solids analysis, the glass petri plates with sample swatches where wrapped in aluminum foil and placed in a muffle furnace. Samples were fired for 1 hour at 550°C. Once the furnace cooled, samples were removed and placed into a desiccator and weighed. To calculate the total volatile solids, it was necessary to determine amount of volatile mass within the membrane itself. This was done by firing six 4 cm x 4 cm membrane swatches cut from an unused RO membrane following the same procedure described above. The values obtained were averaged and then used in the volatile solids calculations.

Results

Data acquired from the total and volatile solids analyses was often nonsensical in all the phases. A great deal of data scatter was observed within each membrane. Volatile solids values were often negative throughout each phase.

Discussion

The methodology of these assays was not sensitive enough to provide accurate results. It was extremely difficult to ensure that the sample swatch size was exactly 16 cm^2. Furthermore, since the membrane itself was manufactured using volatile solids, errors in measurements were compounded by the need subtract out that mass. Total and volatile solids analyses were discontinued by Phase IV.

APPENDIX F

ORGANIC CARBON CONSUMPTION

APPENDIX F: Organic Carbon Consumption

Introduction

This method is based off of the detection of bacterial metabolic activity. The thought is that bacteria in the biofilm will consume total organic carbon (TOC) as it passes through the feed channel of the membrane. As the amount of biofilm increases, so to should the TOC consumption. Therefore, TOC was measured in the feed and retentate streams in the hope that a net loss can be detected. It was also hoped that this loss in carbon would increase as biofouling increases. The collected data was correlated to the actual state of membrane fouling through autopsies.

Materials and Methods

Retentate and permeate TOC samples were collected directly in disposable glass test tubes that were rinsed 4 times with nano-pure water. Feed TOC samples were collected from the feed tank with disposable syringes that were rinsed 4 times with nano-pure water and then transferred to rinsed disposable glass test tubes. All sample tubes and syringes were rinsed at least once with sample before the final sample was taken and stored. Samples were then stored at 4°C and analyzed the same day using a Formacs$^{HT/TN}$ TOC/TN Analyser (Skalar, Model # CA16, Breda, Netherlands) in conjunction with a LAS-160 Autosampler (Skalar, Model # LAS-160, Breda, Netherlands).

Results

TOC data for Phase II (organics) and Phase III (inorganics) was compared. Using measured flow rates and TOC concentrations, mass flow rates were calculated for each

process stream. A TOC mass balance was performed by subtracting the feed mass flow rate from the combined retentate and permeate mass flow rates. Results are displayed in Figure A2.

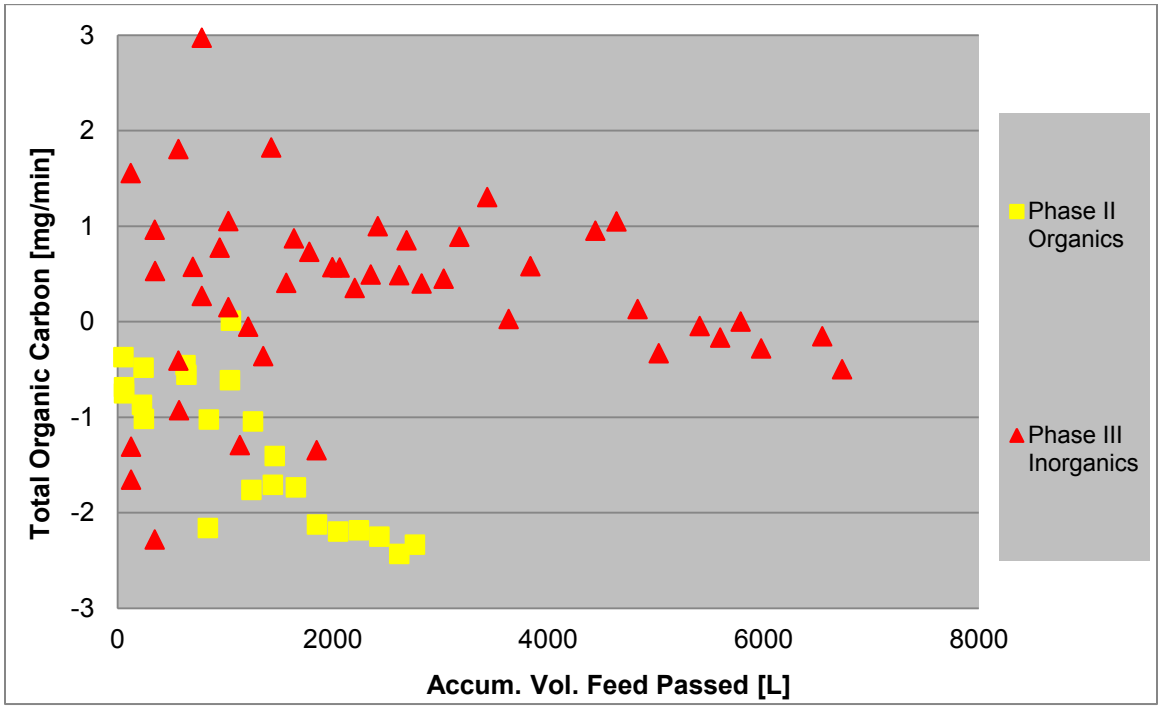

Figure A2: Mass balance (mass rate out – mass rate in) for total organic carbon (TOC) during Phases II and III.

Discussion

Many problems were associated with collecting TOC data during Phase I. Initial sample analysis showed great and nonsensical variability. This was most likely the caused by the use of contaminated glass sample vials. Samples were also frozen prior to analysis and it is believed this also degraded sample quality. By the end of Phase I, these issues were resolved by collecting and analyzing samples in new and clean sample tubes. Also, samples were analyzed the same day they were taken. However, a major issue that

could not be resolved involved the way the Formacs$^{HT/TN}$ TOC/TN Analyser calculated TOC. TOC is calculated by subtracting measured total carbon and inorganic carbon. Under this method, TOC results were adversely affected when inorganic carbon made up more than 30% the total carbon. This was especially a concern in the combined loading cases.

The TOC mass balance for Phase III showed a great deal of initial scatter. This may be because of the aforementioned problems with the way TOC is determined. Furthermore, the difference between the two phases is only 2 mg/min. The fact that the Phase III data scatter encompasses the entire range of the Phase II data leads to the conclusion that the analyses were not sensitive enough to make proper distinction between the two.

APPENDIX G

SESSILE ORGANIC AND INORGANIC CARBON

APPENDIX G: Sessile Organic and Inorganic Carbon

Introduction

Sessile carbon was used to try to enumerate the type and quantity of foulant on the membrane surface. It was hypothesized that the degree of inorganic fouling could be determined by the amount of inorganic carbon as calcium carbonate scraped from the surface. It was further hypothesized that the degree of biofouling could be indicated by the amount of sessile organic carbon.

Materials and Methods

Sampling and Sample Preparation. The procedure used to sample and prepare the membrane swatches is described in detail in the Membrane Autopsy Analytical Methods section of Chapter 3.

Sessile Carbon Concentration Determination. A known volume of the prepared aqueous sample was transferred directly into disposable glass test tubes and diluted appropriately. A new membrane control was also analyzed to determine if the membrane itself contributed carbon to the analyses. The glass tubes were prepared by being rinsed 4 times with nano-pure water. Samples were then analyzed that day using a Formacs$^{HT/TN}$ TOC/TN Analyser (Skalar, Model # CA16, Breda, Netherlands) and a LAS-160 Autosampler (Skalar, Model # LAS-160, Breda, Netherlands).

Results

Phase I and Phase IV autopsies were performed upon membrane failure. For Phase II and Phase III, one membrane was autopsied at 1/3 of the predicted maximum increase in trans-membrane pressure, 2/3 the predicted maximum increase in trans-membrane pressure and membrane failure. Maximum increase of trans-membrane pressure was predicted by subtracting the initial trans-membrane pressure from the maximum pressure the of the RO booster pump.

Sessile inorganic carbon data showed a great deal of variation throughout all the phases.

Phase I (combined) data showed the greatest variation in sessile TOC at the failure point. Sessile TOC in Phase II (organics) increased over the length of the experiment. Phase III (inorganics) sessile TOC did not increase throughout the length of the experiment. Phase IV combined sessile TOC quantities were half those observed in Phase I. Phase IV organics had the overall highest quantities of sessile TOC. Sessile TOC for Phase IV inorganics was half the value of the sessile TOC measured in Phase IV combined. Sessile TOC data is displayed in Figure A3.

Discussion

Sessile inorganic carbon data should not be taken seriously. It is impossible to completely remove scalants from a membrane surface through scraping. This undoubtedly resulted in scalant being left on the membrane surface and not being quantified.

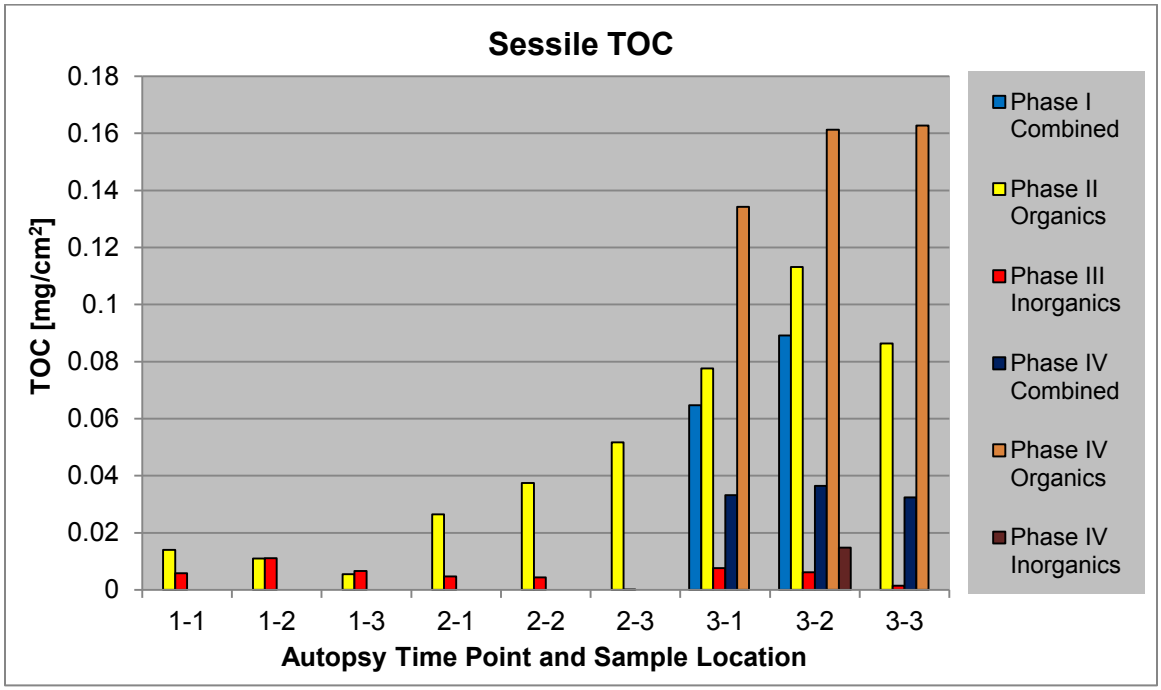

Figure A3: Sessile total organic carbon (TOC). Sample nomenclature is as follows (autopsy time point - sample location). Autopsy time point 1 was at 1/3 the increase to maximum trans-membrane pressure (TMP) drop. Autopsy time point 2 was at 2/3 the increase to maximum TMP drop and autopsy time point 3 was after failure. Sample location 1 was at the beginning of the feed channel where feed water entered the membrane. Sample location 2 was at the center of the membrane. Sample location 3 was at the extreme end of the feed channel where retentate water exited the membrane.

Sessile TOC data is more trustworthy. Biofilm can be removed from the membrane surface through scraping. Sessile TOC data correlated well with biofouling and retentate cell clumping. Membranes with high sessile TOC also had high degree of clumping in the retentate.